Budapest University of Technology and Economics
Faculty of Mechanical Engineering
Department of Polymer Engineering

DEVELOPMENT OF ALL-POLYPROPYLENE COMPOSITES FOR INJECTION MOULDING

PhD thesis

By   **Ákos Kmetty**

MSc in Mechanical Engineering

Supervisor   **Tamás Bárány, PhD**

Associate Professor

Budapest, 2012

Acknowledgements

I would like to express my thanks to my supervisor, Dr. Tamás Bárány for his attention and relentless support of my studies, and his guidance towards a deeper scientific way of thinking. I appreciate the valuable help and advice of Professor József Karger-Kocsis, who has supported my studies from the beginning. I would like to thank to Professor Tibor Czigány for his assistance and assuring the friendly atmosphere during my work. I would like to thank the help and advices of Dr. József Gábor Kovács, Dr. Tamás Tábi and Dr. László Mészáros. I am grateful to my colleagues and friends at the Department of Polymer Engineering for their significant help.

I express my thanks to C. M. Wu for his help, to Dóra Tátraaljai and Dr. Enikő Földes for their help in the FTIR measurements and to Csaba Érseki for his help in development of the special extrusion die. I express my thanks to my students who helped a lot my work.

I express my thanks to the Hungarian Scientific Research Fund (OTKA K75117) for the financial support, to Arburg Hungary Ltd. for the Arburg Allrounder 370S 700-290 machine and to MTA–BME Research Group for Composite Science and Technology for the support.

Finally, I would like to thank my wife, parents and friends for their continuous support in reaching my goals.

Alulírott Kmetty Ákos kijelentem, hogy ezt a doktori értekezést magam készítettem, és abban csak a megadott forrásokat használtam fel. Minden olyan részt, amelyet szó szerint, vagy azonos tartalomban, de átfogalmazva más forrásból átvettem, egyértelműen, a forrás megadásával jelöltem.

Budapest, 2012. november 15.

<div align="right">Kmetty Ákos</div>

A doktori disszertáció bírálata és a védésről készült jegyzőkönyv a

Budapesti Műszaki és Gazdaságtudományi Egyetem

Gépészmérnöki Karának Dékáni Hivatalában megtekinthetőek.

TABLE OF CONTENT

LIST OF SYMBOLS AND ABBREVIATIONS

Lists of symbols

$a_{c,n}$	$[kJ/m^2]$	impact strength (notched)
$a_{c,n,L}$	$[kJ/m^2]$	longitudinal impact strength (notched)
$a_{c,n,T}$	$[kJ/m^2]$	transversal impact strength (notched)
C_1	[-]	constant (proportional to the relaxation of the fibre)
C_2	[-]	constant (proportional to the orientation of the fibre)
D	$[mm]$	diameter of the extruder screw
E_B	$[GPa]$	flexural modulus
E_t	$[GPa]$	tensile modulus
$E_{t,L}$	$[GPa]$	longitudinal tensile modulus
$E_{t,T}$	$[GPa]$	transversal tensile modulus
L	$[mm]$	length of the extruder screw
L_i	$[mm]$	product dimension on defined place
L_m	$[mm]$	mould dimension on defined place
m	[-]	slope of the post shrinkage
p	$[MPa]$	processing pressure
p_A	$[MPa]$	pressure amplitude
p_h	$[MPa]$	holding pressure
S_i	$[\%]$	shrinkage of the product
S_t	$[\%]$	technological shrinkage
T_D	$[°C]$	drawing (stretching) temperature
T_g	$[°C]$	glass transition temperature
T_{proc}	$[°C]$	processing temperature
$T_{proc,opt}$	$[°C]$	optimal processing temperature
T_m	$[°C]$	melting temperature
T_{mould}	$[°C]$	mould temperature
V	$[mm/min]$	extrusion velocity
λ	[-]	draw ratio
σ_B	$[MPa]$	tensile strength
$\sigma_{B,L}$	$[MPa]$	longitudinal tensile strength
$\sigma_{B,T}$	$[MPa]$	transversal tensile strength
σ_F	$[MPa]$	flexural strength

7

σ$_Y$	[*MPa*]	yield stress
BP	[*MPa*]	base pressure for vibration injection moulding

Lists of abbreviations

All-PP(R)	all-polypropylene composite with random polypropylene matrix
All-PP(E)	all-polypropylene composite with polypropylene based thermoplastic elastomer matrix
ATR	attenuated total reflectance
CBT	cyclic butylene terephthalate oligomer
IM	conventional injection moulding
CNF	carbon nanofibre
CP	cross-ply structure
DMA	dynamical mechanical analysis
DSC	differential scanning calorimetry
EDS	energy dispersive x-ray spectroscopy
EDR	extrusion draw ratio
EP	ethylene-propylene copolymer
ePP	polypropylene based thermoplastic elastomer
EPR	ethylene-propylene rubber
FG	fan gate
FTIR	Fourier transform infrared spectroscopy
GF	glass fibre
HDPE	high-density polyethylene
hPP	polypropylene homopolymer
iPP	isotatic polypropylene
LCP	liquid crystalline polymer
LM	length dimension at the middle
LS	length dimension at the side
MD	machine direction
MFC	microfibrillar composite
OPIM	oscillating packing injection moulding
PA	polyamide
PA-6	polyamide-6

PA-6.6	polyamide-6.6
PBA	polybutyl acrylate
PCTG	polycyclohexane-terephthalate glycol
PE	polyethylene
PEEK	polyether-ether-ketone
PEN	polyethylene-naphthalate
PET	polyethylene-terephthalate
PETG	polyethylene-terephthalate glycol
PMMA	polymethyl-methacrylate
POM	polyoxymethylene or polyacetal
PP	polypropylene
PPS	polyphenylene-sulfide
PS	polystyrene
PTFE	polytetrafluor-ethylene
PVC	polyvinyl-chloride
PVDF	polyvinylidene-fluoride
rPP	random polypropylene copolymer
SCORIM	shear controlled orientation in injection moulding
SEM	scanning electron microscopy
SRPM	self-reinforced polymeric material
SRPP	self-reinforced polypropylene
TD	transverse (to machine) direction
TEM	transmission electron microscopy
TMA	thermomechanical analysis
UD	unidirectional alignment, structure
UHMPE	ultra high modulus polyethylene
UHMWPE	ultra high molecular weight polyethylene
VIM	vibration injection moulding
α-PP	isotatic polypropylene (alpha form)
α-rPP	random polypropylene copolymer (alpha form)
β-PP	isotatic polypropylene (beta form)
WF	width dimension at the front
WB	width dimension at the back

1. Introduction

Nowadays different environmental regulations were made due to the greenhouse effect, exhaustion of the not renewable natural resources and the increase of the waste content. Reusability and recyclability of the structural materials has the same importance as their economic parameters, due to the European Union directive concerning the automotive industry [1]. According to this directive, 95% of the vehicle components should be made of reusable/recyclable materials by 2015.

Presently, considerable research activities and accompanying commercial interest are devoted to all-polymeric materials, especially to self-reinforced versions. In the all-polymeric materials, both the reinforcing and matrix phases are given by suitable polymers. In self-reinforced polymeric materials (SRPMs), the same polymer forms both the reinforcing and matrix phases. SRPMs are also referred to as single-phase or homocomposites. Moreover, in the open literature, those polymer composites where the reinforcement and matrix polymers are different but belong to the same family of polymers, are also termed as SRPMs. SRPMs may compete with traditional composites in various application fields based on their performance/cost balance. With respect to their performance, the ease of recycling has to be emphasized because they represent likely the best recycling option (compared to the glass fibre reinforced thermoplastic composites) when reprocessing via remelting is targeted. Accordingly, SRPMs can be considered to be environmentally benign materials. The concepts used to produce SRPMs can also be adapted to biodegradable polymers to improve their property profiles, whereby even the degradation properties can be tailored upon request.

A further driving force for SRPMs is the possibility of manufacturing lightweight parts and structures because the density of SRPMs is well below those of traditional filled polymers. The density of the corresponding composite is usually higher than that of an SRPM because the former contains reinforcements [2] such as glass fibre (density: 2.5-2.9 gcm^{-3}), carbon fibre (density: 1.7-1.9 gcm^{-3}), basalt fibre (density: 2.7-3.0 gcm^{-3}), aramid fibre (density: 1.38-1.44 gcm^{-3}) and/or fillers like talc (density: 2.7-2.8 gcm^{-3}), chalk (density: 1.1-2.5 gcm^{-3}) and silica (density: 2.1-2.6 gcm^{-3}). The basic structural concept of self-reinforcement is the creation of a one-, two- or three-dimensional alignment (1D, 2D or 3D, respectively) within the matrix to fulfil the role of matrix reinforcement. Reinforcing action requires that the generated structure possesses higher stiffness and strength than the matrix and, in addition, is well "bonded" to the matrix polymer. As a consequence, the stress can be

transferred from the "weak" matrix to the "strong" reinforcing structure resulting an optimized anisotropic load-bearing distribution, which is the "working principle" of all composites. The reinforcing structure can be produced during one (*in-situ*) or more processing steps (*ex-situ*). From a historical point of view, the development of SRPMs started with the *in-situ* production of 1D-reinforced materials. This occurred mostly with solid-phase extrusion forming and techniques exploiting melt shearing in solidifying melts. The related operations resulted in 1D, aligned supermolecular structures acting as the reinforcement in SRPMs, whereby the covalent bond strength of the macromolecules was indirectly utilized. The term "supermolecular structure" already suggests that SRPMs are almost exclusively semicrystalline polymer-based systems. Compared to the matrix, the reinforcing structure in them either has different crystalline and/or supermolecular (also referred to as higher-order) structures or is given by a preform, a prefabricate (*e.g.* fibre, tape and their different textile architectures) with higher (and different) crystallinity. The 1D reinforcement can also be generated by multi-step stretching. Related technologies, practiced for example in fibre spinning operations, are grouped into multi-step (*ex-situ*) productions of single-component SRPMs. Self-reinforced polypropylene (SRPP) composites, produced only from fibres or fabrics as preforms, are classified as multi-step products of single-component SRPMs, which may exhibit 1D (unidirectional fibre alignment), 2D (fabric plies) or 3D (*e.g.* braided structure) reinforcements. In other words, when an SRPM is produced solely from preforms, with prefabricates instead of primary granules of a given polymer, it is classified as the product of multi-step processing. A commercial break-through with SRPMs occurred recently. SRPP composites (also called all-PP composites) are now available on the market under the trade names Curv®, Pure® and Armordon®. Curv® is a single-component, multi-step product usually with 2D (fabric) reinforcement, whereas Pure® and Armordon® are two-component, multi-step versions originally with 1D reinforcement (as stretched tapes with different PP grades in the core and surface layers). Disadvantage of these composites is the sheet-like form. Manufacturing of this is strongly limited (only thermoformed products with constant wall thickness, *e.g.* shells, panels etc.). 3D products with complex geometry cannot be produced with conventional technologies (*e.g.* injection moulding).

The main goal of my dissertation is to develop and characterise injection mouldable all-polypropylene composites.

2. Literature overview

The grouping outlined in Figure 1 will be followed in this chapter. Accordingly, the single- and multi-component SRPMs will be treated separately by considering their production (*i.e. in-situ* or *ex-situ*) and spatial reinforcing structure (*i.e.* 1D, 2D or 3D).
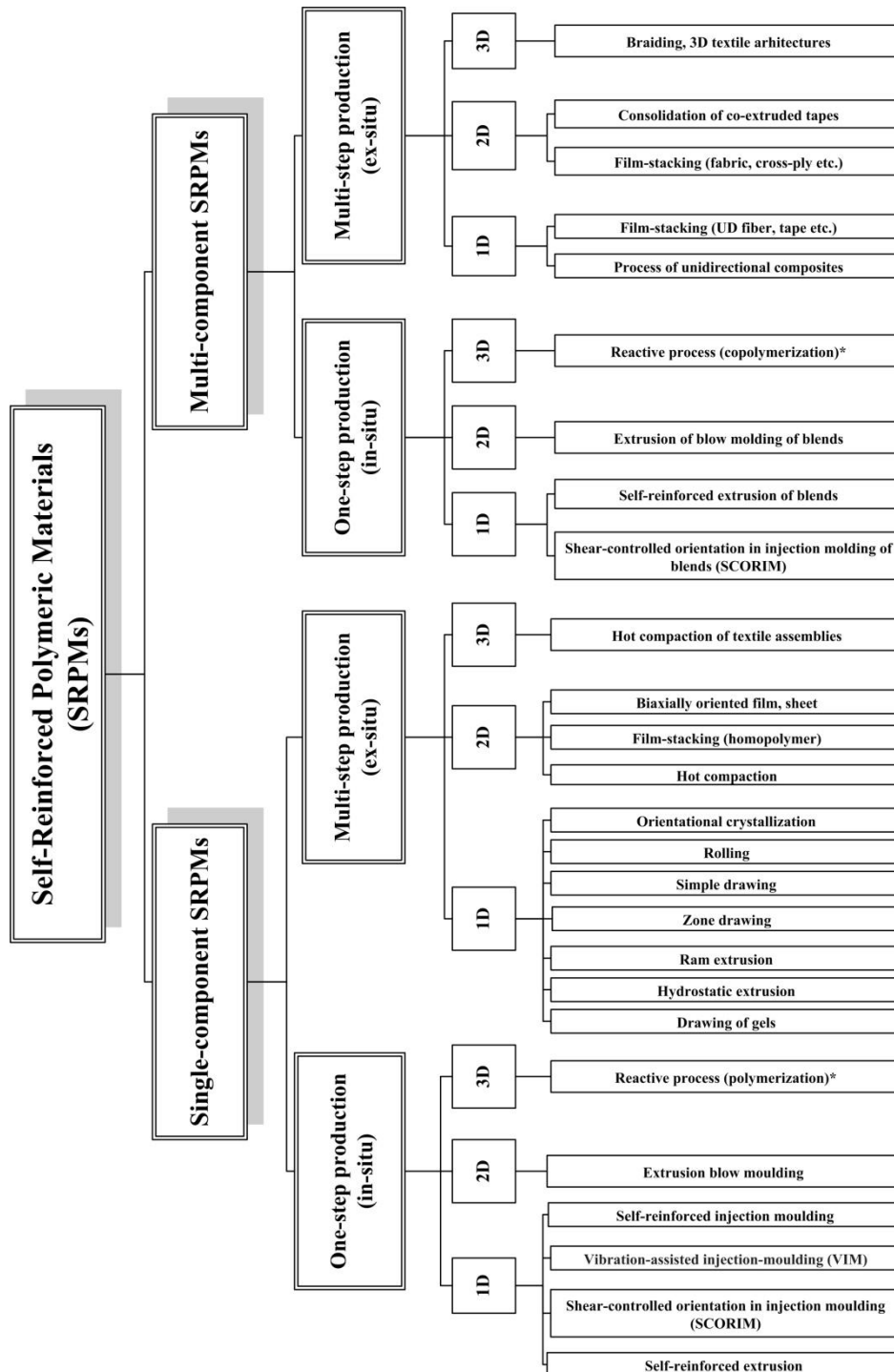

Figure 1. Classification of self-reinforced polymeric materials (SRPMs),*not yet explored [3]

2.1. Single-component SRPMs

In this chapter the single-component self-reinforced polymeric materials will be detailed.

2.1.1. One-step (*in-situ*) production

A 1D self-reinforcing structure can be produced by extrusion moulding whereby the extruder is equipped with a die having a convergent section (*cf.* Figure 2). The convergent section (with an angle of 45° or higher) is foreseen to generate the molecular orientation via extensional flow that is "frozen" in the subsequent sections of the die (calibration zone). Pornnimit and Ehrenstein [4] used this technique to manufacture self-reinforced HDPE. It was shown that the oriented molecules act as (self) row nuclei and trigger the formation of cylindrical and shish-kebab-type supermolecular structures (Figure 2).
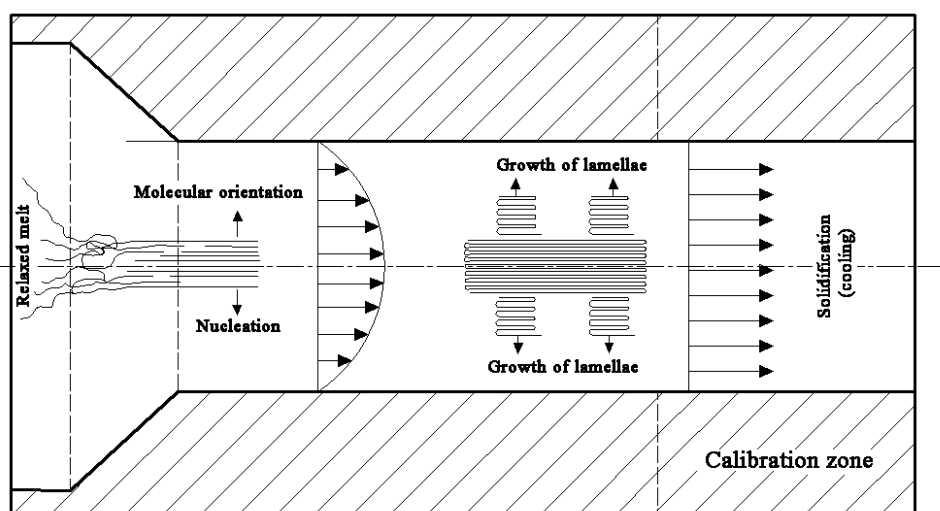

Figure 2. Scheme of the 1D supermolecular structure formation in a die with a convergent section during extrusion moulding [3]

As a controlling parameter of the formation of the self-reinforcement, the temperature program of the die (affecting the pressure build-up within) was identified. Upon cooling the outcoming zone of the die, a high extrusion pressure could be reached, which supported the formation of the shish-kebab crystals. The self-reinforced HDPE rod exhibited considerably higher stiffness and strength and highly reduced thermal shrinkage when measured in the reinforcing direction. Although the shish-kebab structure has been known since the mid 1960s, the mechanism of its formation is still debated. Kornfield *et al.* [5] in their recent work proposed that long chains are not the dominant species of the shish formation as thought

before. Nevertheless, the presence of long macromolecules strongly favours the propagation of shish. The basic prerequisites of the extrusion procedure yielding 1D self-reinforcement were identified as follows [6]: molecular orientation in the melt via forced extensional flow; processing close to the crystallization temperature of the polymer; and "fixing" of the resulting structure in the final section of the die by raising the pressure. DSC investigations showed that the melting peak of the self-reinforced HDPE was shifted towards higher temperatures by approximately 4°C. Farah and Bretas [7] developed shear-induced crystallization layers in iPP via a slit die attached to a twin-screw extruder. The output rate was below 10 kg/h. The die temperatures were set between 169 and 230°C. Rheological studies revealed that the induction time, at a given crystallization temperature, decreased as the shear rate increased. At a given shear rate, higher crystallization temperatures gave longer induction times. It was observed that at a given output rate, the thickness of the shear-induced crystalline layer decreased with the increase of die temperature. Three layers were found by SEM and TEM. Two layers were spherulitic while one layer was composed of highly oriented lamellae.

Huang *et al.* [8-9] produced self-reinforced HDPE by using a convergent die (angle 60°) and an extrusion pressure ranging from 30 to 60 MPa. Similar to the methods in [10], the authors cooled the melt before leaving the die at 128°C. The tensile strength of the resulting 1.5 mm thick sheets was eight times higher than that of the conventionally extruded sheet. The anisotropy in the sheets was detected in mechanical and tribological tests and was also demonstrated by microhardness results. Parallel to the works on PEs, PP was also discovered as a suitable candidate for SRPM [11-12]. Song *et al.* [13] produced self-reinforced PP by a conventional single-screw extruder with pressure regulation (L/D= 30, maximum pressure: 100 MPa), equipped with a convergent die (entrance angle 45°) with two or more calibration (cooling) sections. The properties of the extrudate were superior to counterparts produced by the conventional extrusion moulding. Self-reinforced structures can also be generated by injection moulding. The related techniques differ from one another whether the oriented structure is created outside or within the mould. Prox and Ehrenstein [14] produced self-reinforced material using the technique of converging die injection moulding. They injected the low temperature melt into the cavity just after the melt passed a convergent die section. Note that this concept requires a careful mould construction and well-defined processing conditions to avoid relaxation phenomena reducing the molecular orientation. Those injection moulding techniques that generate the self-reinforcement in the mould have become far more

popular than the above-mentioned variant. They are known under shear controlled orientation in injection moulding (SCORIM)) [15-16] or oscillating packing injection moulding (OPIM). The common characteristic of these techniques is that the molecular orientation is set in the mould by shearing/oscillation of the solidifying melt via a suitable arrangement of pistons. The pistons start to work when the cavity is already filled. The related mould construction may be very different [17], although in SCORIM three basic operation modes exist (*cf.* Figure 3).
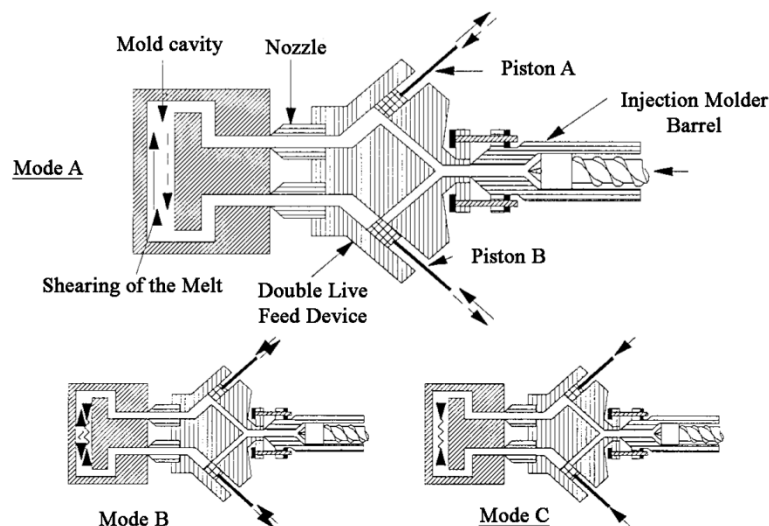

Figure 3. Scheme of the function of the SCORIM procedure along with the three basic operations (A, B and C)- Mode A: the pistons are activated 180° out of phase; Mode B: pistons are activated in phase; Mode C: the pistons are held down a constant pressure [18]

Guan *et al.* [19] used the OPIM to produce self-reinforced HDPE. An injection pressure of ca. 41 MPa was superimposed by an oscillating packing pressure (varied between 32 and 48 MPa) with a frequency of 0.3 Hz. An operation mode "A" in Figure 3 was chosen, and 220 and 42°C were set for the temperatures of the melt and mould, respectively. The moulded parts were subjected to mechanical and morphological tests. The stiffness and strength of the OPIM mouldings were superior to the conventional ones. Morphological studies revealed the presence of a microfibrillar structure. The TEM study showed that the microfibrillar structure was composed of shish-kebab formations. Based on DSC measurements, the authors concluded that the microspherulitic structure melts at 132°C, whereas the shish-kebab crystals melt at 137°C. In a follow-up work, Guan *et al.* [20] adapted the OPIM on PP. Studying the effects of processing conditions, the authors concluded that the mechanical properties of the mouldings strongly depend on the operation mode and to a lesser extent depend on the oscillation frequency, frequency/mode and frequency/time

combinations. Chen and Shen [21] produced biaxial self-reinforced (*i.e.* 2D) PP by OPIM. An operation mode "A" in Figure 3 was selected, and 195 and the range of 20–80°C were chosen for the temperatures of the melt and mould, respectively. The products exhibited quite balanced (*i.e.* less anisotropy) static mechanical properties (strength improvements compared to conventional injection moulding in the melt flow direction and transverse to it at 55–70 and 40%, respectively), but further on a pronounced anisotropy in respect to impact strength was seen (improvement to conventional moulding in the melt flow direction and transverse to it at 400 and 30–40%, respectively). Kalay *et al.* [18, 22] investigated the influence of PP types on the corresponding SCORIM products and deduced the basic rules on how to prepare products with optimum properties. It is important to emphasize that the basic advantage of SCORIM/OPIM is the pronounced orientation of the molecules in the whole cross-section of the moulded parts. This is because of the repeated shearing/oscillation movements in the melt that are acting until the melt solidifies. This suppresses the relaxation of the oriented molecules. A further variant of the injection moulding resulting in self-reinforcement is vibration injection moulding (VIM), which was pioneered by Li *et al.* [23]. The working principle of VIM is depicted in Figure 4.
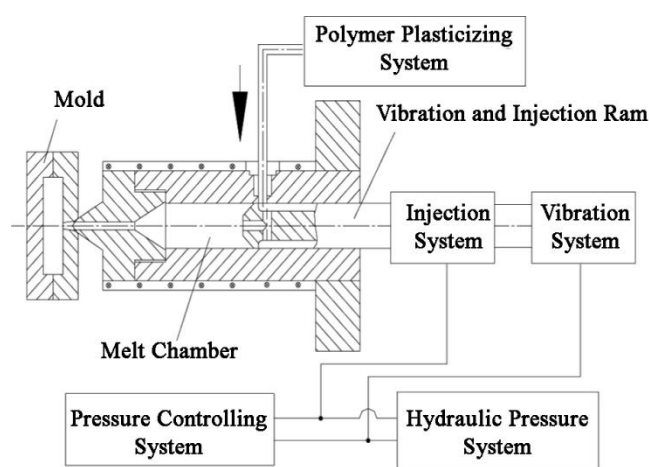

Figure 4. Working principle of the vibration injection moulding [23]

The ram itself is a part of both the injection and vibration systems. Without vibration, the setup works as a conventional injection moulding (IM) unit. However, working in the VIM mode, pulsations occur in the injection and holding pressure stages. This causes an effective compression and decompression of the melt and shearing at the melt–solid interface. Note that solidification progressed from the surface to the core of the moulding in the cavity. For this VIM device, the main processing parameters are vibration frequency and vibration pressure amplitude. In the cited study, the authors used a single screw extruder as the

16

plastification unit. The PP melt was vibrated for 25 s, and the cooling time was fixed at 20 s. The injection pressure for IM and the base pressure (BP) for VIM was 49.4 MPa. In the latter case, the pressure amplitude was fixed at 19.8 MPa. The mechanical properties and morphology of the specimens were determined. It was found that the mechanical properties of the VIM-produced parts were enhanced compared to conventional injection moulding. The yield stress steeply rose with the vibration frequency in the range of 0–1 Hz. Afterwards, a constant value was noticed for the range of 1–2.5 Hz. The tensile strength increased with increasing vibration frequency. The impact strength of PP was doubled compared to the conventional moulding using VIM at 2.33 Hz. The crystalline structure of the VIM-produced PP showed the simultaneous presence of the crystalline α, β- and γ-modifications of PP.

In a companion study [24] using HDPE and setting the vibration frequency at 2.33 Hz and the pressure amplitude at 19.8 MPa, the authors observed the formation of a shish-kebab along with row-nucleated crystalline lamellae. Their presence resulted in an upgrade of the mechanical properties of HDPE. Attention should be paid to a widely practiced design method in injection moulded items, to the film or "plastic" hinge. It was recognized early-on that the convergent (hinge) section of the moulded parts of both semicrystalline and amorphous thermoplastics has a peculiar performance: it withstands multiple bending movements. Now, this design principle has been incorporated into many products of everyday life, especially for dispensing packages.

Morphological studies on such hinges [25] demonstrated the presence of strongly oriented (1 or 2D) supermolecular structures, including shish-kebab types. The hinges consist of two highly oriented surface layers and one almost isotropic core in between. The core exhibits a small-sized spherulitic structure whereas the oriented surface layers contain shish-kebab structures. The mechanical behaviour of the oriented layers is similar to that of "hard elastic fibres", which show a high stiffness and a high strain recovery. So, products with film or 'plastic' hinges represent nice examples of the one-step (in situ) produced SRPCs, although only a given section of them is really self-reinforced. Some results of the previously presented methods are summarized in Appendix Table 5 – *cf.* Figure 1.

2.1.2. Multi-step (ex-situ) production

Single-component SRPCs can also be produced by multistep production methods, such as die- and zone-drawing, ram extrusion, hydrostatic extrusion, rolling (using various solid "preforms that are eventually produced on-line), gel drawing or spinning (where the

"preform" is a dilute polymer solution). As the reader will see, in many cases the preparation of the "preform" and the generation of the reinforcing structure within occur on-line, but in different stages or steps. This is the reason why they are listed among the multi-step production methods. When the orientation and thus the creation of the reinforcing structure takes place in the solid state of the polymer (*i.e.* below its melting temperature), the related methods are referred to as solid-state processes [13].

2.1.2.1. Solid phase extrusion

Developed in the early 1970s, ram extrusion involves the pressing of a solid preform through a metallic die of conical (convergent) shape. This technique was successfully adapted to many thermoplastics, covering not only semicrystalline (PE, PTFE, PP, PET, and PA) but also amorphous versions (PS) [26]. Major problems with the ram extrusion include: a very low output rate due to the very high friction between the solid polymer and the die surface and the coexistence of different morphological superstructures through the cross-sections of the extrudate [27]. Legros *et al.* [28] studied the effects of the processing conditions (additional use of lubricant, variation in the extrusion speed, use of a take-up device) of the ram extrusion on the properties of HDPE and PP rods. The experiments were performed at a barrel area/die exit area ratio of 6. The maximum draw ratio, $\lambda \sim 6$, was obtained with a low extrusion speed of 0.1 mm/s. At higher speeds, like at high extrusion temperatures, λ was markedly reduced for PP. For HDPE, the decrease in the draw ratio as a function of experimental conditions was less pronounced than for PP. An increasing draw ratio was accompanied with enhanced crystallinity, as expected. By the take-up device, the relaxation phenomena in the rod, after leaving the die, could be reduced. Note that this technique is nowadays well established for the manufacturing of various PTFE-based products.

Using hydrostatic extrusion [26], some drawbacks of ram extrusion can be circumvented. For example, the extrudate has a homogeneous reinforcing structure. In this process the polymer preform is pressed with the help of a hydraulic fluid through a conical die and the outcoming extrudate is pulled away (*cf.* Figure 5).
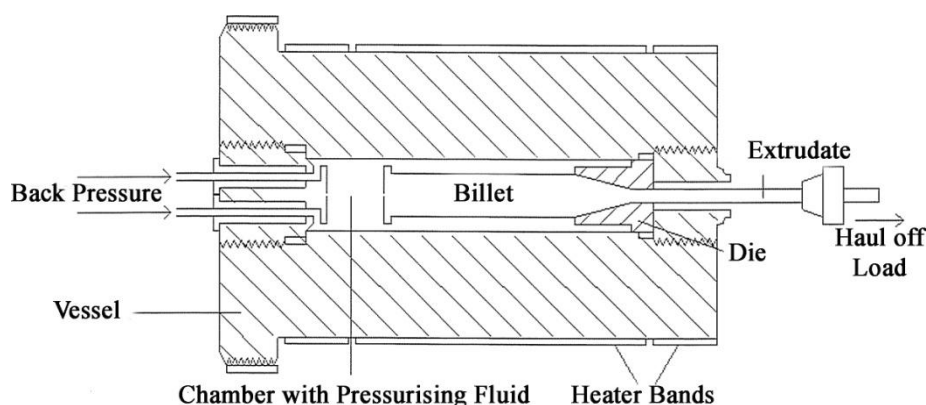
Figure 5. Working principle of the hydrostatic extrusion process schematically [26]

The hydrostatic extrusion was successfully adapted to manufacture high-modulus tapes and fibres even from filled (hydroxyapatite/PE) and reinforced polymers (discontinuous glass fibre-reinforced POM). Disadvantages of this process include discontinuous operation and the very high flow stress at the exit of the die. The polymer has the highest strain rates at the exit of the conical die, where the plastic strain is the greatest. The strain-rate sensitivity of flow stress in solid-state extrusion increases rapidly with plastic strain. As this situation incurs very high flow stresses as the polymer reaches the die exit, high extrusion pressures are therefore required [26]. The die-drawing, credited to Ward *et al.* [26], is a further development in this field. The change in the morphology due to the die/drawing is depicted schematically in Figure 6.
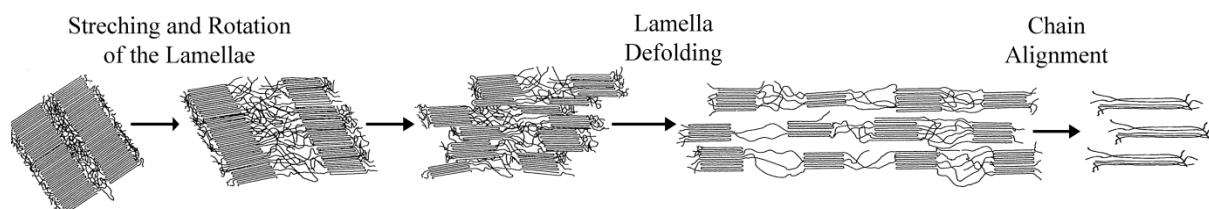

Figure 6. Scheme of chain orientation [3]

The advantage of the die-drawing is that the draw ratio can be set accordingly. This technique was used for different polymers, like PE [29], PP [30-31], PVC [26], PET [26], PEEK [26], PVDF [26] and POM [32]. Owing to the high molecular orientation, the related products exhibited pronounced improvements in the E-modulus, strength, barrier and solvent resistance. In addition, the extrudates were less prone to creep than the conventionally produced counterparts. This method is used to produce PE (gas, water) and PVC pipes (drainage) and PET containers (food storage) [26].

2.1.2.2. Super drawing

A two-stage drawing technique was applied to the super-drawing of PTFE virgin powder by Endo and Kanamoto [33]. In the first-stage, the compression-moulded PTFE film was solid-state coextruded (extrusion draw ratio (EDR) between 6 and 20) at 10°C below the T_m. The second-stage draw was made by applying a pin-draw technique in the temperature range covering the static T_m of PTFE. The maximum achieved total draw ratio was 160. The maximum tensile modulus and strength at 24°C reached 102±5 and 1.4±0.2 GPa, respectively.

2.1.2.3. Rolling

Rolling processes can induce a permanent deformation in the morphology by transforming the initial spherulitic structure to a fibrillar structure. This can be achieved by series of pairs of rolls (heated or not) and temperature-conditioning steps. Rolling is usually preferred for semicrystalline instead of amorphous polymers because the latter show more pronounced relaxation behaviour [26, 34]. PE and PP are used for room temperature rolling, whereby a thickness reduction ratio of up to ~5:1 can be reached. At high speeds (as high as 20 m/min), rolling occurs adiabatically. As a consequence, the chemical and thermal stability of the polymer should be considered. The rolling process increases the crystalline and amorphous molecular orientations and thus enhances both the strength and E-modulus of the polymer [35]. It is well known that the plastic deformation of crystalline polymers, especially upon drawing, is associated with cavitation. Cavitation, however, can be suppressed by applying compressive stress during orientational drawing. This was demonstrated by Polish researchers, whom developed a method called rolling with side constraints [36-39]. The materials used were mostly HDPE and PP. Galeski [40] reviewed the structure–property relationships in isotactic PP and HDPE produced by rolling with side constraints. Rolling was done in a specially constructed apparatus at various speeds (0.5-4 m/min for iPP and 200 mm/min for HDPE) and at different temperatures. Both the tensile modulus and ultimate tensile strength increased with increasing deformation ratio. The maximum strength/deformation ratio values were 340 MPa/10.4 and 188 MPa/8.3 for iPP and HDPE, respectively. Mohanraj *et al.* [41] prepared highly oriented polyacetal (POM) bars via a constrained rolling process. In this process, the heated polymer billet is deformed in a channel given by the circumference of the bottom roll, which provides lateral constraint to the material when it deforms. POM was rolled below the crystalline melting temperature. The

modulus and strength parallel to the rolling direction increased almost linearly with the compression ratio.

2.1.2.4. Gel drawing

Via gel drawing (spinning), films and fibres can be produced from dilute polymer solutions. This requires, however, a polymer with a high mean molecular weight and suitable molecular weight distribution characteristics. If the molecules are less entangled in the gel, this guarantees drawing to high degrees [42-44]. Oriented synthetic fibres of UHMWPE (Dyneema (www.dsm.com) and Spectra (www51.honeywell.com)) can be formed by gel spinning (gel drawing process) to have tensile strengths as high as 2.8 GPa. These fibres are mostly used to produce ballistic vests covers, safety helmets, cut resistant gloves, bow strings, climbing ropes, fishing lines, spear lines for spear guns, high-performance sails, suspension lines in parachutes etc. (tensile strength of the ballistic materials ~3.5 GPa).

2.1.2.5. Orientation drawing

Elyashevich and coworkers [45-46] prepared high-modulus and high-strength PE fibres via orientation drawing. Drawing took place between the glass transition (T_g) and melting temperature (T_m) of the given polymer. During orientation, the folded chain crystal lamellae rotate, break-up, defold and finally form aligned chain crystals (*cf.* Figure 6).

Fibres with very high orientation (draw ratio) were produced in one or more drawing steps. In the latter case, the isothermal drawing temperature was increased from one to the next drawing step. Elyashevich *et al.* [45-46] manufactured (with one-step orientation) PE fibres having an E-modulus and tensile strength of 35 and 1.2 GPa, respectively. Baranov and Prut [47] produced ultra high modulus PP tapes by a two-step isothermal drawing process. The isothermal drawing of the parent film was done in a tensile testing machine equipped with a thermostatic chamber. The first drawing occurred at 163–164°C, while the second one was at 165°C. The E-modulus and strength of the tapes were 30–35 GPa and 1.1 GPa, respectively. PP and PET tapes and strips are widely used for packaging purposes. Their tensile strength ranges are 220–350 and 430–570 MPa for PP and PET, respectively. Morawiec *et al.* [48] demonstrated that the strength of PET, even from scrap (recycled beverage bottles), may reach 700 MPa when suitable orientation conditions prevail. This was demonstrated using an on-line, two-step extrusion drawing unit. The structural "basis" of high-strength and high-modulus polymers is well reviewed by Marikhin and Myasnikova

[49]. This chapter helps the interested reader to also trace pioneering activities of researchers in the related fields.

Alcock *et al.* [50] produced highly oriented PP tapes by extrusion and drawing steps. The tensile deformation was achieved by pulling a tape from one set of rollers at 60°C through a hot air oven to a second set of rollers at 160–190°C. The tapes were classified into two series; Series A describes PP tapes drawn to varying draw ratios at the same drawing temperatures, while Series B covers PP tapes drawn to λ=13 at a range of drawing temperatures in the second drawing stage. The results showed that the density was approximately constant with an increasing draw ratio up to λ=9.3, above which it sharply dropped. The decrease in density was associated with a change in opacity of the tape due to the onset of microvoiding within the tape. Karger-Kocsis *et al.* [51] noticed that microvoiding in stretched iPP tapes takes place even at λ=10. In the study of Alcock *et al.* [50], the density reached 0.73 gcm^{-3} at λ= 17, which indicates an almost 20% reduction compared to the undrawn tape. PP tapes possess ∼15 GPa tensile modulus and ∼450 MPa tensile strength by a high drawn ratio (λ= 17).

2.1.2.6. Hot compaction

Ward *et al.* [52-53] developed a new method to produce SRPCs that they called "hot compaction". The related research started with highly oriented PE fibres and tapes. When these preforms were put under pressure and the temperature was increased, their surface and core showed different melting behaviours. This finding was exploited to melt the outer layer of the fibres and tapes, which after solidification (crystallization) became the matrix. The residual part of the fibres and tapes (*i.e.* their core section) acted as the reinforcement in the resulting SRPC (*cf.* Figure 7).
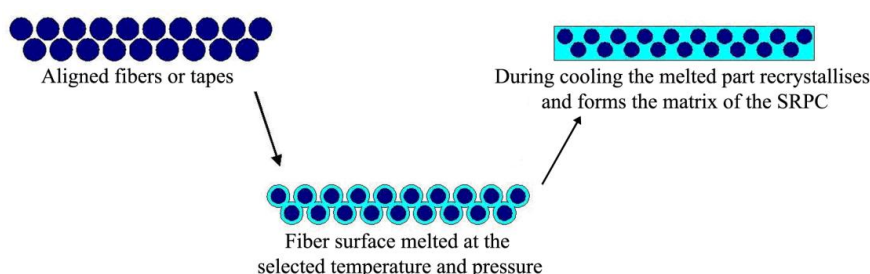

Figure 7. Principle sketch of hot compaction on the example of unidirectional (UD) arranged fibres [3]

It was found that hot compaction works well for semicrystalline, liquid crystalline and amorphous thermoplastics as well [54]. By hot compaction, different high-strength SRPMs

were produced from PET [55-56], PE [57-58], PEN [54], PA-6.6 [59], PPS [54], POM [60], PP [61], PMMA [62] and PEEK [54]. It is intuitive that the processing window during the hot compaction of single component polymeric systems is very narrow. When the compaction temperature approaches the melting temperature of the fibre, the transverse strength of composites with UD-aligned (*i.e.* 1D) reinforcement increases, albeit at a cost to the stiffness and strength measurable in the longitudinal direction [63] (*cf.* Figure 8). Figure 8 also displays the narrowness of the temperature range for the productions of SRPMs.
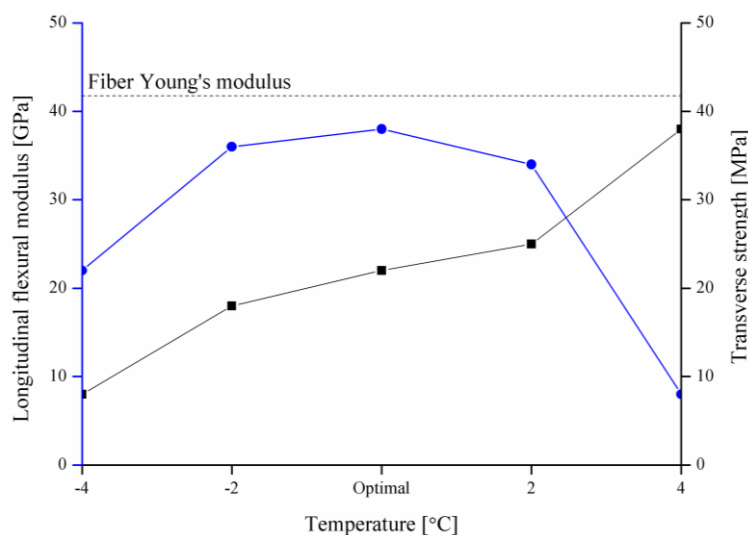

Figure 8. Longitudinal flexural modulus (●) and transverse strength (■) *vs.* compaction temperature of melt spun polyethylene fibres [3]

It was also reported that in order to set optimum mechanical properties, a given amount of the fibre should melt and work later as the matrix. This was given by ca. 10% of the cross-section (*i.e.* outer shell) of the fibre. This value is very closely matched with the amount that is required to fill the spatial voids between those fibres that adapt a hexagonal-like cross-section owing to the acting pressure. The hexagonal shaping of the initially spherical fibres along with the formation of a transcrystalline layer between the residual fibre (core) and formed matrix have been proven [63]. Ratner *et al.* [64] experienced an additional surface crosslinking during hot compaction of UHMWPE fibres. The surface of the fibres was coated by a solution containing peroxide prior to the hot compaction (T = 140–150°C, pressure: 31 MPa, time: 30 min). In this way, the stress transfer between the residual fibre (reinforcement) and the newly formed matrix has been improved compared to non-treated versions. Here it is appropriate to draw attention to the effect of the transcrystalline layer, which is controversial from the point of view of fibre/matrix adhesion. Though the development of the transcrystalline layer is necessary, its internal build-up may be of great

23

relevance, as outlined by Karger-Kocsis [65]. Ratner *et al.* [66] found that the crosslinked interphase between fibre and matrix is more beneficial than the usual transcrystalline one, especially when long-term properties like fatigue are considered. Hine *et al.* [57] produced SRPMs using fabrics (*i.e.* 2D reinforcement) composed of high-modulus PE fibres (E-modulus: 42 GPa). With increasing hot compaction temperature, it was established that the melted proportion of the fibres increased and the crystallinity of the formed matrix became markedly less than that of the initial fibres. A further important finding was that the processing temperature for 2D fabrics was higher than for UD (1D) aligned fibres. This is because an assembly of woven fabrics has more interstitial space to be filled with the matrix than a parallelized 1D fibre one. The quality of the related SRPM was measured by interlayer T-peel tests. The T-peel strength increased steeply with the matrix fraction (up to 30%) and reached a constant value afterwards.

Based on tensile tests and detailed morphological studies, the authors quoted that the final matrix content should be between 20 and 30% in order to set optimum properties for SRPMs from woven fabric layers. It was also emphasized that the processing window for 2D fabrics is even smaller than that for 1D fibres or tapes. However, UHMWPE loses its stiffness and strength and becomes prone toward creep with increasing temperature. To overcome this problem, the UHMWPE fibres were exposed to γ-irradiation to trigger their crosslinking [54]. Orench *et al.* [67] performed a comparative study on SRPMs produced from commercially available high-strength fibres and tapes (Spectra$^{®}$, Dyneema$^{®}$). Due to the low temperature resistance of PE, the hot compaction research shifted to PP [61]. This direction yielded new insights, such as that PP should be kept under high pressure during heating to the compaction temperature to prevent its thermal shrinkage.

Hine *et al.* [68] compacted PP tapes from fibrillated woven PP in both open and closed moulds. Based on flexural tests and morphological inspection, the optimum processing conditions were defined. Teckoe *et al.* [69] manufactured 2 mm thick sheets from woven fabrics consisting of high-strength PP fibres. The fabric layers were subjected to a 2.8 MPa pressure until the compaction temperature (varying between 166 and 190°C) was reached. This temperature was kept for 10 min before raising the pressure suddenly to 7 MPa and maintaining this during cooling to 100°C, when demoulding took place. At low compaction temperatures, the voids within the woven structure were not completely filled, while at high temperatures too much matrix was produced and thus the reinforcement content diminished. It was claimed that the final matrix content should be between 20 and 30% for good quality

products. It is worth noting that the heating of the related preform to the compaction temperature is accompanied by the release of its internal stress state. Due to the high pressure applied, the material melts under constraint conditions, so its melting occurs at a higher temperature than under normal conditions. This is the reason why the optimum hot compaction temperature is close, and even above, the usual melting under unconstrained conditions. Jordan and coworkers [70-72] studied the effects of hot compaction on the performance of PE and PP tapes and fabrics. The latter differed in their mean molecular weights, which influenced the consolidation quality assessed by tear tests.

Bozec *et al.* [73] investigated the thermal expansion of self-reinforced PE and PP containing 2D (*i.e.* woven fabric) reinforcements. Good quality products were received under the following conditions: PE: p = 0.75 MPa, T = 139°C; PP: p = 3 MPa, T = 183°C. The shrinkage, E-modulus and linear thermal expansion coefficient of the corresponding SRPMs were determined. It was reported that especially the PP systems were sensitive to changes in the compaction conditions. Hine *et al.* [74] devoted a study to determine whether the insertion of film layers between the fabrics to be compacted results in improved consolidation quality, as well as whether this "interleaving concept" can widen the temperature window of the processing. Note that this method is basically a combination of hot compaction and film stacking (to be discussed later). This strategy yielded the expected results: the consolidation quality was improved (well reflected in the mechanical property profile), the interlayer tear strength enhanced, and the processing temperature interval enlarged. This approach was also followed for PP fibres.

McKown and Cantwell [75] studied the strain-rate sensitivity of a hot-compacted, self-reinforced PP composite. The SRPP specimens were subjected to strain rates ranging from 10^{-4} to 10 s^{-1}. The SRPP composite showed similar characteristics to the neat PP material in respect to the stress–strain behaviour with increasing strain rate. Stiffening of the material in the elastic region was followed by enhanced yield stress and maximum stress with increasing strain rate. Parallel to that, the strain-to-failure was reduced. The failure mode of the SRPP composite was characterized by longitudinal fibre fracture with varying degree of inter-ply delamination over the dynamic tensile loading range studied. Prosser *et al.* [76] investigated the thermoformability of hot compacted PP sheets with 2D reinforcement (woven fabric). It was reported that the self-reinforced PP sheets experienced considerable work hardening, according to in-plane tensile tests performed at high temperatures (*cf.* Figure 9).
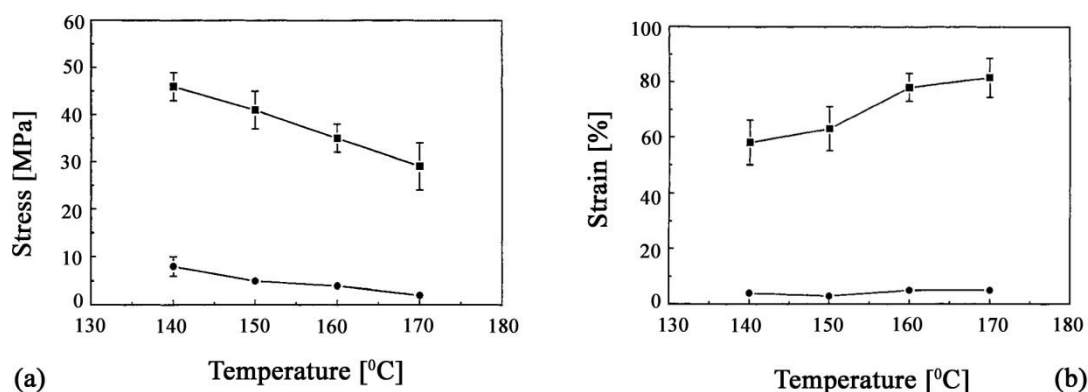
Figure 9. Effects of testing temperature on the stress-strain behaviour of self-reinforced PP with 2D reinforcement, schematically. (a) dependence of yield stress (●) and failure stress (■) on test temperature (b) Dependence of yield strain (●) and failure strain (■) on test temperature [76]

The authors observed that the optimum thermoforming temperature is very close to that of the melting of the matrix formed by recrystallization of the melted part of the parent fibre/tape. Romhány et al. [77] studied the fracture and failure behaviour of woven fabric-reinforced self-reinforced PP (Curv®), making use of mechanical fracture concepts and recording the acoustic emission during the loading of the specimens. The latter technique proved to be well suited to characterize the consolidation quality. Jenkins et al. [78] prepared a range of flat hot-compacted single-polymer composite panels from oriented PP and PE. The panels differed in their dynamic modulus and damping capacity values. SRPMs were subjected to mechanical excitation, allowing their acoustic frequency responses over the audio bandwidth to be measured. The results showed the correlation of mechanical and acoustic frequency response functions with the dynamic modulus, damping and specific modulus of the panel materials. The ideal combination of material properties to maximize the acoustic output of the panels was given by: high stiffness and low density to reduce the impedance of the panel and low damping to enhance the efficiency. One major goal of the hot compaction technology was to offer lightweight and easily recyclable thermoplastic composites to the transportation sector. As further application fields, sporting goods, safety helmets, covers and shells (also for luggage) were identified. Hot compacted PP sheets from woven PP fabrics are marketed under the trade name of Curv® (www.curvonline.com). As mentioned before, the hot compaction method was successfully transferred to many other polymers, like multifilament assemblies of PET and PEN [55, 79], PA-6.6 [59], POM and PPS [54], PEEK [54] and even PMMA [62]. Needless to say, the optimum compaction conditions are strongly material-dependent.

2.1.2.7. Production by film stacking

During film stacking, the reinforcing layers are sandwiched in-between the matrix-giving film layers before the whole "package" is subjected to hot pressing. Under heat and pressure, the matrix-giving material, that has a lower melting temperature than the reinforcement, melts and infiltrates the reinforcing structure accordingly. Recall that both the matrix and the reinforcement are given by the same polymer or polymer family. The film stacking procedure is highlighted in Figure 10.
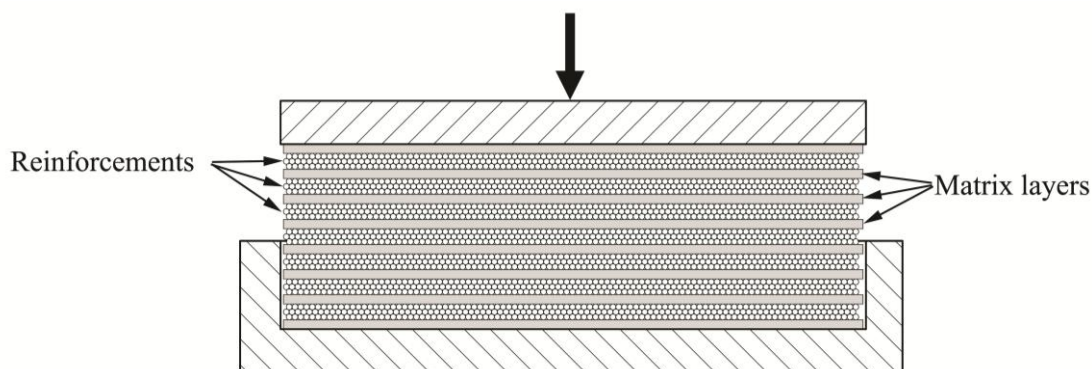

Figure 10. Scheme of the composite processing via film stacking [3]

The necessary difference in the melting temperatures between the matrix and the reinforcement can be set by using different polymer grades (*e.g.* copolymers for the matrix and homopolymers for the reinforcement, which per definition belongs to the multi-component SRPMs) or polymorphs (*e.g.* lower melting modification for the matrix and higher melting one for the reinforcement; this concept yields a single-component SRPM). It is of great importance to have a large enough difference between the melting temperatures of the composite constituents. Accordingly, the matrix-forming grade melts and wets out of the reinforcing structure without causing a temperature induced degradation in the stiffness and strength of the reinforcement, or at least keeping it at an acceptable level. Those thermoplastic systems, which can be used to produce single- and multi-component SRPMs via film stacking, are summarized in Table 1.

Composite	Matrix	Reinforcement	Processing temperature range (ΔT)
PE	LDPE	UHMWPE fibre	20-40°C
	HDPE	UHMWPE fibre	20-40°C
PP	β-PP*	highly oriented iPP fibre	20°C
	random PP copolymer	highly oriented iPP fibre	25°C
	iPP*	highly oriented iPP fibre	8-10°C
Polyester	PETG	PET fibre	40-60°C
	PETG	PEN fibre	15-20°C
	CBT[x]	PBT	60-80°C
LCP	LCP	LCP (Vectran® M)	25°C

Table 1. Possible polymer pairs to produce SRPMs; * single component SRPM; [x] production occurs via liquid composite moulding [3]

In the follow-up section, we shall treat only the single component SRPM versions. Bárány *et al.* [80-83] produced different PP-based SRPMs. For reinforcement, highly oriented fibres in different textile architectures (carded mat, carded and needle-punched mat, in-laid fibres in knitted fabrics) were used, whereas for matrices either PP fibres of lower orientation (the same textile assemblies as indicated above) or beta-nucleated PP films were selected. Note that some of the above preforms do not even contain interleaving films and thus do not fall strictly under the heading of film stacking. The matrix-giving phase in them is either a discontinuous fibre or a knitted fabric. Nevertheless, their consolidation occurs by hot pressing as in the case of film stacking. One consideration is that the melting temperature of the beta-modification of isotactic PP is more than 20°C lower than the usual alpha-form [84]. The beta modification can be achieved by incorporating a selective beta nucleating agent in the PP through melt compounding [85]. The concept of this alpha (reinforcement)/beta (matrix) combination should be credited to Karger-Kocsis [86]. The consolidation quality of the all-PP composites produced by Bárány *et al.* [87] was mostly studied as a function of processing conditions, *viz.* temperature. With increasing temperatures, the stiffness and strength increased and the resistance to the out-of-plane-type perforation impact decreases. The consolidation quality of the layered composite laminates could be well qualified by the interlaminar tear strength. Bárány *et al.* [81-82] later used PP fabric (woven type from split yarns) as the reinforcement and beta-nucleated PP film as the matrix-giving material. As mentioned above, the benefit of the beta-modification is the widening of the melting temperature range between the reinforcement and the matrix [88]. With increasing processing (pressing) temperature, the consolidation quality was improved. Parallel to that, the density, the tensile and flexural stiffness and the strength increased, whereas the penetration impact

28

resistance diminished. The authors proved by polarized light microscopy the presence of a transcrystalline layer between the PP reinforcement and PP matrix (*cf.* Figure 11).
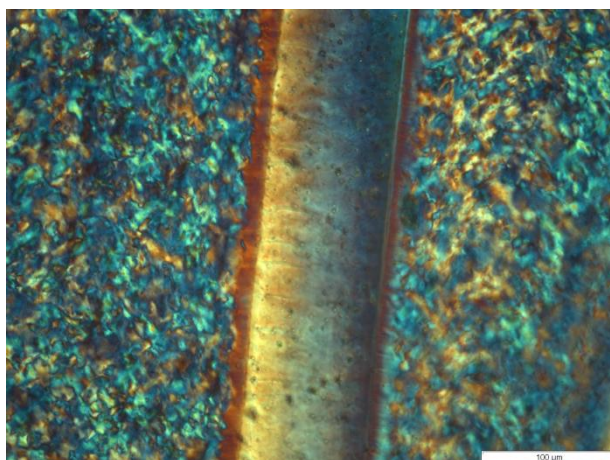

Figure 11. Transcrystalline layer of PP fibre and β-rPP matrix [3]

Izer and Bárány [83] manufactured all-PP composites by direct hot pressing of suitable textile assemblies. As indicated above, these assemblies contained both the reinforcement and matrix-giving phases in form of fibres with different orientations (draw ratios). Recall that the latter is the guarantee for a small difference in the melting temperatures, which was used in this case. Abraham *et al.* [89] produced all-PP composites with tape reinforcement by exploiting the difference in the melting behaviour of alpha and beta-polymorphs. The alpha-PP tapes were arranged in UD and cross-ply (CP) manners by winding, putting beta-nucleated PP films in-between the related reinforcing tape layers. The stiffness as a function of temperature of the corresponding composites was determined by dynamic mechanical thermal analysis (DMTA).

Bhattacharyya *et al.* [90] prepared an SRPM by combining hot compaction and film stacking. High tenacity PA-6 yarn was used as reinforcement, and PA-6 film (from pellets) was used as matrix. The yarn was subjected to annealing in a vacuum (3 h at 150°C) in order to get a higher melting point. Two yarn layers were sandwiched in between two matrix films and subjected to compression moulding at 200°C for 5 min under a pressure of 15 MPa. With the combination of these two techniques, good wetting properties were achieved and materials with excellent mechanical properties were produced. The tensile modulus and strength of the composites were improved by 200 and 300–400%, respectively, compared to the initial isotropic matrix film. An overview on the production methods, conditions and product characteristics of single-component SRPMs produced in multi-step (*ex-situ*) processing is given in Appendix Table 6. – *cf.* Figure 1.

2.2. Multi-component SRPMs

SRPMs can also be produced by the combination of polymers that belong to the same family of polymeric materials. The major goal during their preparation is the achievement of good adhesion (bonding) between the reinforcing and matrix-giving polymer phases. Like the single-component SRPMs, the reinforcing structure may be generated in single- (in situ) or multi-step (*ex-situ*) operations. Accordingly, a similar grouping as before can also be followed here. Next, the different variants will be briefly introduced.

2.2.1. Single-step (in situ) production

2.2.1.1. Multi-component extrusion yielding self-reinforced structures

The extrusion die with a convergent section allowed us to set a unidirectional (1D) molecular alignment in situ, which will work as the reinforcement owing to the supermolecular structure formed by the crystallization. Chen *et al.* [91] solved the problem of biaxial orientation (2D), however, by using a specially designed fish-tail shaped (bi-cuneal shape) extrusion die, as depicted in Figure 12.
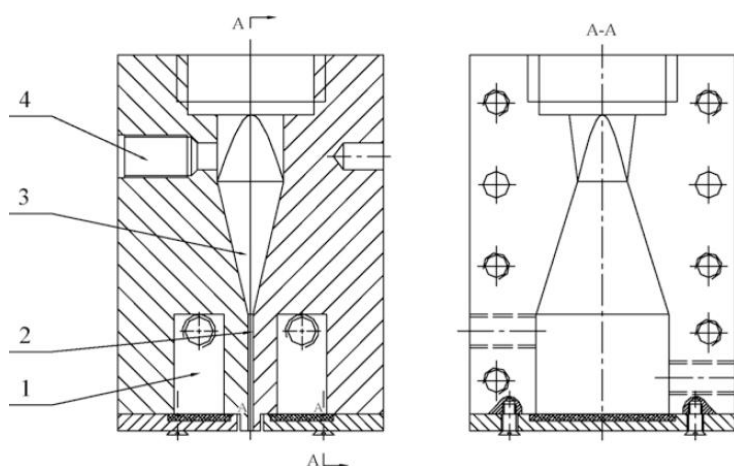

Figure 12. Schematic representation of the self-reinforcing sheet extrusion die: (1) temperature controlling oil bath, (2) the straight section, (3), the convergent section, and (4) double functional temperature–pressure sensor [91]

Composites with planar reinforcement were produced via this die from HDPE and HDPE/UHMWPE blends using a single-screw extruder. The mould temperature was controlled with oil (T = 126–137°C), and the optimum processing pressure was between 15 and 30 MPa. Under conventional extrusion conditions, the tensile strength of the extruded sheet was comparable to conventionally moulded HDPE samples. The tensile strength was

almost the same in both the machine (MD) and the transverse directions (TD). The tensile strengths of the HDPE/UHMWPE in the extrusion and transverse directions were six and three times higher, respectively, than those of the related traditionally produced sheet (HDPE).

2.2.1.2. Multi-component SCORIM/OPIM

Zhang *et al.* [92-93] processed LDPE/HDPE and HDPE/PP blends by the earlier introduced OPIM technique (oscillation frequency: 0.3 Hz). It was established that with increasing LDPE content the tensile strength diminishes, whereas the toughness increases for the LDPE/HDPE blends. Morphological studies confirmed the onset of a shish-kebab-type supermolecular structure. The tensile strength of the HDPE/PP blends could also be markedly increased (fivefold) when the PP content remained below 10 wt%. Zhang *et al.* [94] investigated the performance of HDPE/UHMWPE when processed by the SCORIM technique. Tribological tests showed that the wear resistance of the related system was ca. 50% better than that of traditionally molded specimens. Appendix Table 7 displays the production methods, conditions and product characteristics of multi-component SRPMs produced in single-step (in situ) processing - *cf.* Figure 1.

2.2.2. Multi-step production

The first publication of this processing version should be credited to Capiati and Porter [95]. They combined HDPEs with different melting characteristics. The high modulus fibres (reinforcement) melted at 140°C, while the matrix-giving HDPE melted at 131°C. The HDPE fibre was embedded in the melted HDPE using a special rheometer. After cooling/solidification, the fibre in this single-fibre reinforced composite was subjected to a pull-out test. It was reported that the interfacial shear strength was comparable with that of the glass fibre/epoxy system. Moreover, the presence of a transcrystalline layer was detected at the fibre/matrix surface.

2.2.2.1. Consolidation of coextruded tapes

The development of SRPMs is best reflected by searching for options that amplify the difference between the melting of the reinforcement and the matrix. Recall that this range was highly limited for hot compaction. Peijs [96] developed a coextrusion technique for which the melting temperature difference between the composite constituents reached 20–30°C. The invention was to "coat" a PP homopolymer tape from both sides by a copolymer through a

continuous coextrusion process. Note that a copolymer melts always at lower temperatures than the corresponding homopolymer, owing to its less regular molecular structure. The coextruded tape was stretched additionally in two-steps (*cf.* Figure 13).
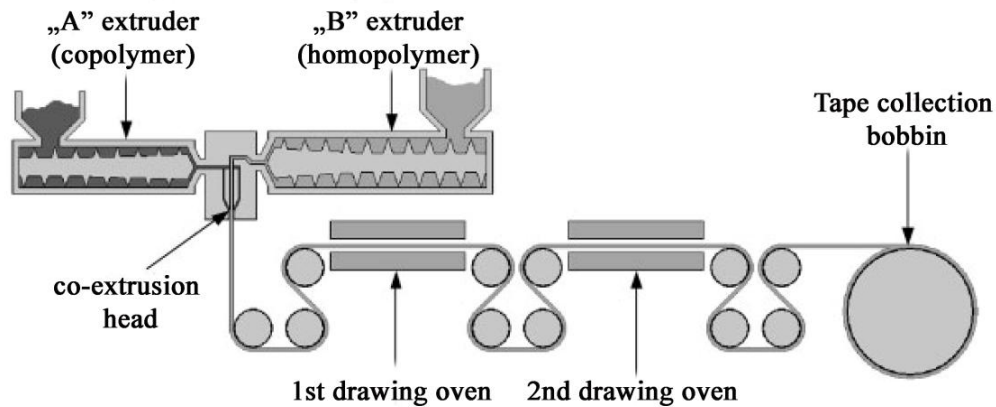

Figure 13. Co-extrusion technology with additional stretching to produce high-strength tapes [97]

This resulted in high-modulus, high-strength tapes. The primary tapes could be assembled in different ways: as in composite laminates (ply-by-ply structures with different tape orientations, such as UD (*cf.* Figure 14) and CP) or integrated in various textile structures (*e.g.* woven fabrics).
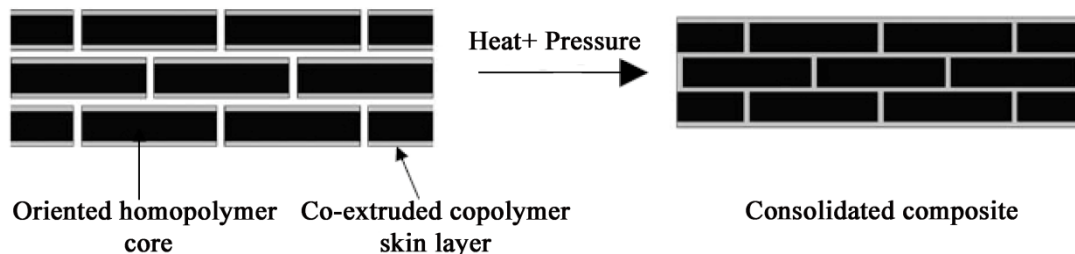

Figure 14. Production of composites with UD tape alignment from coextruded tapes [3]

The consolidation of the related assemblies occurred by hot pressing. The advantage of this method is that the reinforcement (core) content of the tape may be as high as ca. 80%. This, along with the high draw ratio, yielded tapes of excellent mechanical properties (E-modulus > 6 GPa, tensile strength > 200 MPa). Cabrera *et al.* [98] prepared all-PP composites from UD and woven fabric assemblies of coextruded tapes. For the consolidation of the UD composites, a 17 MPa pressure was used and the temperature covered the range between 140 and 170°C. The time was kept constant (15 min) during hot pressing. The E-modulus of the laminates, measured both in the tape direction and transverse to it, was not much affected by the processing temperature. In contrast, the interlaminar tear strength was improved by

increasing the temperature, well reflecting the improvement in the consolidation quality. The woven fabric-reinforced composites were subjected to falling dart (perforation impact) tests. Based on the related specific (*i.e.* thickness-related) perforation impact energy data, the all-PP composites outperformed both the glass fibre (GF) mat- (three times higher) and flax mat-reinforced counterparts (six times higher). Alcock *et al.* [99] manufactured UD composite sheets by winding the coextruded tapes on a metallic frame that was later put in-between the plates of a press operated in the temperature interval of T = 140–160°C.

The properties of the composites were determined in mechanical investigations, whereas the reinforcement content (reaching 90 wt%) was determined via microscopic investigations. As usual, for all UD-reinforced composites, both the tensile E-modulus and strength decreased with increasing angle between the reinforcing and loading directions (off-set) during their testing. The transverse compressive strength (10 MPa) was not affected by the pressing temperature. The results received were compared with those measured on 50 wt% UD GF-reinforced PP composites. Although the UD-GF PP composite performed better than the all-PP material, the latter took the lead with respect to the related specific (*i.e.* density-related) properties. In follow-up studies, Alcock *et al.* [97, 100-103] investigated the structure–property relationships in all-PP composites produced from woven fabrics composed of coextruded tapes. When the consolidation took place at low temperatures (T = 125°C) and under low pressures (p = 0.1 MPa), the sheets exhibited excellent resistance to the perforation impact. This was traced to an intensive delamination between the fabric layers that was triggered during this high-speed perforation process.

Up to a 2 mm sheet thickness, the perforation energy increased linearly with the sheet thickness. Ballistic test results confirmed that the performance of composite sheets from Pure® tape is comparable with that of the state-of-art ballistic materials. The authors draw attention to the fact that the mechanical performance of the all-PP composites, which contain fabrics of coextruded tapes, can be optimized upon request by selecting suitable textile architectures and hot pressing/consolidation parameters (pressure, temperature). Barkoula *et al.* [104] investigated the fatigue performance of PP tapes and woven tape fabric-reinforced all-PP composites. They found that the endurance limit (or fatigue threshold, below which no fatigue-induced property reduction occurs), controlled by the onset of delimitation, is strongly affected by the processing temperature. The fatigue threshold of the optimum processed composite was at 65% of the static tensile strength. This is markedly higher than that of GF mat-reinforced PP composites, which show a range of 30–40% [105]. Banik *et al.* [106-107]

studied the short-term creep performance of coextruded tape-reinforced PP composites with both UD- and CP-type tape lay-ups. The related sheets were produced by vacuum bagging in an autoclave (which is almost exclusively used for thermoset composite production) under a 2.4 MPa pressure and at T = 138°C. The flexural creep tests were performed in a DMTA device in the temperature range of 20–80°C. It was reported that the creep depends on the composite lay-up. By adopting the temperature-time superposition principle to the short-term creep results, a master curve was constructed that predicted the long-term creep at a given temperature.

Kim *et al.* [108] also studied the creep response of all-PP composites and emphasized that small changes in the processing conditions have a pronounced effect on the creep behaviour. It is noteworthy that composites from coextruded PP tapes in different assemblies were produced by various techniques, such as hot pressing, tape winding [109], stamp forming and vacuum bag/autoclaving [110-111]. Moreover, the related sheets were used for the face-covering of different sandwich structures with cores including honeycomb structures and foams. The face sheeting occurred with or without additional primer [112]. Recall that the coextruded PP tapes are known under the trade names of Pure® and Armordon® (www.purecomposites.com; www.armordon.com).

2.2.2.2. Film stacking

This technique is usually used for SRPMs in which the constituents are from the same polymer family. Shalom *et al.* [113] produced high-strength PE fibre- (Spectra®) reinforced HDPE composites by winding the fibre in a unidirectional manner and sandwiching the HDPE films in-between the wound fibre layers. The reinforcing fibre content in the UD assembly was 80 wt%. Its consolidation occurred by hot pressing (T = 137°C, p = 16.5 MPa). Samples were subjected to tensile tests with variation of the loading direction in respect to the UD fibre alignment (off-axis tests). As expected, the tensile modulus, yield stress and resistance to fracture were all higher when the off-axis angle was smaller. Houshyar and Shanks [114] used a mat from PP homopolymer fibres as the reinforcement (fixed at 50 wt%) and PP copolymer film as the matrix-giving material. The difference in their melting temperatures was ca. 16°C according to DSC results. The fibre diameter in the mat was varied. The hot consolidation occurred between 155 and 160°C. It was found that with increasing diameter of the mat fibres, both the stiffness and the strength of the composites increased. The surface of the homopolymer PP fibre acted as a heterogeneous nucleator and initiated transcrystalline growth. In follow-up studies [115-116], it was demonstrated that

with increasing diameter of the reinforcing PP fibre, the void content in the composite can be reduced. The maximum strength was reached when the diameter of the fibre was ca. 50 µm. The creep results of the related composites, which were also modelled by the Burgers model, demonstrated that increasing reinforcing fibre content was accompanied by increasing resistance to creep.

The objective of further studies of the Shanks' group [117-118] was to deduce possible effects of different textile architectures (covering both non-woven and woven ones) on the mechanical properties of the related all-PP composites. During the consolidation, they were subjected to a low pressure (ca. 0.01 MPa) at T=158°C for 15 min. The mechanical results showed that the properties of the woven composites strongly depend on the woven geometry. The composite with the satin cloth delivered the best properties. This was due to the advantages of the satin parameters, such as the long float length, high fibre content, few interlace points and loose pattern. It is noteworthy that the authors used the term "compaction" even though this is reserved for those techniques in which a part of the reinforcing phase becomes melted and thus overtakes the role of the matrix after cooling. This is not the case in film stacking, where the melting temperature of the reinforcing fibre or tape is usually not surpassed. In order to improve the energy absorption capability of the resulting composites, Houshyar and Shanks [119] modified the matrix. This was done by extrusion melt compounding of the matrix-giving PP copolymer with ethylene-propylene rubber (EPR; up to 30 wt%) with follow-up sheeting.

Bárány *et al.* [120] prepared composites using random PP copolymer films and carded and needle punched mats as matrix and reinforcing phases, respectively. The nominal reinforcement content was 50 wt%. The consolidation was performed at different temperatures in the range of T=150–165°C. Consolidation at 150°C resulted in poor performance, whereas that above T=165°C did not yield additional property improvement. Bárány *et al.* [81-82] also studied the perforation impact resistance of all-PP composites containing fabrics woven from highly stretched split PP yarns as reinforcement and films composed of both alpha and beta-phase random PP copolymers as matrix-giving materials. The beta-modification was produced by using a selective beta-nucleant (Calcium salt of suberic acid (Ca-sub)). The perforation impact resistance of the composite with beta-nucleated random PP copolymer was higher that the alpha variant. Izer and Bárány [121] estimated the long-term flexural creep of self-reinforced polypropylene composites based on short term creep tests performed at different temperatures. An Arrhenius-type relationship

was used to shift the related creep data along the time axis. It was found that with improved consolidation (increasing processing temperature) the creep compliance decreased. Moreover, good correlations were found between the creep compliance and density and between the creep compliance and interlayer peel strength.

Abraham *et al.* [89] produced high-strength alpha PP homopolymer tapes by a single-step hot stretching technique and used this as UD or CP reinforcement in alpha- and beta-phase random PP copolymer matrices. The interphase between the reinforcement and matrix was composed of a transcrystalline layer that was larger in the beta- than in the alpha-phase random PP copolymer matrix. This finding was traced to the fact that the composite with beta-nucleated matrix performed better than the alpha version. Kitayama *et al.* [122] produced SRPMs from PP homopolymer fibres (reinforcement) and a random PP copolymer (matrix) by film stacking and studied the interphase formed. Here, a transcrystalline layer was resolved, the structure of which changed with the consolidation temperature (*cf.* Figure 15).
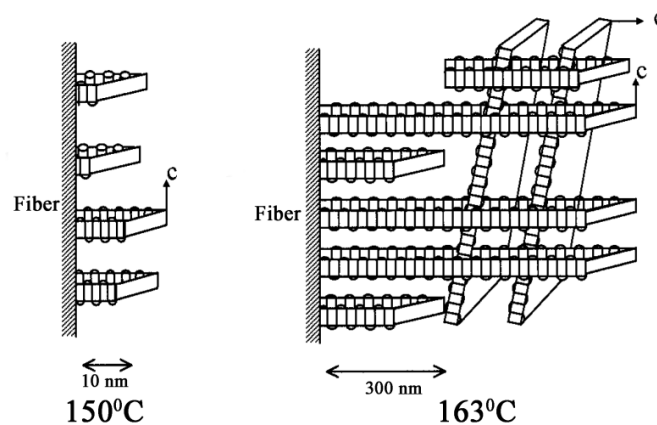

Figure 15. Lamellar structure within the transcrystalline layer as a function of the consolidation temperature [122]

The lamellar structure, depicted in Figure 16, can be stretched upon loading without detaching from the surface of the reinforcing PP homopolymer fibre, which is very beneficial in composites. Recall that the lamellar structuring in the transcrystalline layer for optimum stress transfer from the matrix to the fibre, proposed by Karger-Kocsis *et al.* [123], is very similar to that in Figure 15 (*cf.* Figure 16).
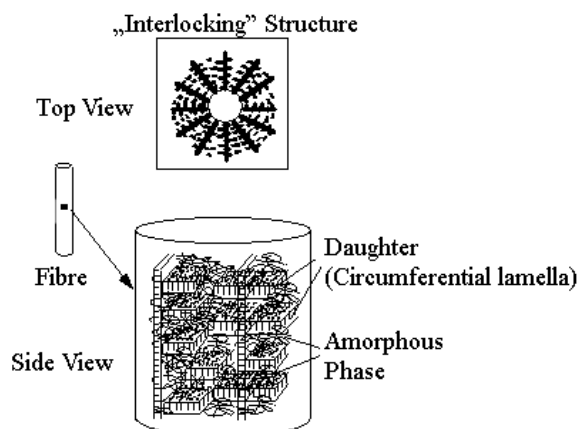
Figure 16. Hypothesized interphase with lamellar interlocking and amorphous phase as adherent for the transcrystalline layer initiated by flat-on type lamellar growth on fibre surface [123]

The recycling via melt processing of one- and two component all-PP composites has already been topic of investigations [124]. Ruan *et al.* [125] manufactured nanoparticle-filled self-reinforced PP composites, for which they used fumed SiO_2 as the nanoparticle. The nanoparticles were preheated at 140°C under vacuum for 5 h. Then, the mixture of monomer (butyl acrylate) and the nanoparticles and a certain amount of solvent was irradiated by 60Co -ray in air at a dose rate of 80 kGy. The resultant, poly(butyl acrylate) (PBA) grafted nano-SiO_2 (SiO_2-g-PBA) with a percent grafting of 3.35%, was used for the subsequent composite manufacturing. Untreated or treated nano-silica was melt compounded with iPP at 180°C in the mixer. The content of nanosilica in all of the composites was 1.36 vol%. The sheets of SiO_2/PP were produced by hot pressing, and then the sheets were hot drawn under a temperature slightly lower than the melting temperature of PP (150°C) at a constant velocity. A film with a thickness of 0.05 mm was blown from the random PP copolymer by extrusion film blowing. Finally, the stretched sheets were film-stacked with copolymer films by a specially designed mould and were hot pressed at different processing temperatures (T = 150–175°C) and holding pressures (p = 2.0–5.0 MPa) for a constant holding time of 10 min. According to the mechanical properties reported, the incorporation of nanoparticles into the polymer matrix improved the mechanical properties of the self-reinforced composites.

Pegoretti *et al.* [126-128] used thermoplastic liquid crystalline polyester fibres for both the reinforcement (Vectran[®] HS, T_m = 330°C) and the matrix (Vectran[®] M, T_m = 276°C). Unidirectional composites were prepared in a two-stage process. At first, both Vectran[®] M and HS as-received fibres were wound on an open metal frame, and after winding the LCP was consolidated in a hot press. An optimum processing temperature of T = 275°C was

deduced and was associated with the lowest void content and highest mechanical strength. Matabola *et al.* [129] used PMMA electrospun nanofibres as reinforcement and PMMA foil as matrix material. Composite structure was hot pressed following film-stacking method. Processing temperature of 150°C was adequate for the preparation of a good composite. Dynamic mechanical tests were performed in a DMA device. The results showed that the composites generally showed an improvement in compared to the neat PMMA matrix. The increases in the stiffness (up to 83%) and glass transition temperatures (up to 10°C) of the composites were pronounced in the case of a 10 wt% nanofibre loading.

Chen *et al.* [130] prepared self-reinforced PET composites with film-stacking method. For the composite biodegradable polyester matrix and PET yarn applied. Results showed that the self-reinforced PET composite display significant improvement in their tensile, flexural, and impact properties when compared to the polyester matrix material. The absorbed impact energy of the best composites was 63 times that of pure polyester resin. Wu *et al.* [131] investigated self-reinforced PET composite with biodegradable polyester matrix also. Appendix Table 8 lists the production methods, conditions and product characteristics of multi-component SRPMs produced in multi-step (ex situ) processing - *cf.* Figure 1.

2.3. Fibre reinforced polymer composites by conventional injection moulding

The injection moulded products can be filled and reinforced with natural and artificial fillers (*e.g.* glass beads, wood, carbon black, carbon nanotube) and reinforcement (*e.g.* glass, carbon, basalt fibre) to change the properties of the raw material (thermoplastic matrix (*e.g.* PP, PA)). Using these materials the mechanical properties (impact and abrasion resistance, stiffness, antistatic behaviour and strength) can be increased and the shrinkage, heat expansion can be decreased [132-133].

The number of the publications about the injection moulded fibre reinforced composites is very numerous and articles about the injection moulded self-reinforced (or all-polymer) composites with multi component have not been published yet. In this chapter general properties of the (glass) fibre reinforced composites produced by injection moulding technique will be summarized.

2.3.1. Shrinkage and warpage of the injection moulded products

The dimensional accuracy is the one of the most important property of the injection moulded products. Shrinkage means the decreasing dimension under the cooling while the warpage means the deformation of the product which is caused by shrinkage on different areas. Shrinkage depends on the applied materials, processing parameters and the mould (product) geometry. Two types of shrinkage can be separated. The first is a linear (depends on the mould geometry) and the second is the volumetric shrinkage (forecast of the sink mark). The shrinkage (S_i) of the injection moulded products can be calculated with the following equation [134]:

$$S_i = \frac{L_M - L_i}{L_M} \cdot 100 \ [\%],\tag{1}$$

where the L_M is the mould and the L_i is the product linear measure on defined place.

The shrinkage depends on time therefore three phases can be separated in time. The first is the in-mould shrinkage, the second is the technological (as-mould) shrinkage which is interpreted after the mould opening (~1 h) and the third is the post shrinkage which is caused by long-term post-crystallization, aging, and other morphological effects. The non-uniform shrinkage and warpage are reducible to the different shrinkage in flow and transversal direction (caused by different orientation (Figure 17)), non-uniform cooling, material anisotropy and thermal stresses which caused by geometry.
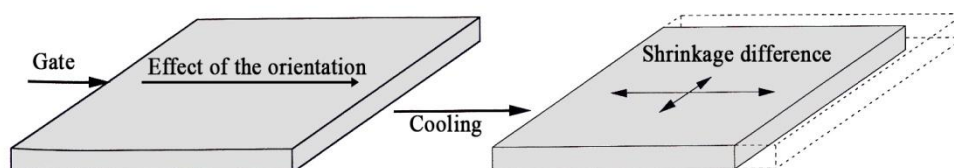

Figure 17. Effect of the orientation on the shrinkage [134]

In the injection moulded products skin-core structure usually forms by the melt flow which makes the fibre orientation different through the cross section (Figure 18).
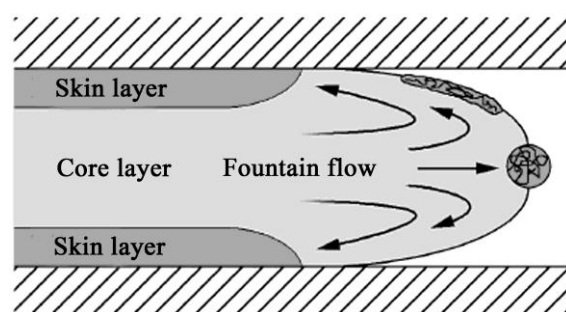
Figure 18. Skin-core structure under injection moulding [134]

Shrinkage can be reduced in many ways. The most important alternatives are the followings: increases of the holding pressure, even of the wall thickness; tube or rib and gate configuration; optimizing injection points, application of constant mould temperature and use of filler materials. Due to material morphology shrinkage could vary, high crystallinity shows higher shrinkage effect because the volume difference of the melt and solid (order) phase is high. The publications are shown that using reinforcements (*e.g.* glass fibres) the shrinkage in flow direction can be decreased, much more than in cross flow direction [135]. The warpage is increased with shrinkage difference [134, 136-137] which can be decreased with optimizing the processing parameters [138-139].

2.3.2. Effect of the fibre length and content on the properties of injection moulded fibre reinforced composites

Advantage of the fibre reinforced thermoplastic polymer composites is the better strength/weight and stiffness/weight ratio compared to the metals. The properties of the thermoplastic polymer composites are influenced by the length and concentration of the applied reinforcement. As reinforcement material short (fiber length = 0.2-0.4 mm) and long fibre (fibre length = 3.0-6.0 mm) can be applied [140]. Thomason *et al.* [141-143] demonstrated that using long (initial length=12.5 mm) glass fibre and PP matrix significant improvements in (room temperature) tensile and flexural strength and unnotched impact resistance could be achieved. Long fibre reinforced PP shows increasingly higher modulus over Short fibre reinforced PP as the strain is increased. The applied fibre contents (0-73 wt%) show that the modulus of the composites increases linearly with fibre volume fraction. Strength and notched impact performance show a maximum in the 40-50 wt%. It was found that the fibre content increases as the average fibre length decreases. Kumar *et al.* [144] used 3, 6 and 9 mm pellets to produce long fibre reinforced composite for injection moulding.

Results demonstrated that flexural strength, stiffness and impact strength increased by increasing fibre length.

The biggest disadvantages of the glass fibre reinforcement are the fibre breaking (under the process), abrasion load to the screw, nozzle and mould. Achievable reinforcing efficiency depends on the following parameters [140, 145-146]:

- Available fibre,
- Critical fibre length (calculated from Kelly-Tyson relation),
- Fibre orientation.

Aspect of the technology, skin-core structure (fibre orientation) is very important. Fibre direction in the skin layer is parallel to the flow direction while in the core region it is distributed perpendicular to the flow.The parameters of the technology affect the skin-core structure. When the filling time is short thus the injection speed is high thin skin layer can be achieved.

2.4. Summary of the literature, aims of the dissertation

The literature overview confirmed that the literature of the self-reinforced polymer materials and composites is very wide. The self-reinforced polymer materials have been intensively explored for a long time but it has not yet been grouped. Besides the achieved results (mechanical properties, reinforcing directions/dimensions etc.) with different processing techniques cannot be summarized. Consequently a new grouping of the self-reinforced material could be made which has not yet been published. From the applied components two large groups (single and multi-component SRPMs) can be made. These groups can be separated in many small subgroups which show the steps of the material/composite production and the dimension of the evolved reinforcement structure. From the literature it can be concluded that the reinforcing part in the materials can be assured by molecular orientation (molecular chain orientation and defrosting) or with pre-oriented structure (*e.g.* highly oriented PP fibre). Using molecular orientation technique self-reinforced product can be directly produced in pre-set direction (using *e.g.* hydrostatic or self-reinforced extrusion).

To produce pre-oriented structure (number of related articles is the highest) hot compaction, consolidation of coextruded tapes and film-stacking methods are widespread. In hot compaction technique oriented thermoplastic fibers were used and laid to a metal mould. Putting these preforms under pressure and temperature, their surface and core showed

different melting behaviour. This finding was exploited to bring the outer layer of the fibers and tapes into melt, which after solidification (crystallization) overtook the role of the matrix, whereas their residual part (*i.e.* core) acted as the reinforcement in the resulting composite. The product of this technique has very good mechanical properties. The disadvantage of this method is the narrow processing window (3-5°C) which requires a highly controlled production. This technique was initially developed for melt-spun polyethylene fiber and later adapted to practically all fiberforming semicrystalline thermoplastics (*e.g.* PE, PP, PET, PA66 *etc.)* from which fibers can be produced.

To enlarge the processing window of hot compaction and thereby to improve consolidation coextrusion and film-stacking techniques were developed. With coextrusion the invention was to "coat" a PP homopolymer tape from both sides by a copolymer through a continuous coextrusion process. Note that a copolymer always melts at lower temperature than the corresponding homopolymer owing to its less regular molecular structure. The coextruded tape was stretched additionally in two-steps. This resulted in high-modulus, high-strength tapes. The primary tapes could be assembled in different ways: as in composite laminates (ply by ply) structure with different tape orientation, such as UD or integrated in various textile structures (e.g. woven fabrics).

The third method to improve the consolidation was the film-stacking. During this technique the reinforcing layers are sandwiched in between the matrix-giving film layers before the whole "package" is subjected to hot pressing. Under heat and pressure the matrix, having lower melting temperature than the reinforcement, melts and infiltrates the reinforcing structure accordingly. Recall that both matrix and reinforcement are given by the same polymer or polymer family. The advantage of these methods is an enlarged processing window from the viewpoint of the temperature (20-40°C).

The achived results of the different (*in-situ*; *ex-situ*) techniques are concluded in the appendices in tabular form. The main disadvantages of the developed techniques are the design problems (*in-situ* techniques) of the reinforcement phase in the product and the strongly limited forms (only thermoformed products with constant wall thickness, e.g. shells, panels etc. (*ex-situ* techniques)).

Processing technique to produce self-reinforced/all-polymer composites with multi component (matrix-reinforcement) and conventional material (e.g. polypropylene) in large-scale (*e.g.* with injection moulding) have not yet been developed. Analysis of the suitable pre-

products for injection moulding has not yet been published as well. Based on the above the aims of this PhD thesis are the followings:

- Development of all-polypropylene composites for injection moulding and determine suitable material (matrix-reinforcement) pairs.
- To determine the effect of the processing parameters (type of gate and nozzle, temperature) on the properties of the injection moulded composites.
- To determine the effect of wider processing window (by selecting matrix material with lower melting temperature) on the properties of the injection moulded composites.
- To analyse the shrinkage behaviour of the injection moulded all-PP composite specimens.

3. Experimental part

In this chapter at first the preliminary tests (for determine the applicable materials and develop the processing technique) and thereafter the used materials, their processing, and the applied testing methods are described. Finally the results of the all-polypropylene composites are analysed.

3.1. Preliminary tests

In the pre-experiments two kinds of material pairs were selected. The first aim was to assure the different melting temperature between the matrix and reinforcement. The material combinations were the followings (matrix/reinforcement):

   a) Random polypropylene copolymer (TVK Tipplen R959A, Hungary) / Highly oriented homo-polypropylene multifilament (Innegra Technologies, Innegra S, USA)

   b) Random polypropylene copolymer (TVK Tipplen R959A, Hungary / Borealis RJ470MO, Austria) / Highly oriented homo-polypropylene multifilament (Stradom S.A., Poland)

Each kind of reinforcement was tested with morphological (Differential Scanning Calorimetry (DSC)), mechanical tests (tensile tests on single fibres according to the EN ISO 527 standard, the cross-head speed was set to 5 mm/min, and each test was performed at room temperature (24°C); at least 60 single fibres from each material were tested). The sizing agent of the single fibres surface was tested by Energy Dispersive X-Ray Spectroscopy (EDS). The matrix materials were characterized by DSC (from the first melting curve, 10°C/min). These results show that the difference between the melting temperatures of the materials is higher than 20°C. It was pointed out by EDS tests that there is sizing agent on the fibre surface except for the Stradom hPP fibres (*cf.* Figure 19).
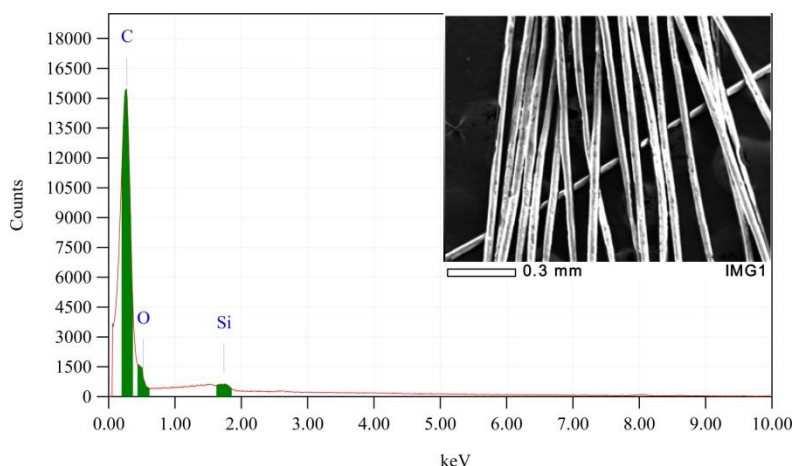
Figure 19. EDS test on the highly oriented hPP fibres (Stradom S.A.)

3.1.1. Mixing method

In the first series to produce pre-product for injection moulding mixing technology was applied. Polypropylene in pellet and powder form was mixed with the highly oriented polypropylene multifilament by powder mixer (Thyssen Henschel FMA10). The mix was subsequently injection moulded at 160°C with an Arburg Allrounder 320C machine. The results showed that the hPP multifilament became roughened and formed agglomerates (due to electrostatic charge), and a cold slug formed that blocked the standard flat nozzle, which has 2 mm diameter holes. The reinforcement fibre content could not be guaranteed, and even distribution of reinforcement fibres could not be achieved. In the next step new pre-product material was developed.

3.1.2. Extrusion coating method

To avoid agglomeration of reinforcing fibres, extrusion coating was developed and applied prior to injection moulding in the second series. One or two bobbins of multifilament (hPP) were used, and these were continuously coated in a special extrusion (based on the electric cable coating method) die by melted matrix material (rPP) (Figure 20). The plan of the developed die can be seen in Appendix (Figure 80).
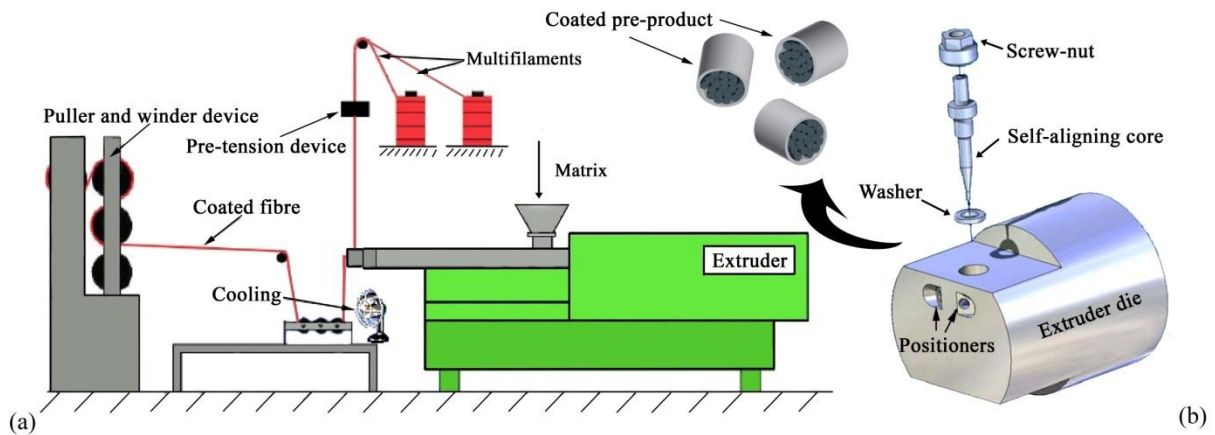
Figure 20. Scheme of the coating system (a) and the cylindrical shaped pellets with extruder die (b)

During the process coated multifilaments could be produced until 40 wt% reinforcement content. The coated multifilament was granulated into 1-10 mm long cylindrical pellets and used for injection moulding (Figure 21).
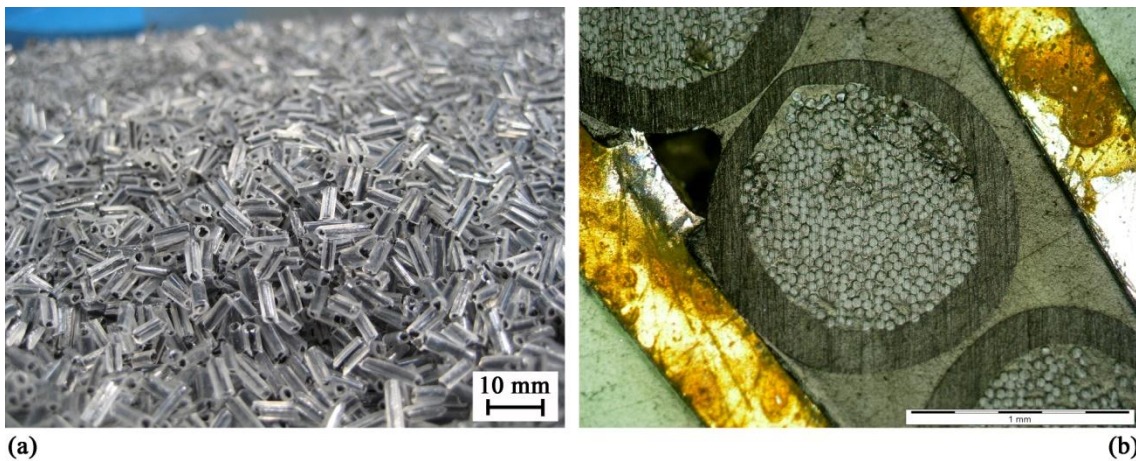

Figure 21. 10 mm long cylindrical pellets for injection moulding (a) and the cross section of the pellet (b)

The PP-based pre-product could be injection moulded (using heated flat nozzle which had 4 mm hole diameter), and the results showed that the thermoplastic reinforcement did not melt in the core section of the specimens during manufacturing (Figure 22). However, in the skin section of the specimens melted fibres could be detected which was caused by the shear heat.

**Figure 22. Single fibres in the dumbbell specimens of the all-PP composite
(fibre content was ~10 wt%)**

During the injection moulding of PP-based pre-product different parameters (applied processing temperature and fibre length) were analysed. Firstly, the effects of the applied processing temperatures (nozzle temperature was 150, 160 and 170°C) were characterized. At 150°C the matrix did not melt perfectly (rigid parts of the matrix could be seen in the melt) and specimens could not be produced. At 170°C the thermoplastic fibres melted and formed blend with the matrix. At the processing temperature of 160°C the injection moulding became stable and the reinforcing fibres kept their form and could be found in the moulded specimen. Varying fibre did not affect the mechanical properties.The mechanical tests of the all-PP systems revealed that a slight reinforcing effect (yield stress ~10% higher compared to the matrix) could be detected. The microscopic images showed that neither the distribution of the single fibres nor the impregnation of matrix material was perfect (Figure 23).
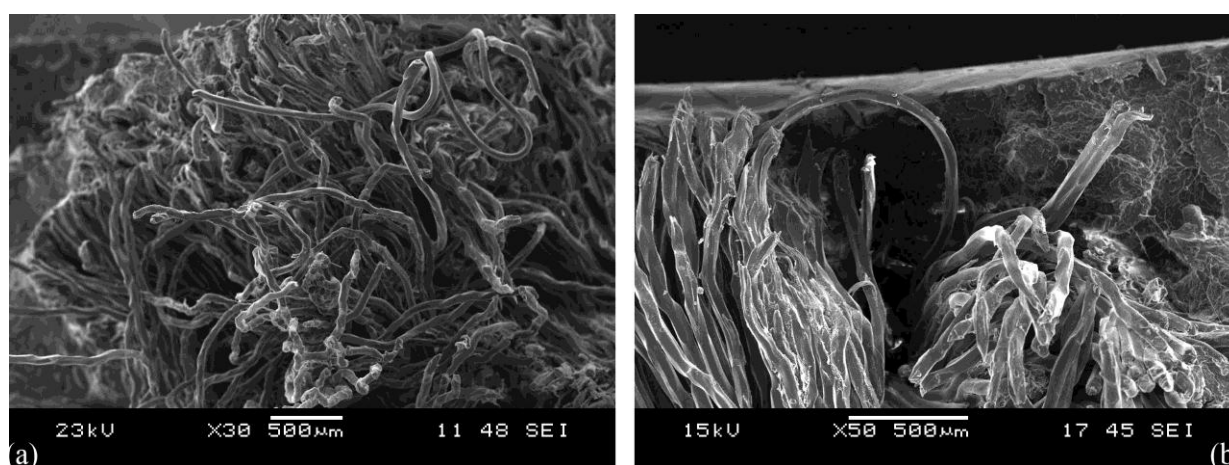
Figure 23. Single fibre distribution and fibre-matrix impregnation of the injection moulded all-PP composites (micrographs were taken after the tensile tests from the fracture surface) a) single fibre in multifilament form; b) gap between the multifilaments

47

These problems must arise from the improper impregnation of the coated pre-product. The melted matrix could not interpenetrate between the single fibres under the injection molding. Althought the thermoplastic reinforcement was successfully injected to the mould but the distribution of the single fibres were worse; so it was concluded that the impregnation process had to be improved.

3.2. Materials, processing and testing

In this part the selected materials and their processing will be described. The manufacturing of the all-PP composites and characterization and the applied testing methods will be detailed.

3.2.1. Materials

During the materials selection the primer aim was to assume wider melting temperature between the matrix and the reinforcement. Further aim was to select polypropylene as matrix material with high melt flow index (>25 g/10 min) which provide the good fibre impregnation at low processing temperature (<170°C). The processing temperature of the injection moulding should be below the melting temperature of the reinforcement. The properties of the selected reinforcement and matrix materials are summarized in Table 2.

Material	MFI [g/10 min] (2.16 kg, 230/160ºC)	Yield stress [MPa]	Tensile modulus [MPa]	Melting temperature [ºC]
Single hPP fibre (Stradom S.A.)	-	581.0±30	6432±490	172.1
rPP (TVK Tipplen R959A)	45/8	24.7±0.4	985±20	148.4
ePP (Dow Versify 4200)	25/4	6.6±0.2	100±30	79.2

Table 2. Properties of the selected materials

Reinforcement

Highly oriented homo-polypropylene multifilament (Stradom S.A., Czestochowa, Poland) was selected and used as reinforcement. The linear density of the multifilament was 3300 dtex. The reinforcing multifilament has a melting temperature of 172.1°C (determined by DSC (TA DSC Q2000) from the first melting curve, 10°C/min) (Figure 24 (a)). Tensile stress and tensile modulus of single fibre were 581±30 MPa and 6432±490 MPa (The tensile tests were carried out by a universal ZWICK Z005 tensile machine according to the EN ISO 527 standard at room temperature (24°C), the crosshead speed was set to 5 mm/min; at least 60 single hPP fibres and 5 hPP multifilaments were tested). Average value and the deviation of the single tests were calculated (Figure 24 (b)). The average single fibre diameter was

40.1±1.8 μm. The multifilament form (~ 400 pieces single hPP fibre) has 336±1.8 MPa yield stress and 2536±377 MPa tensile modulus.
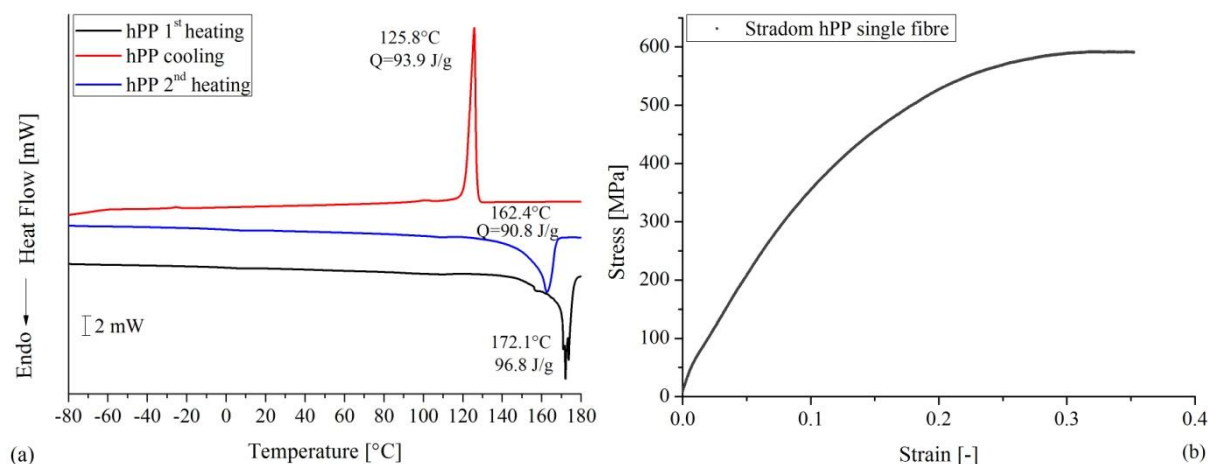

Figure 24. DSC curves (a) and the typical stress-strain curve (b) of the hPP multifilament

The sizing material which was occasionally applied by the producer was studied by EDS tests earlier (during the preliminary tests but sizing material was not detected). To certain that the selected hPP fibres did not content sizing agent EDS tests were completed with Attenuated Total Reflectance (ATR) spectroscopy (Bruker Tensor 27; munber of scanning: 16; range of the wave number: 400-4000 cm^{-1}; picture resolution: 2 cm^{-1}). The ATR test was performed on the original fibres before and after immersing them in chloroform and acetone for 1 h. The spectra of the hPP fibres are shown in Figure 25.
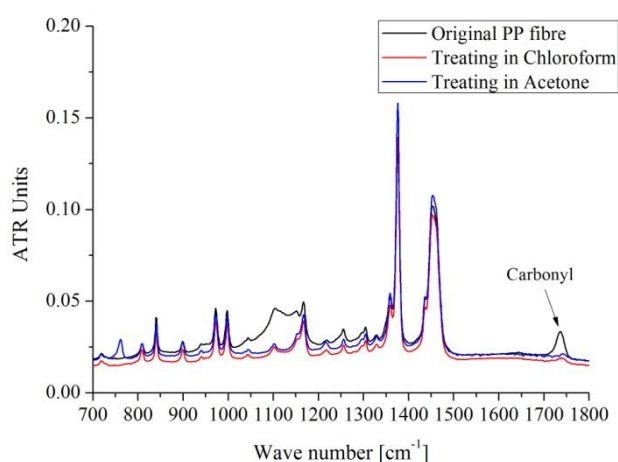
Figure 25. ATR spectra of the hPP fibre

The difference of the spectra of the original and the treated fibres can be seen. Carbonyl absorbance can be found at 1750 cm^{-1} which means that sizing agent (ester or carboxylic acid)

exists on the surface. This means that the adhesion between the matrix and the reinforcement has to be qualified after the injection moulding (with e.g. SEM micrographs).

Matrix materials

Two kinds of materials were used as matrix. The first was a random polypropylene copolymer (rPP) (Tipplen R959A) was produced by TVK Nyrt. (Tiszaújváros, Hungary). The rPP has a melting temperature of 148.4°C (determined by DSC from the first melting curve, 10°C/min) (Figure 26) and a Melt Flow Index of 45 and 8.2 g/10 min (CEAST 7027.000, 2.16 kg, 230°C and 160°C).
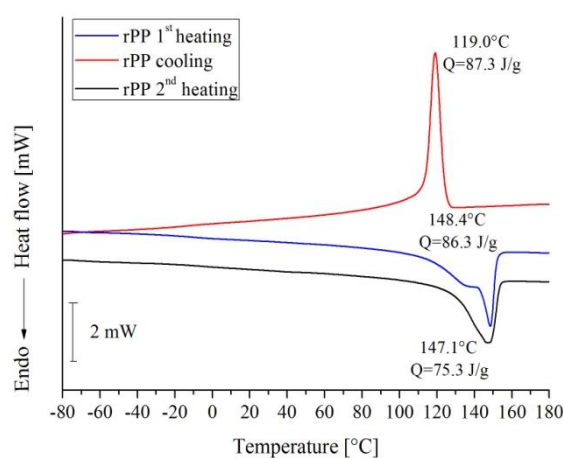
Figure 26. DSC curves of the rPP matrix material

From the initial rPP granules, a 50 µm thick film was produced using extrusion film blowing technique (with Labtech LF-400 film blowing machine at 170°C (Figure 27)).

Figure 27. Producing of rPP film by film blowing technique

To produce all-PP composites with wider processing window (than for rPP) polypropylene-based thermoplastic elastomer (Versify 4200 (ePP)), was produced by Dow Chemical Company, Horgen, Switzerland) was selected. The ePP has 25 g/10 min Melt Flow Index at 230°C and 2.16 kg. The same as rPP material characteristic was demonstrated by Fourier transform infrared spectroscopy (FTIR) tests (Figure 28).
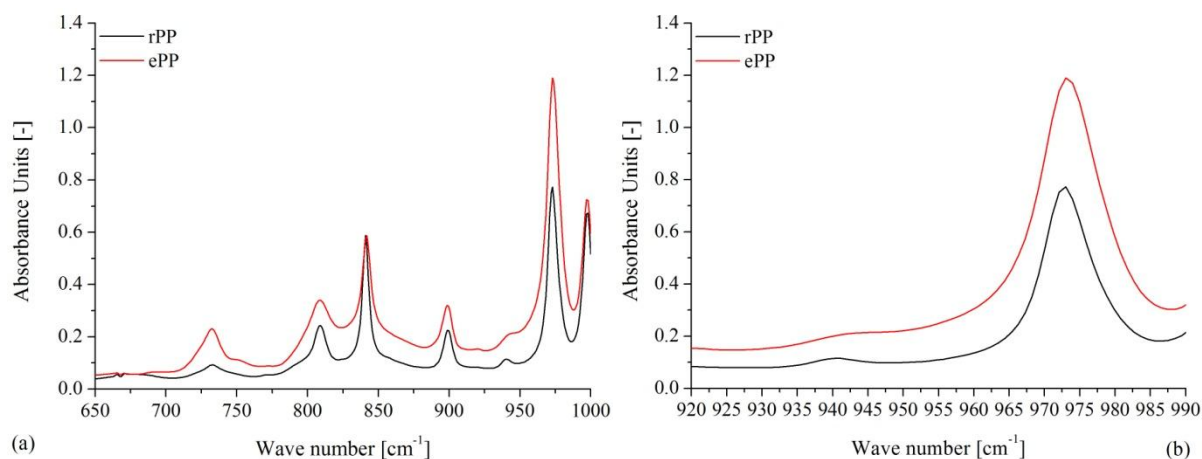

Figure 28. FTIR spectra of the selected matrix materials (rPP, ePP) (a) and the curves between 920-990 cm^{-1} (b)

Comparing the FTIR spectra of rPP copolymer and PP-based TPE (ePP) the difference in the intensity of the peaks and no other peak(s) can be observed. These results means that cross-linked elements (e.g. cis-vinylene on 675-715 cm^{-1} or trans-vinylene on 965 cm^{-1}) of the materials cannot be found so this matrix is a polyproplyne based thermoplastic elastomer where the soft segment is the ethylene-propylene copolymer and the hard segment is propylene. This result means that the two selected matrix materials belong to the same polymer family.

The melting and cooling peaks of the material were analysed by DSC tests (Figure 29 (a)) and the MFI values (with the load of 2.16 kg) at different temperatures (120-160°C) are shown in Figure 29 (b).
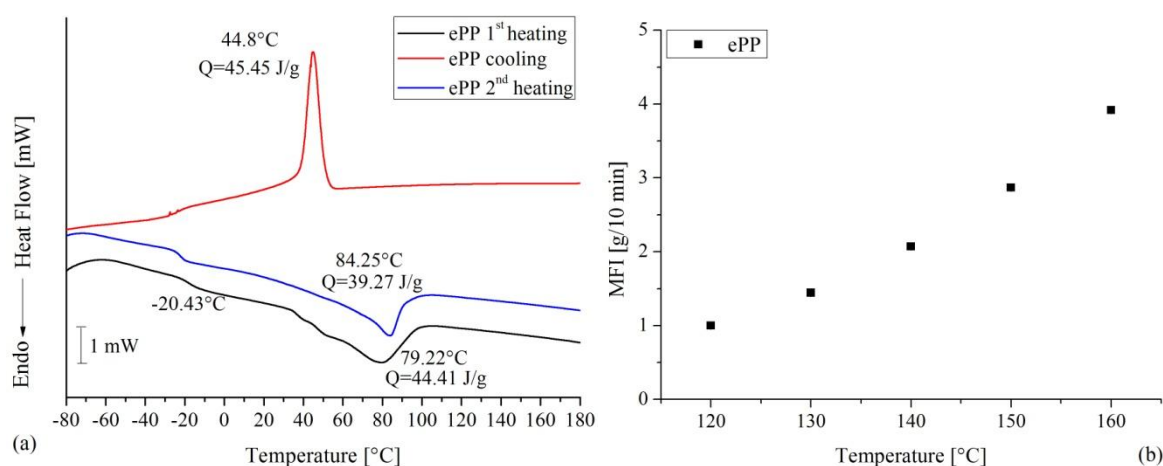
Figure 29. DSC curves (a) and MFI values (b) of the ePP at different temperatures

Comparing the melting temperature of the ePP (melting peak in Figure 29) and the hPP reinforcement (melting peak in Figure 24 (a)) wide processing window (90°C) can be stated which significantly (~50°C) higher than for rPP/hPP. The MFI results show that the flow capability is increasing with increasing temperature. Comparing of the MFI values at 160°C one can state that this value for ePP is half of the value of the rPP material (MFI=8.2 g/10 min (2.16 kg, 160°C)). From the ePP pellets a 50 µm thick foil was prepared by flat film extrusion with Labtech LF-400 film blowing machine at 195°C.

Figure 30. Producing of ePP film by flat film extrusion technique

3.2.2. Manufacturing of the pre-impregnated material

The matrix film and the reinforcing hPP multifilament were laminated prestressed onto an aluminium core with filament winding according to the film-stacking method (to improved the impregnation of the fibres and decrease the relaxation of the fibres), which resulted in unidirectionally aligned (UD) fibres, shown in Figure 31 (a).
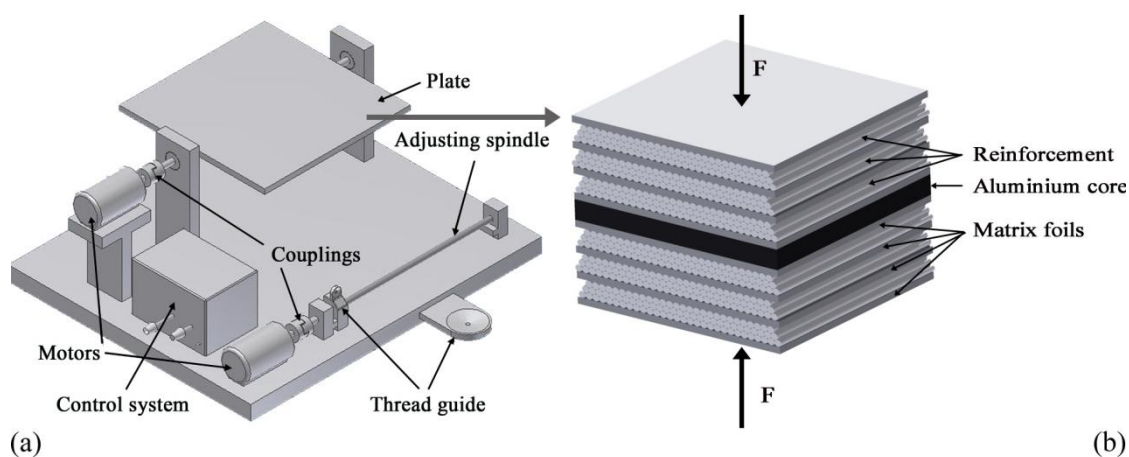
Figure 31. Preparation of unidirectional, all-PP composites with filament winding (a) and with subsequent compression moulding (b)

Random polypropylene based all-polypropylene composite (designated further as all-PP(R)) sheets with thicknesses of 1.7 mm and with varying reinforcing multifilament content (50, 60, 70 and 80 wt%) and elastomeric PP based all-polypropylene composite (designated further as all-PP(E)) sheets with thicknesses of 1.6 mm with 70 wt% reinforcement content were produced by compression moulding, as shown in Figure 31 (b). The consolidation temperature was 180°C (all-PP(R)) and 140°C (all-PP(E)). The filament-wound, film-stacked package was inserted into preheated moulds and held for 240 s (all-PP(R); all-PP(E)) without pressure, then consolidated for 240 s (all-PP(R)) and 480 s (all-PP(E)) with pressure of 5.26 MPa. Thereafter it was cooled to 45°C. To achieved rigid properties of the consolidated sheets they were cooled down under the glass transition temperature of the matrices (rPP= -14°C and ePP= -38°C determined by DMA traces see in chapter 3.3.1 and 3.3.2) liquid nitrogen and chopped (with Labtech LZ-120/VS granulator machine) for small pellets having a dimension of 5x5 mm (width x length).

In order to investigate the effect of the reinforcing fibre length 70 wt% reinforcement containing all-PP(R) composites were also chopped for 5x2 and 5x8 mm. Note that the length of the pre-products determined the length of the reinforcing fibres. The chopped pre-products (Figure 32) were used thereafter for injection moulding.

Figure 32. 5 x 8 mm sized chopped all-PP(R) pre-impregnated pellets for injection moulding

The density (which was measure by immersion method with ethanol) of the produced composite sheets is shown in Figure 33 (a). The results demonstrated that the density of the all-PP(R) composite was quasy constant as a function of the fibre content. This means that the fibre impregnation was closely same and the structure did not contain air between the single fibres The density measures was completed by the measure of the ePP matrix and the all-PP(E) composites which was made with 70 wt% nominal fibre content. The red point in the Figure 33 shows that the density of the all-PP(E) composite was 0.86 g/cm^3.To check the consolidation quality and the fibre impregnation the cut surface of the composite was inspected by SEM. Figure 33 (b) (for all-PP(E) composite) evidenced that the consolidation was adequate and the fibres were well wetted by the matrix.
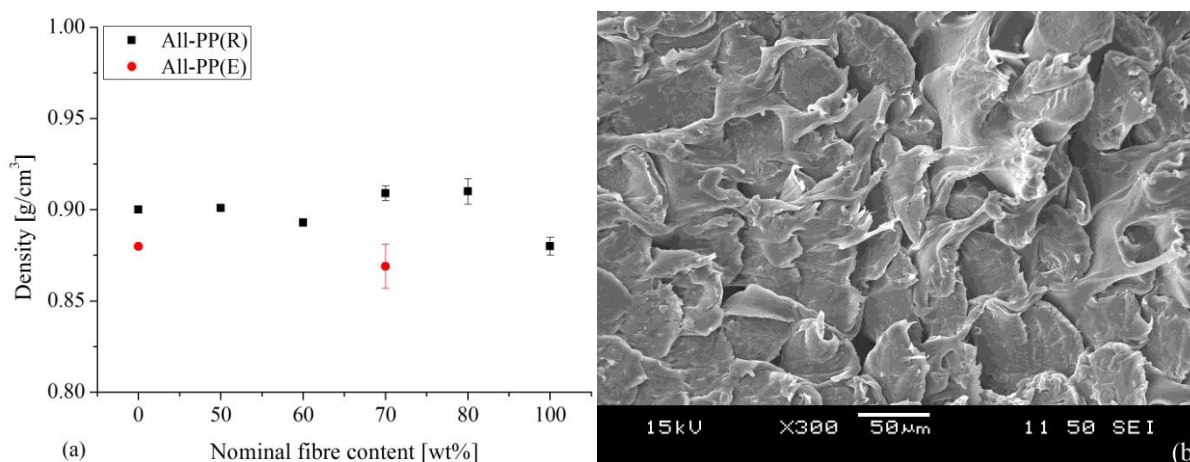

Figure 33. Density of the consolidated sheets (a) and the SEM picture of all-PP(E) composite (b)

3.2.3. Injection moulding

From the pre-impregnated pellets 2.0 mm (all-PP(R) composites) and 2.1 mm (all-PP(E) composites) thick 80 x 80 mm plaque specimens were injection moulded with an Arburg Allrounder 370S 700-290. The injection moulding parameters for all-PP(R) composites as well as the all-PP(E) ones are listed in Table 3.

Injection moulding parameters		Material	
Parameter	Unit	All-PP(R)	All-PP(E)
Injection volume	[cm^3]	50	44
Injection rate	[cm^3/s]	50	50
Switch over point	[cm^3]	10	10
Holding pressure	[bar]	500	400
Holding time	[s]	10	10
Residual cooling time	[s]	15	15
Screw rotational speed	[m/min]	15	15
Back pressure	[bar]	20	20
Decompression volume	[cm^3]	5	5
Decompression rate	[cm^3/s]	5	5
Temperature of Zone 1 (Nozzle)	[°C]	160	120/140/160
Temperature of Zone 2	[°C]	160	115/135/155
Temperature of Zone 3	[°C]	160	110/130/150
Temperature of Zone 4	[°C]	155	105/125/145
Temperature of Zone 5	[°C]	155	100/120/140
Mould temperature	[°C]	40	20

Table 3. Injection moulding parameters

To avoid cold slug formation, heated flat nozzle with 4 mm hole in diameter was used during injection moulding process. To compare the effect of the gate height on the characteristics of the produced injection moulded specimens two different gate types were used (Figure 34): conventional film gate (gate thickness: 1 mm) and fan gate (FG; gate thickness: 2 mm).
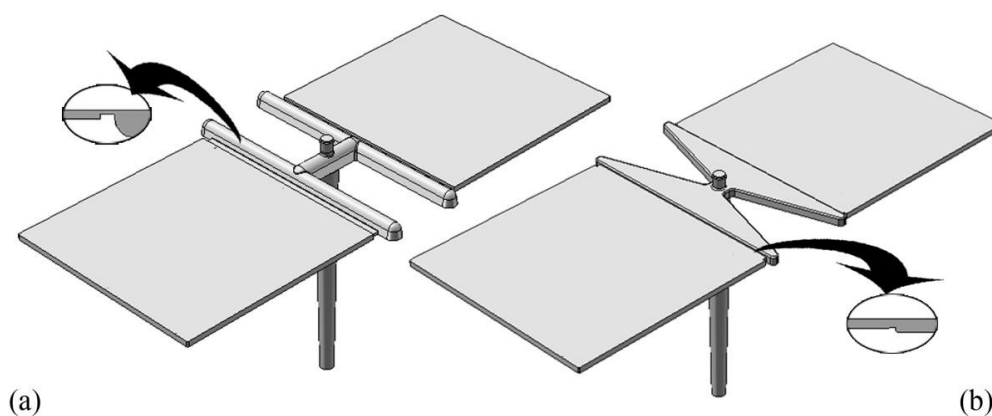
Figure 34. Plaque specimens with a conventional film gate (a) and a fan gate (b)

3.2.4. Testing methods

Quasi-static tensile tests

Static tensile tests were performed on compression moulded sheets (20 x 150 mm) and injection moulding plaque specimens. Dumbbell-shaped specimens (EN ISO 8256 Shape 3) were cut from injection moulding plaque specimens by water jet cutting in-flow and perpendicular to the flow directions (Figure 35). The tensile tests were carried out by a universal ZWICK Z020 tensile machine according to the EN ISO 527 standard. The cross-head speed was set to 5 mm/min, and each test was performed at room temperature (24°C); at least 5 specimens from each material were tested.
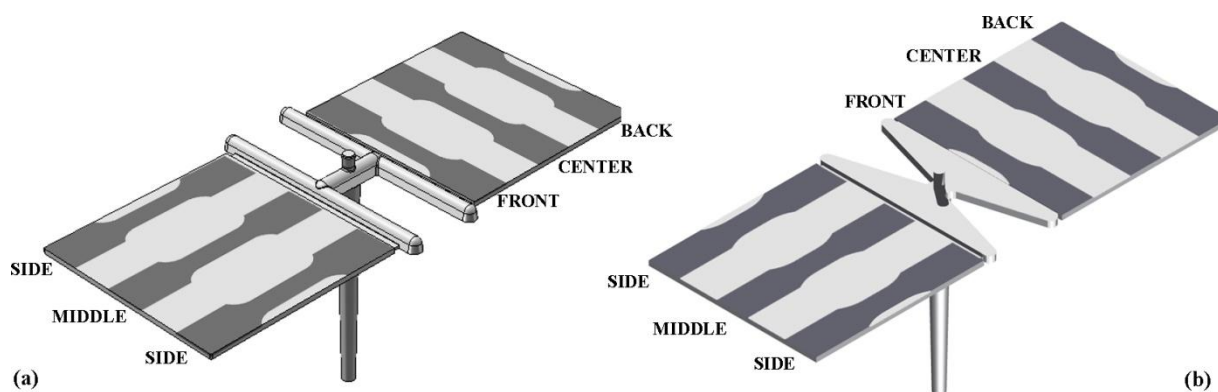

Figure 35. Preparation of dumbbell specimens from the plaque specimens with conventional film gate (a) and fan gate (b) in the parallel and perpendicular to the flow directions

From the static tensile tests results yield stress and tensile modulus were calculated. When a specimen is loaded beyond the elastic limit the stress increases and reaches a point at which has maximum. This first maximum point of stress-strain curve is called yield stress.

Instrumented falling weight impact tests

Instrumented falling weight impact (IFWI) tests were performed on a Fractovis 3789 (Ceast, Italy) machine with the following settings: 131.84 J maximal energy; 20 mm dart diameter; 40 mm support rig diameter; 13.62 kg dart weight; and 1 m drop height. The samples were tested at room temperature (24°C) and at -30°C; at least 10 specimens were tested. Specimens size were 80 (wide) x 80 (length) x 2.0 mm (all-PP(E)) and 2.1 (all-PP(E)) mm (thick).

Dynamic mechanical analysis

Dynamic mechanical analysis (DMA) tests were performed on a DMA TA Instruments Q800 machine with the following parameters:

- To analyse the relaxation of hPP single fibres, the decreasing of the fiber length (shrinkage) was investigated in tensile arrangement with two methods. First the fibre was heated up with the rate of 5°C/min and the strain was registered as a function of temperature between 0 and 165°C. Second the fibre relaxation (strain) was measured isothermally at 100, 120, 140°C for 20 min. For both cases 0.001 N preload was set. After isothermal tests the relaxed fibres were tensile tested with the cross head speed of 0.5 N/min.
- The single hPP fibres were characterised in the range of -80…170°C with the heating rate of 5°C/min, the amplitude of 20 μm and the frequency of 1 Hz.
- The single hPP fibres were tested in tensile test mode at room temperature (24°C) with the crosshead speed of 0.5 N/min.
- The injection moulded all-PP composites were tested with using 3 point bending arrangement with the following parameters: support distance: 50 mm; frequency: 1 Hz; temperature range: -100…150°C; strain: 0.08%; heating rate: 5°C/min. Specimens (Dimensions: 60x10x2 mm) were cut in the flow direction from the plaque specimens (Figure 35 'Side'), were used for these tests.

Light microscopy

Light microscopy (LM) images were taken from the polished cross sections of injection moulding specimens in the flow and transverse directions by an Olympus BX51M device. Cross sections were cut from injection moulding specimens and were embedded in epoxy resin (Figure 36). After the samples were prepared, they were polished in a Struers

polisher in four steps using 320-, 1000-, 2400- and 4000-grit SiC papers and water as a lubricant.
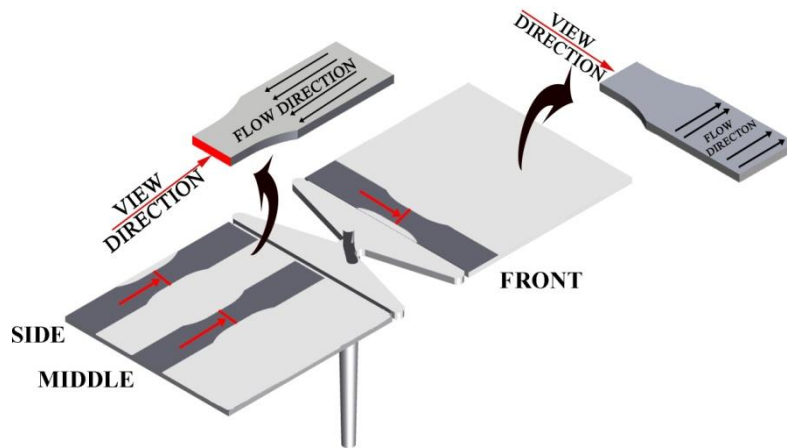

Figure 36. Positions at which the cross-sections of the injection moulding specimens were analysed by light microscope

Scanning electron microscopy (SEM)

Scanning electron micrographs were taken from fracture surfaces with a Jeol JSM-6380LA SEM. Prior to test the samples were sputter-coated with gold/palladium alloy.

Shrinkage tests

Shrinkage was measured at different times after injection moulding (1, 4, 24, 48, and 168 h) and on different positions of the plaque specimens by digital calliper (Figure 37). At least 5 specimens from each material were tested.
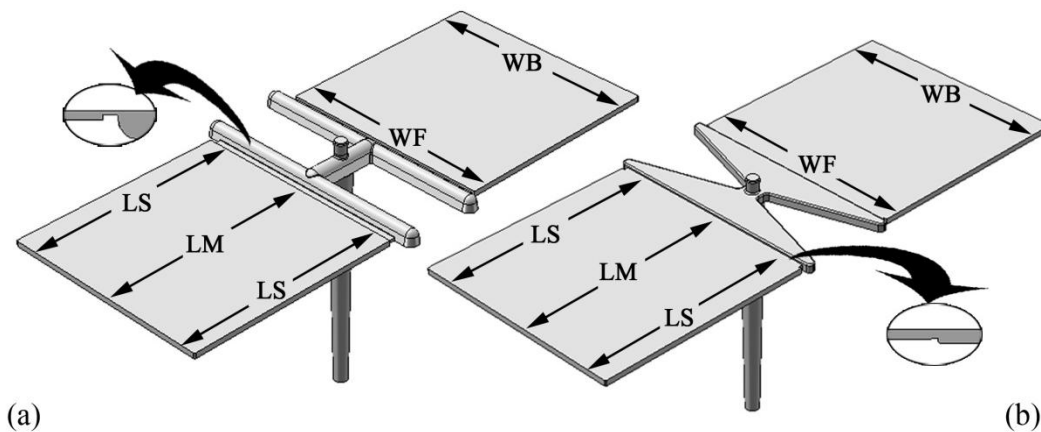

Figure 37. Shrinkage measurement positions. Dimensional abbreviations are as follows: LM – length dimension at the middle; LS – length dimension at the side; WF – width dimension at the front; WB – width dimension at back

3.3. Results and discussion

In this chapter the results of the single hPP fibre and two types of all-polypropylene composites will be discussed. Furthermore the effect of the applied fibre length and nominal fibre content of the pre-impregnated pellets, and gate types will be detailed. In this chapter the shrinkage of the all-PP composites will be outlined as well.

3.3.1. Relaxation of single fibres

Dynamic mechanical analysis was carried out to show the single fibre properties at different temperature. Figure 38 shows the relaxation (shrinkage) of a single fibre as a function of the temperature.
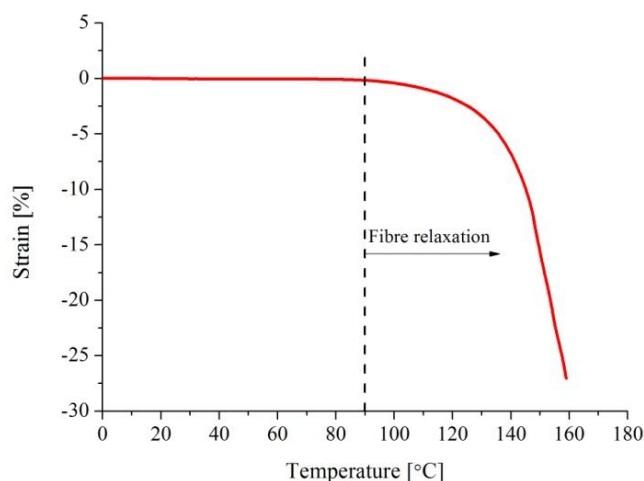

Figure 38. Relaxation of a single hPP fibre as a fuction of temperature

The results show that with increasing temperature the length of the fibre did not change until 90°C. At 90°C the fiber started to shrink and this process increased continously with rising temperature up to 160°C. At 160°C the shrinkage reached 27%.

To characterise the fibre relaxation during injection moulding isothermal DMA tests were performed at 100, 120, 140°C for 20 min test time (Figure 39).
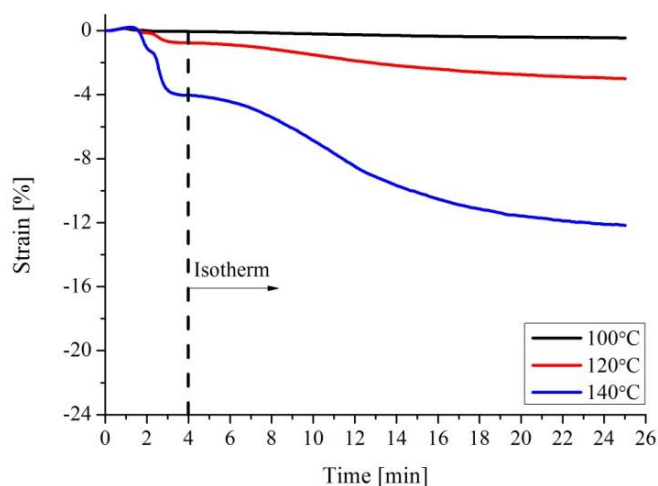
Figure 39. Single hPP fibre relaxation at different isotermal temperature

The results showed that increasing the processing temperature and holding time in the plastification device the fibre relaxation increased. The effect of the fibre relaxation manifested in decreasing tensile modulus values (Figure 40).
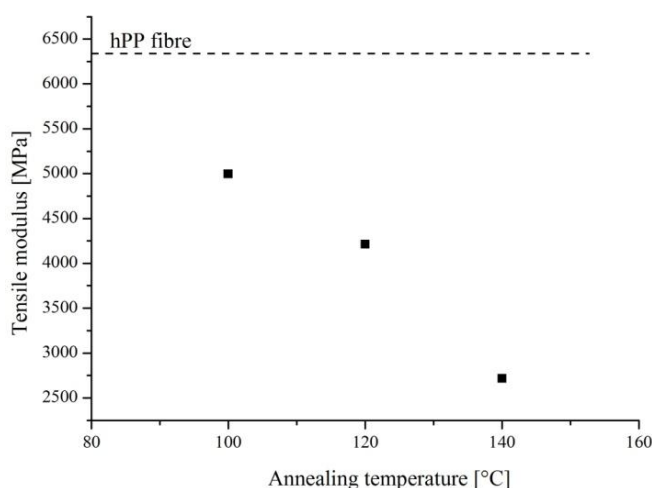

Figure 40. Tensile modulus of the single hPP fibres as a function of different annealing temperature

3.3.2. Random polypropylene based all-PP composite (all-PP(R))

Static tensile tests

   To characterize the all-PP(R) composites, firstly the consolidated sheets were analysed by static tensile test in parallel to the fibre direction. The mechanical properties of the compression-moulded sheets are shown in Figure 41.
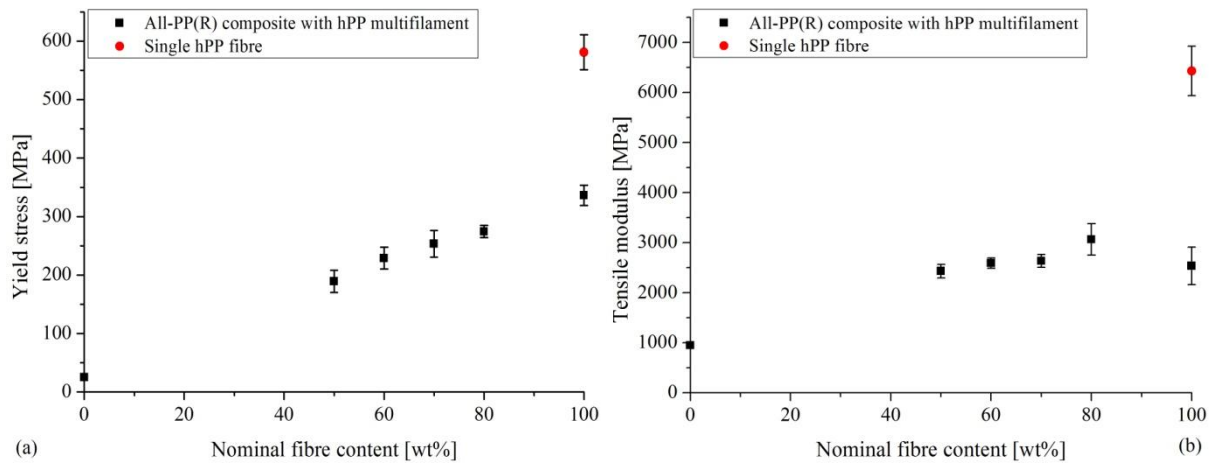
Figure 41. Yield stress (a) and the tensile modulus (b) of the single hPP fibreand the all-PP(R) compression moulded sheets as a function of nominal fibre content

Based on the results in Figure 41, it is obvious that the tensile properties of rPP can be significantly increased by using this filament winding and compression moulding technique. The yield stress and tensile modulus increased with increasing nominal fibre content. This difference in the tensile properties can well be seen in the stress-strain curves in Figure 42.
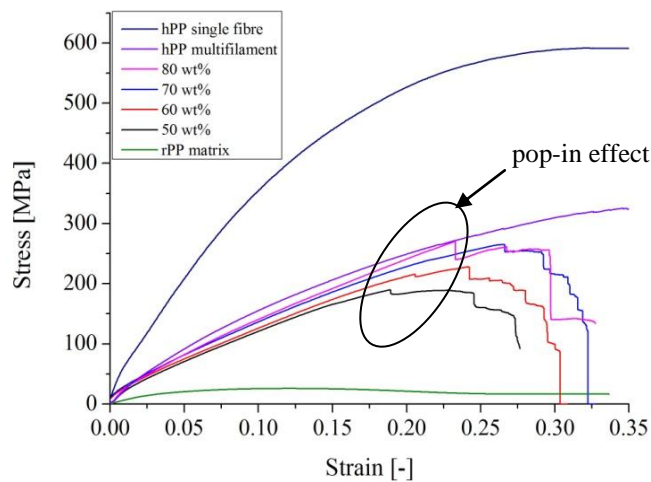

Figure 42. Typical stress-strain curves of the single hPP fibre, hPP multifilament and the different nominal fibre reinforced all-PP(R) composites which was made by compression moulding

In Figure 42 one can also see the pop-in effect where the crack propagation came off in several cracks. The demonstrated results are in close agreement with previously published results for self-reinforced polypropylene composites produced by film-stacking process [3].

From the above mentioned all-PP(R) consolidated sheets different pre-impregnated pellets were produced and applied for injection moulding (*cf*. 3.2.2). The effect of the applied pre-impregnated pellet fibre length on the yield stress and tensile modulus of injection

moulded specimens can be seen in Figure 43 and 44. Yield stress of the all-PP(R) composites in flow direction increased up to 38 MPa if the length of the fibre is increased to 5 mm. Rising further the fibre length (to 8 mm) yield stress remained constant. In perpendicular to the flow direction a slight increase (~20%) can be achieved comparing to the matrix. The values in the three analysed sample places were the same.
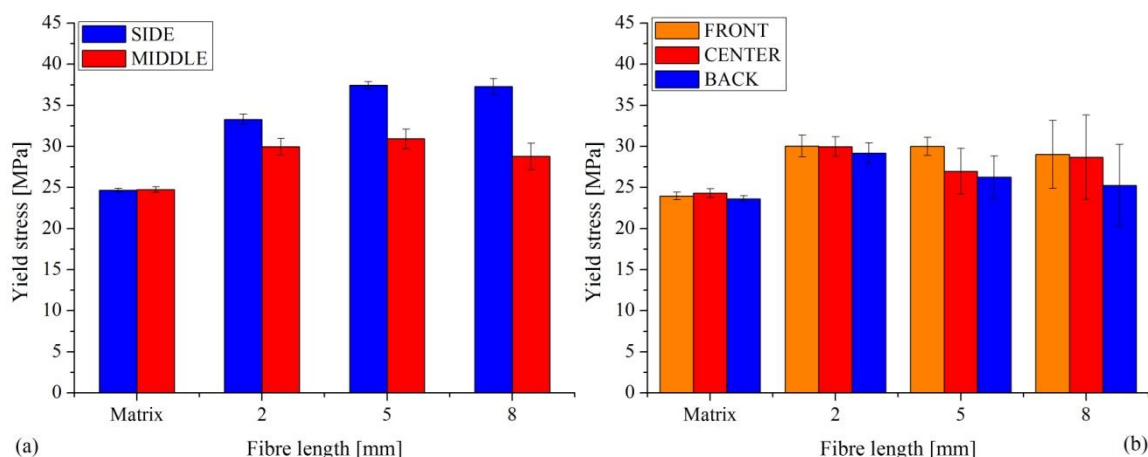

Figure 43. Yield stress of the all-PP(R) composites (fibre content 70 wt%) in flow (a) and perpendicular (b) to the flow direction as a function of fibre length

Based on the results difference in the tensile modulus (Figure 44) cannot be detected in parallel and perpendicular to the flow direction. The values were similar to the value of the matrix, ~1000 MPa.
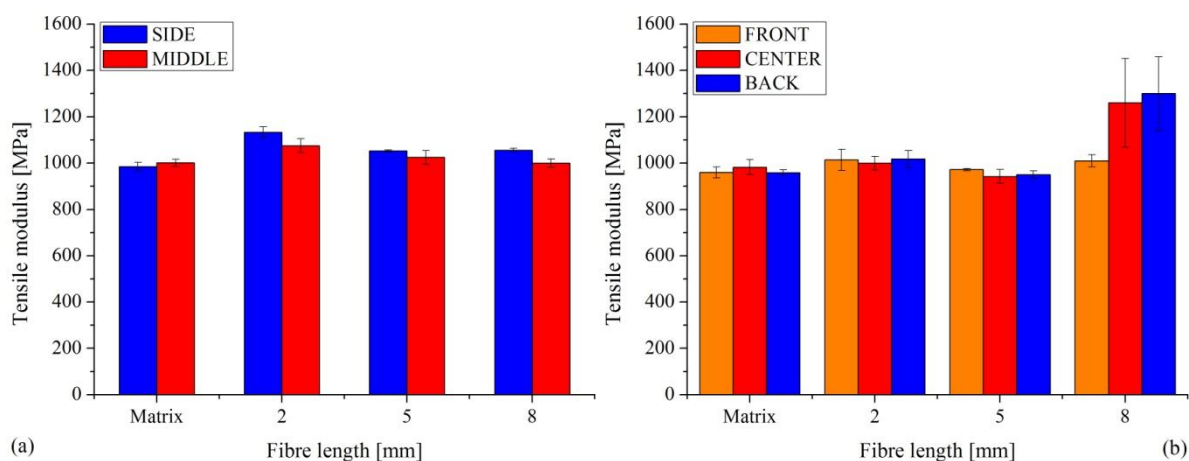

Figure 44. Tensile modulus of the all-PP(R) composite (fibre content 70 wt%) in parallel (a) and perpendicular (b) to the flow direction as a function of applied fibre length

The results of the all-PP(R) composites with different fibre length shows that the highest values with lower deviation can be achieved when the reinforcing fibre length is 5 mm (stable

injection moulding processing could be achieved without injection volume problem) hence for the further studies this value was applied.

The effect of the applied nominal fibre content of the pre-impregnated pellet on the yield stress of injection moulding specimens is shown in Figure 45.
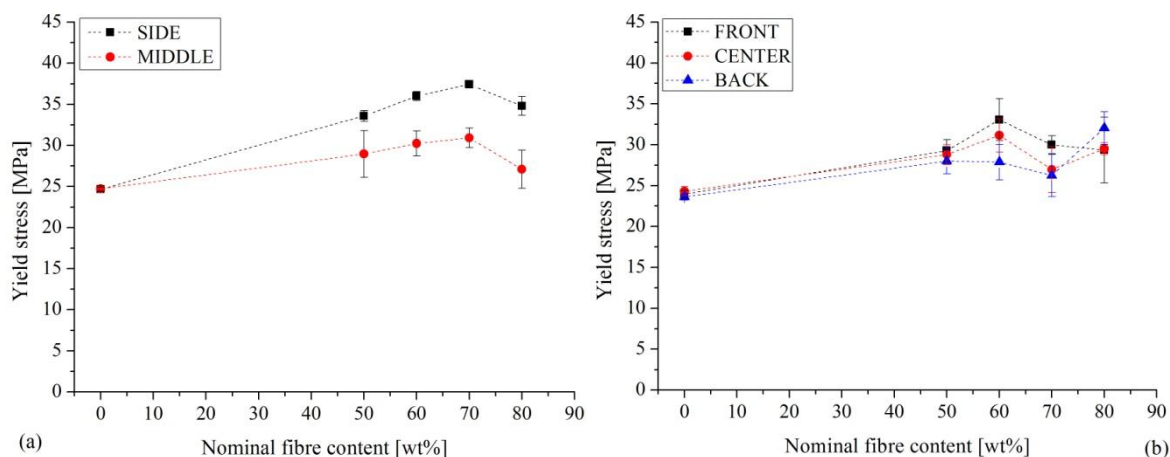

Figure 45. Yield stress of the all-PP(R) in parallel (a) and perpendicular (b) to the flow direction

The yield stress increased in the flow direction with increasing nominal fibre content of the composites until it reached 70 wt%. Composites with 70 wt% fibre reinforcement produced the largest yield stress value, ~38 MPa, which corresponds to a 52% improvement compared to the matrix material. At 80 wt% nominal fibre content, the yield stress is slightly lower, which is attributed to improper consolidation of the composite structure (This observation is also confirmed by SEM micrographs *cf.* Figure 60.).

If analysing the filling pattern the mechanical test results followed expectations. Samples taken from the middle of the plaques had lower yield stress than those taken from the side. This effect is caused by the orientation of the fibres inside the specimens. A slight deviation in yield stress can be observed in perpendicular to the flow. The tensile modulus remained constant with increasing nominal fibre content of the composites until the fibre content reached 70 wt%, after which the modulus increased markedly (Figure 46).
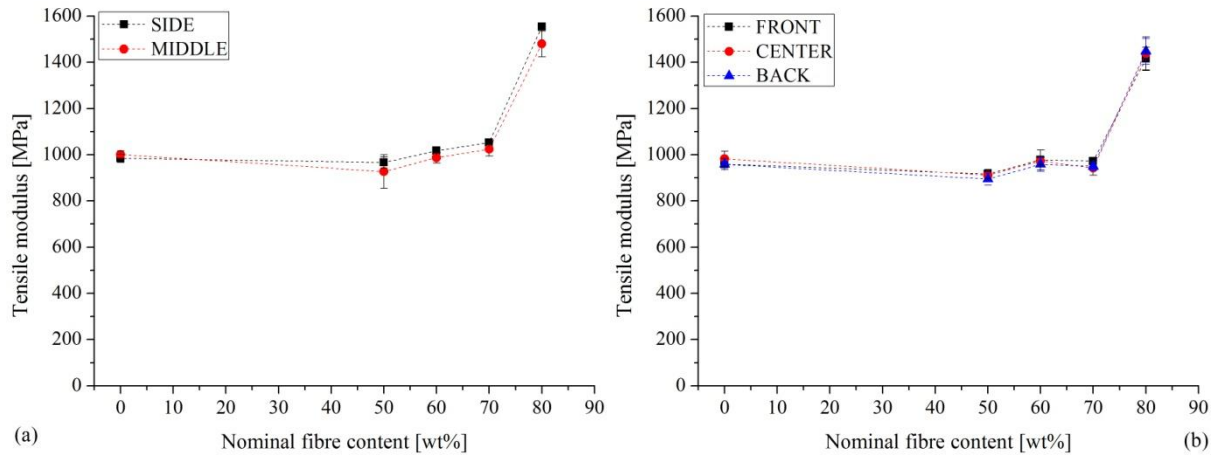
Figure 46. Tensile modulus of the all-PP(R) in parallel (a) and perpendicular (b) to the flow direction

This increasing effect of the all-PP(R) composite with 80 wt% nominal fibre content can be seen also in the typical stress-strain curves of the all-PP composite (Figure 47).
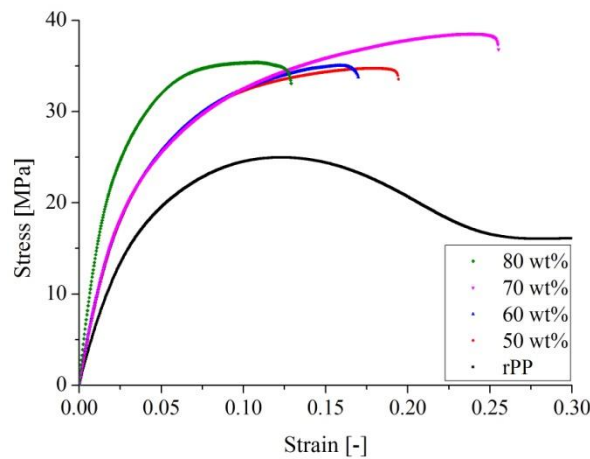

Figure 47. Typical stress-strain curves of the different nominal fibre reinforced all-PP(R) composites which was made by injection moulding

Increased tensile modulus is due to considerably more single fibres being aligned parallel to the load direction. The tensile modulus was calculated in the beginning section of the curves (according to the ISO 527-1 standard) where the consolidation effect was not significant contrast to the number of the single fibre which parallel to the load direction. In this area the fibres kept their reinforcement effect and increased the tensile modulus. When the stress reached the maximal point (yield stress) the poor consolidation was the determinant which decreased the yield stress value compared to the other all-PP(R) composites. This observation is also confirmed by LM *cf.* Figure 57. The effect of the gate types (conventional film gate and fan gate (FG) on the mechanical properties was also analysed (Figure 48). The results show that with a fan gate, the deviation in properties across the three zones of

64

specimens decreased, *i.e.* the mechanical behaviours became more similar. Using the fan gate, the filling patterns became more even. In perpendicular to the flow, the yield stress increased compared to the one injection moulded with film gate.
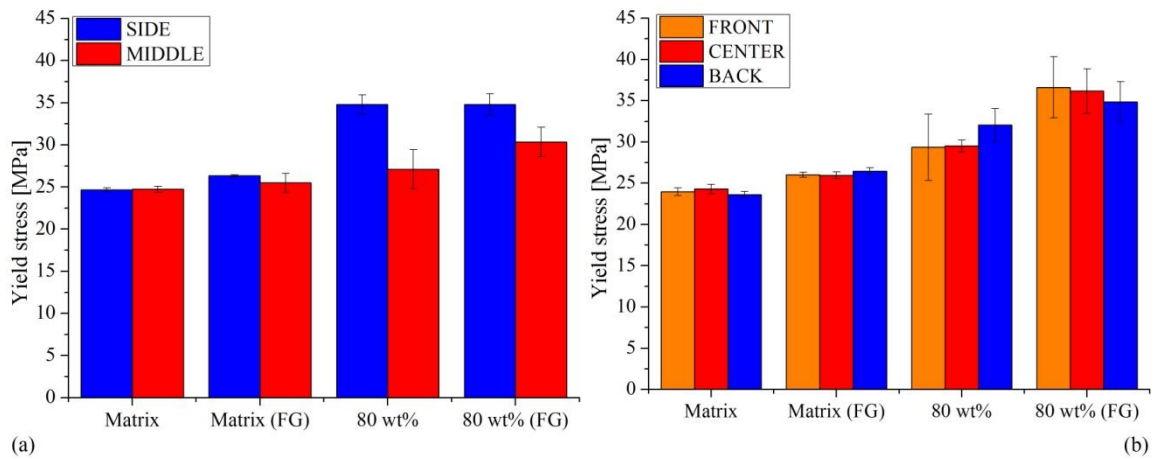

Figure 48. Effect of the gate type on the yield stress of all-PP(R) in the parallel (a) and perpendicular (b) to the flow direction (FG: fan gate)

The tensile modulus (Figure 49) in the flow direction did not change, but in perpendicular to the flow direction, it increased due to lower friction heat in the gate zone.
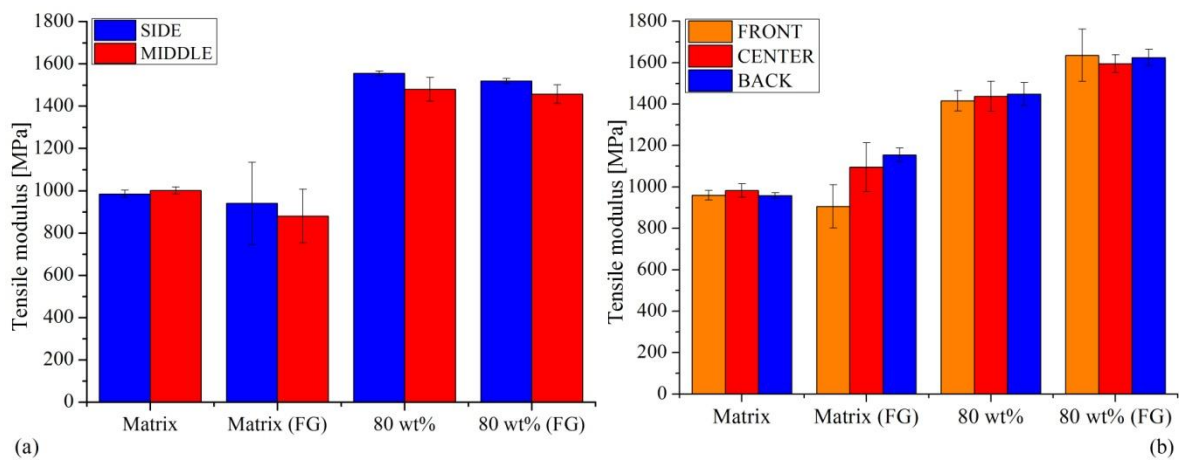
Figure 49. Effect of the gate type on the tensile modulus of all-PP(R) in the parallel (a) and perpendicular (b) to the flow direction (FG: fan gate)

Instrumented falling weight impact tests

To analyse the effect of reinforcing fibre length, content and gate type on the energy-absorbing capacity of the injection moulded plaque specimens, instrumented falling weight impact tests were performed. Typical force-time curves of the composites are shown in Figure 50.

Figure 50. Force-time curves of the all-PP(R) composites with different fibre length (70 wt%) (a) and content (b) at 24°C

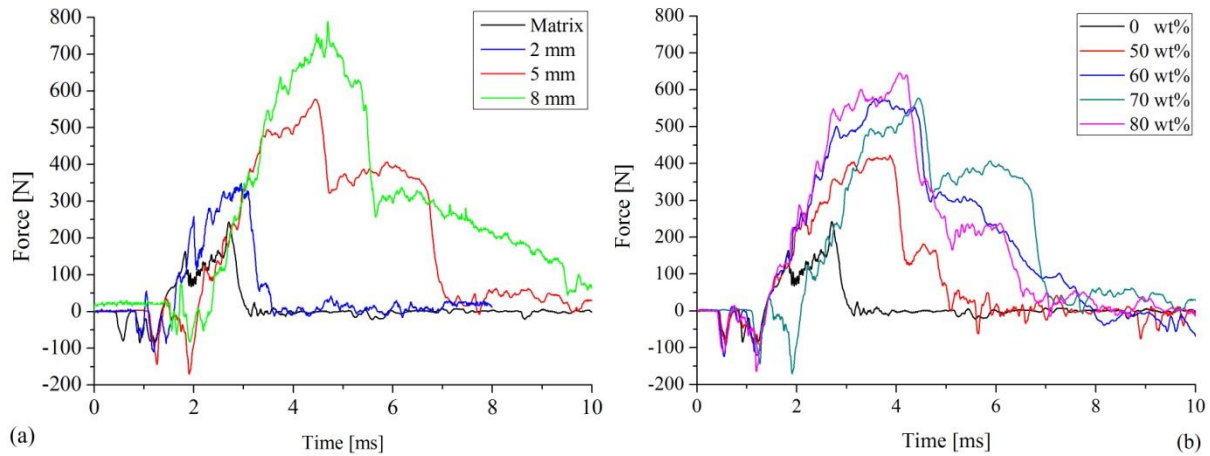These results show that the maximum of the force-time curves increased with increasing fibre length and content of the composites which attributes to higher energy absorbance of the all-PP(R) composite compared to the value of the matrix.

Figure 51 shows the perforation energy (impact energy related to the thickness) of all-PP(R) composite and matrix specimens. These results show that with increasing fibre length the perforation energy increased up to 5.5 J/mm at room temperature which is caused by the decreasing consolidation. At -30°C 5 and 8 mm length of fibre showed similar 2.5 J/mm energy values which is again much more than that of the matrices.

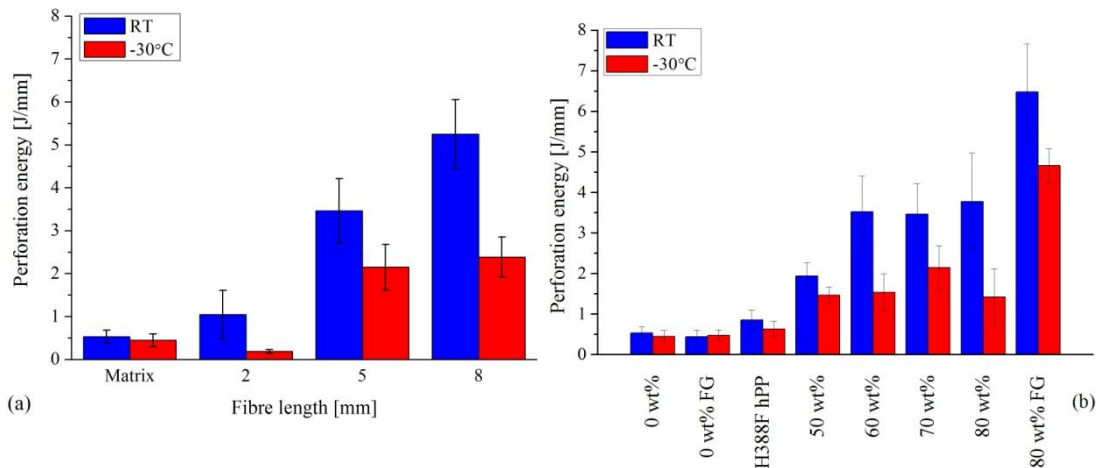**Figure 51. Effect of the reinforcement fibre length (70 wt%) (a) and content (b) on the perforation energy at room temperature and -30°C**

By analysing the effect of the fibre content it can be concluded that increasing the fibre content up to 60 wt%, the perforation energy increased. Above that value, the perforation energy (~3.5 J/mm) remained constant. Using fan gate (FG) led to higher perforation energy

66

(above 6 J/mm) compared to the conventional film gate. This is due to the better fibre distribution in the specimen. Analysing the effect of the testing temperature, significant difference can be seen between the results at 24°C and -30°C than the matrix materials. The perforation energy of all-PP(R) composite was compared to that of a conventional polypropylene homopolymer (Tipplen PP H388F, TVK, Hungary); value obtained is in accordance with the literature [51]. It can be concluded that fibre reinforcement increases the perforation energy significantly compared to the matrix. The perforation energy can be increased up to 1200% compared to the conventional raw material.

Dynamic mechanical analysis

The storage modulus (E′) curves of the injection moulded rPP based self-reinforced composites are shown in Figure 52 which were compared to the conventional polypropylene homopolymer, single hPP fibre and the used rPP matrix.
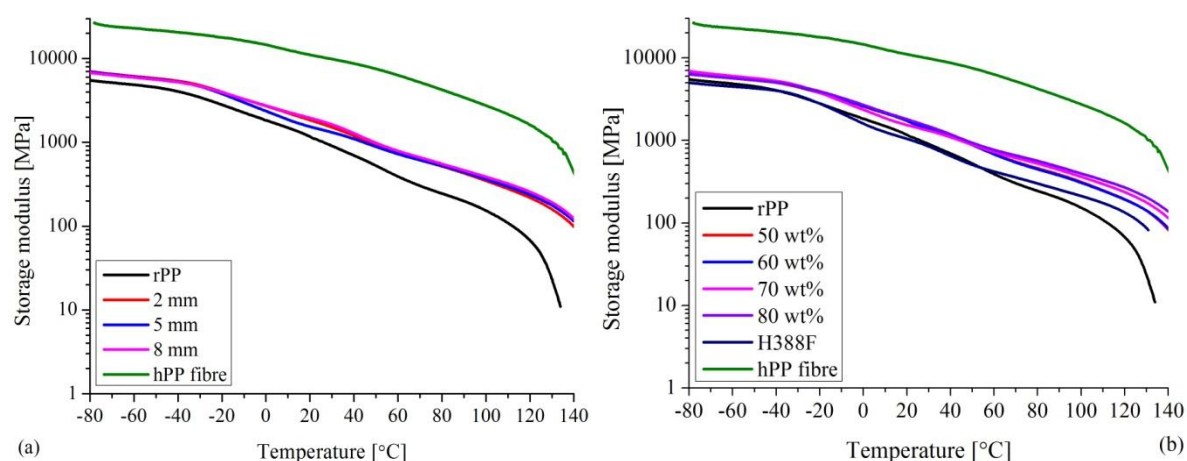
Figure 52. Storage modulus of raw materials and composites with varying fibre length (a) and content (b) with a conventional film gate. * Note that the hPP fibre was tested in tensile mode.

The all-PP(R) composites have higher storage modulus compared to those of the matrix and commercially available PP homopolymer (Tipplen H388F PP). While fibre reinforcement typically leads to a higher storage modulus, increasing the fibre length and content did not affect this parameter significantly. This can be attributed to the relaxation of the reinforcing fibres. Note that the tensile modulus of hPP fibres decreased significantly due to molecular relaxation (cf. Figure 40.) Replacing the conventional film gate (1 mm gate thickness) to fan gate (with 2 mm gate thickness) the storage modulus (Figure 53) did not change owning to the reduced strength of the relaxed fibres.
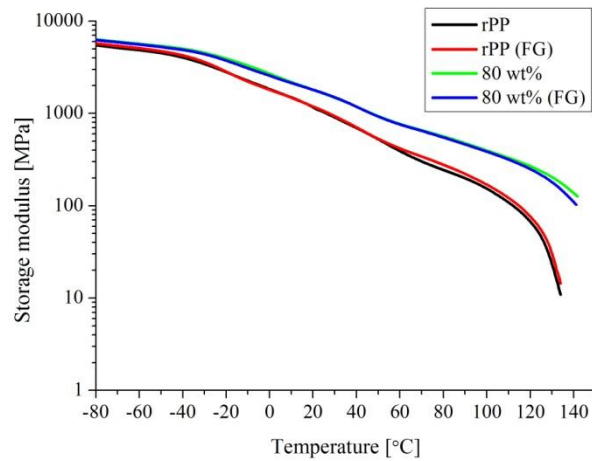
Figure 53. Storage modulus of the all-PP(R) composite (80 wt%) with conventional film and fan gate (FG)

Upon analysis of the glass transition temperature (T_g, derived from the maximum peak of tanδ curves), a slight shift to a higher T_g can be observed with increasing reinforcing fibre content (*i.e.* increasing homopolymer content), as shown in Figure 54.
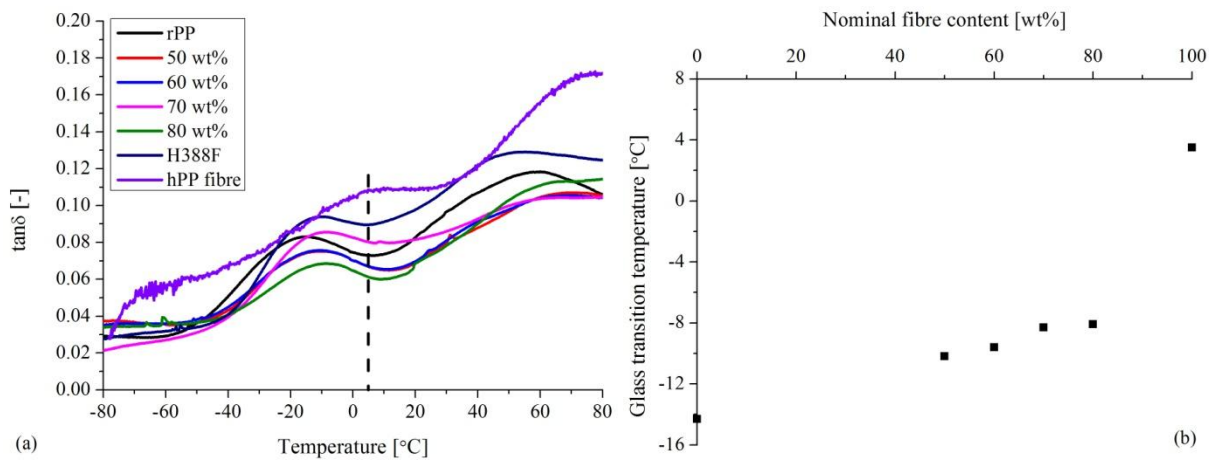
Figure 54. tanδ curves (a) and the glass transition temperature as a function of reinforcing fibre content of the all-PP(R) composites (b)

Light microscopy

Figure 55 shows the cross section of the all-PP(R) specimens in flow direction. On the pictures circular single fibres and skin-core structure can be observed. In case of 8 mm fibre length the fibre distribution becomes poorer. The single fibres were bunched multifilament state.
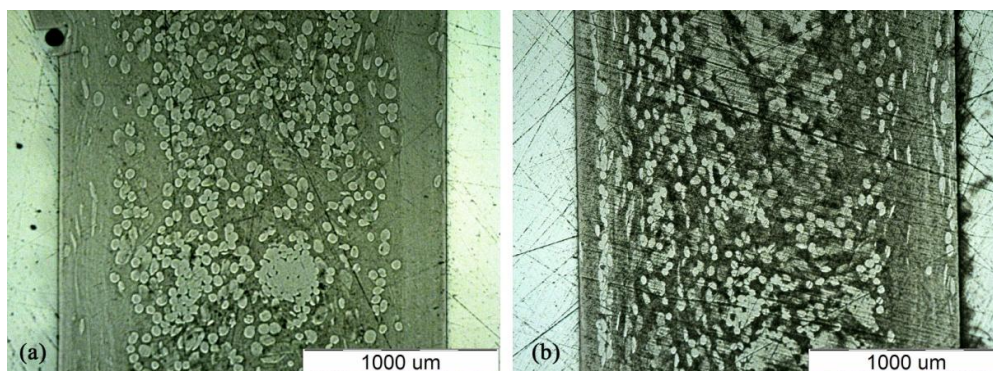
Figure 55. LM micrographs of the all-PP(R) composites in the flow direction (Side)
fibre length of the pre-impregnated pellet was 2 mm (a) and 8 mm (b)

Decreasing fibre distribution can be found when applied 8 mm length of fibre. The single fibres remained in multifilament state and were connected together. Figure 56 shows the single-fibre distributions in the specimens perpendicular to the flow direction (Front) near the gate. The distribution of single fibres is imperfect, and skin-core structure formed. For 80 wt% fibre content, many more single fibres are aligned in the flow direction, which significantly increased the tensile modulus compared to the results in Figure 46 (b).
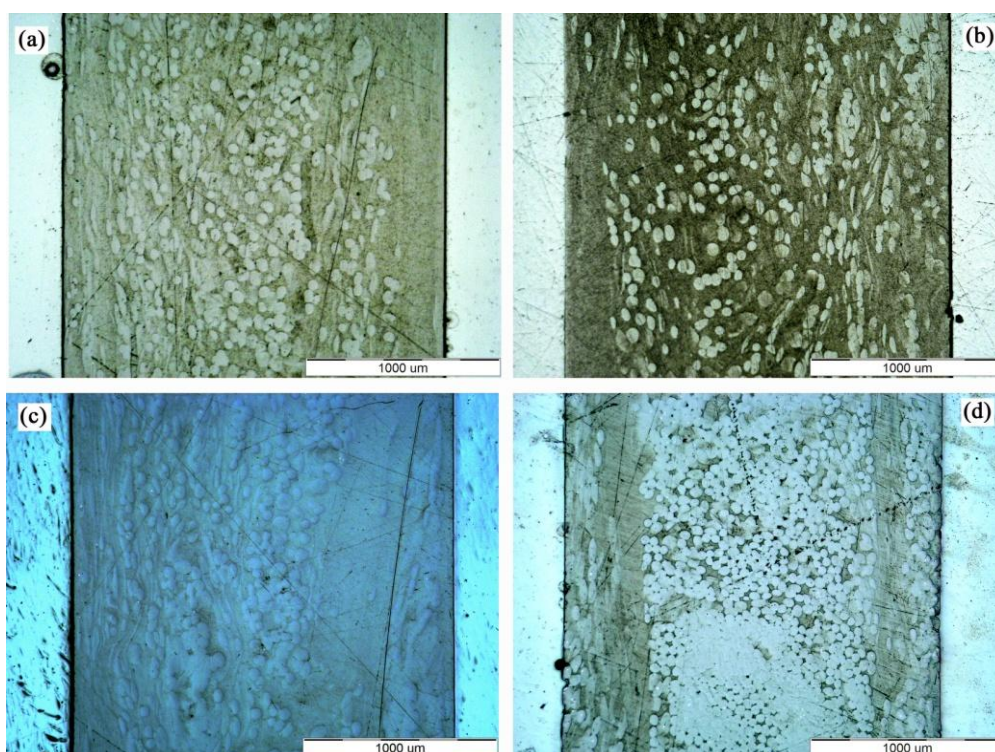
Figure 56. LM micrographs of all-PP(R) composites perpendicular to the flow direction (Front)
a) 50 wt%; b) 60 wt%; c) 70 wt%; d) 80 wt%

LM images taken from the specimen cut in flow direction (Side) are shown in Figure 57. A skin-core layer can also be found with a thickness that is similar to that of specimens cut in the perpendicular to the flow direction. For 80 wt% fibre content, there is a better fibre distribution (Figure 57 d) than for other composites, a trend similar to that in Figure 56 d.
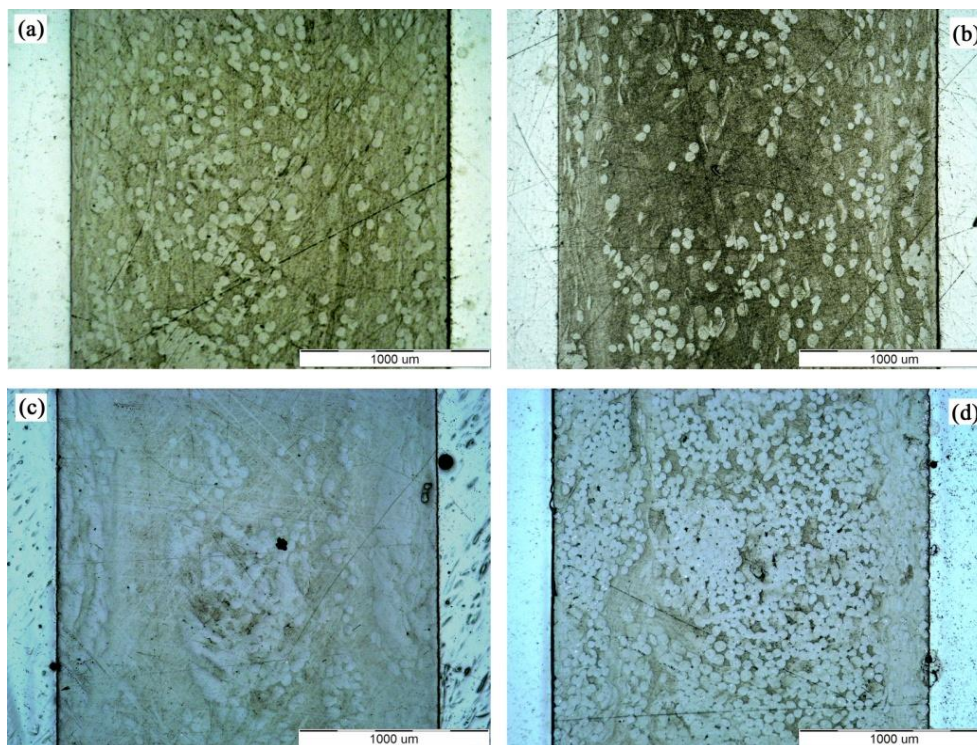
Figure 57. LM micrographs of the all-PP(R) composites in the flow direction (Side)
a) 50 wt%; b) 60 wt%; c) 70 wt%; d) 80 wt%

The cross section of the 80 wt% all-PP(R) composites with a fan gate is presented in Figure 58. There is no skin layer formed in the cross direction. Furthermore, the fibre distribution is better than that for the conventional film gate, which explains the improved mechanical properties.
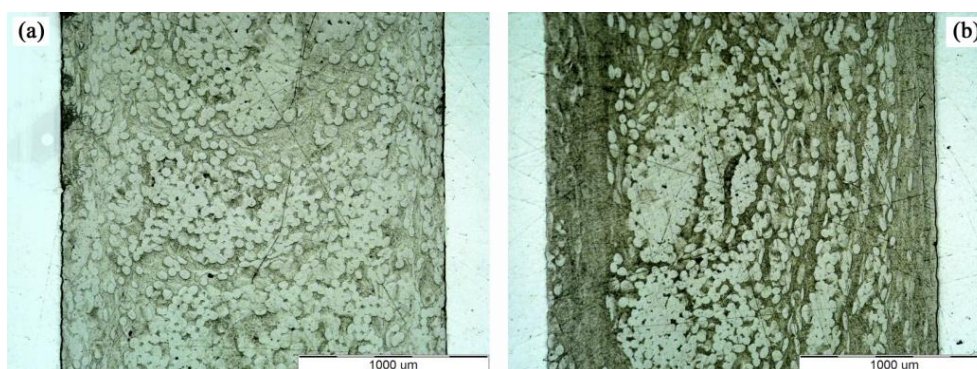
Figure 58. LM micrographs of the all-PP (R) composite (80 wt%) with fan gate in perpendicular (a) and
parallel (b) to the flow direction

Scanning electron microscopy (SEM)

SEM micrographs were taken from the fracture surface of the all-PP(R) composite specimens with different pre-impregnated pellet length of fibre (Figure 59).
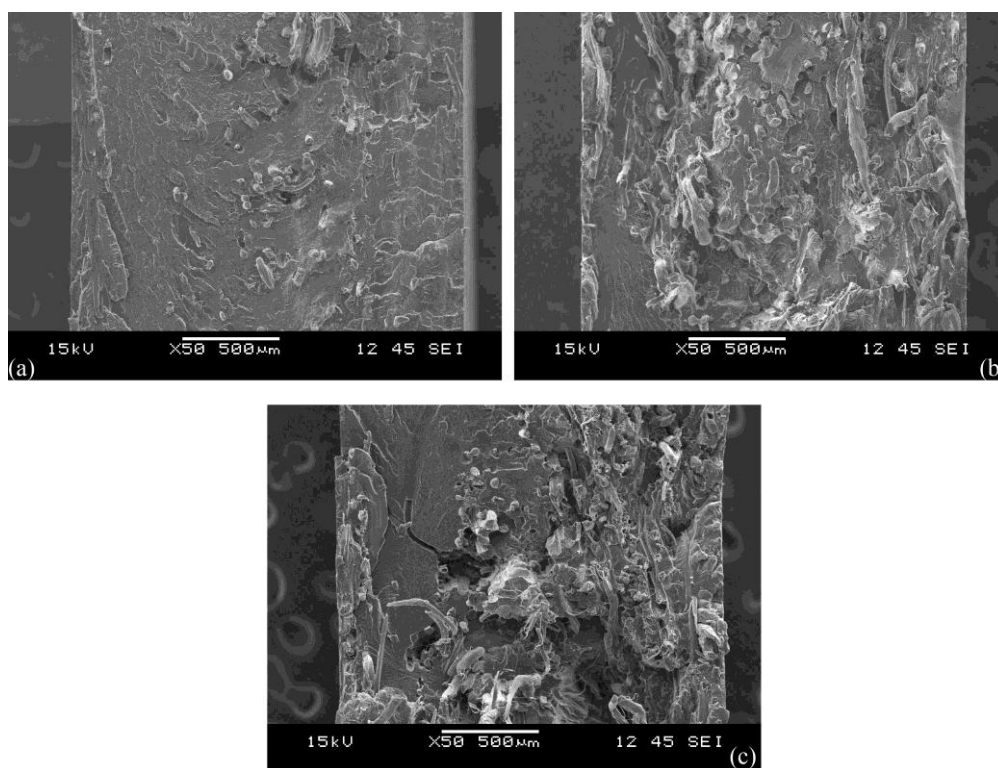
Figure 59. Fracture surface of the all-PP(R) composite (70 wt%) with different fibre length of pre-impregnated pellet in the flow direction (Side)
a) 2 mm; b) 5 mm; c) 8 mm

Figure 59 shows the effect of the different fibre length of the pre-impregnated pellet. It can be concluded that fibre impregnation decreased with increasing fibre length up to 8 mm. Applying 8 mm length poor consolidation was found in the cross section of the specimen.

In Figure 60 one can observe that the consolidation and fibre distribution worsen with increasing fibre content. Voids formed among the fibres, indicating that the matrix material could not fully fill the space between the fibres. Moreover, for the 80 wt% sample, there is poor adhesion between the matrix and fibres in the core region (Figure 60 d).
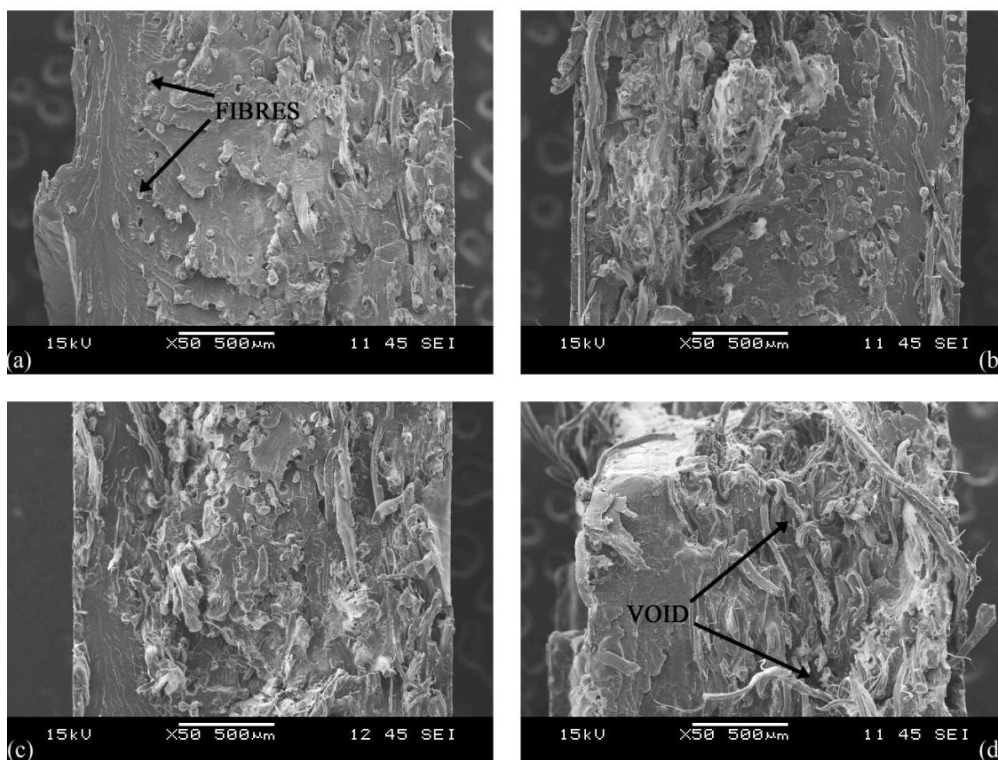
Figure 60. Fracture surface of the all-PP(R) composite in the flow direction (Side)
a) 50 wt%; b) 60 wt%; c) 70 wt%; d) 80 wt%

Figure 61 shows the effect of the gate type used. With a fan gate, the cross section of the specimen became more homogeneous, and the core could not be distinguished from the skin region.
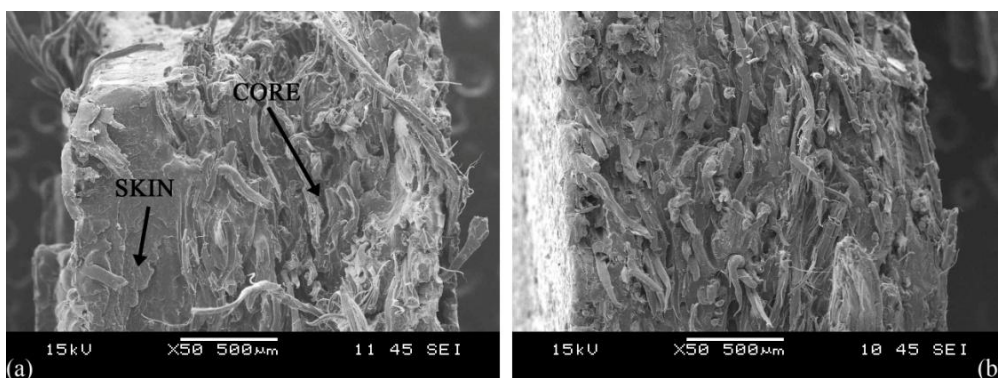
Figure 61. Fracture surface of all-PP(R) composite prepared by a conventional film gate (a) and a fan gate (b) in the flow direction (Side)

Shrinkage tests

Effect of the thermoplastic reinforcement on the shrinkage of the all-PP(R) composite produced with different fibre lengths is shown in Figure 62.
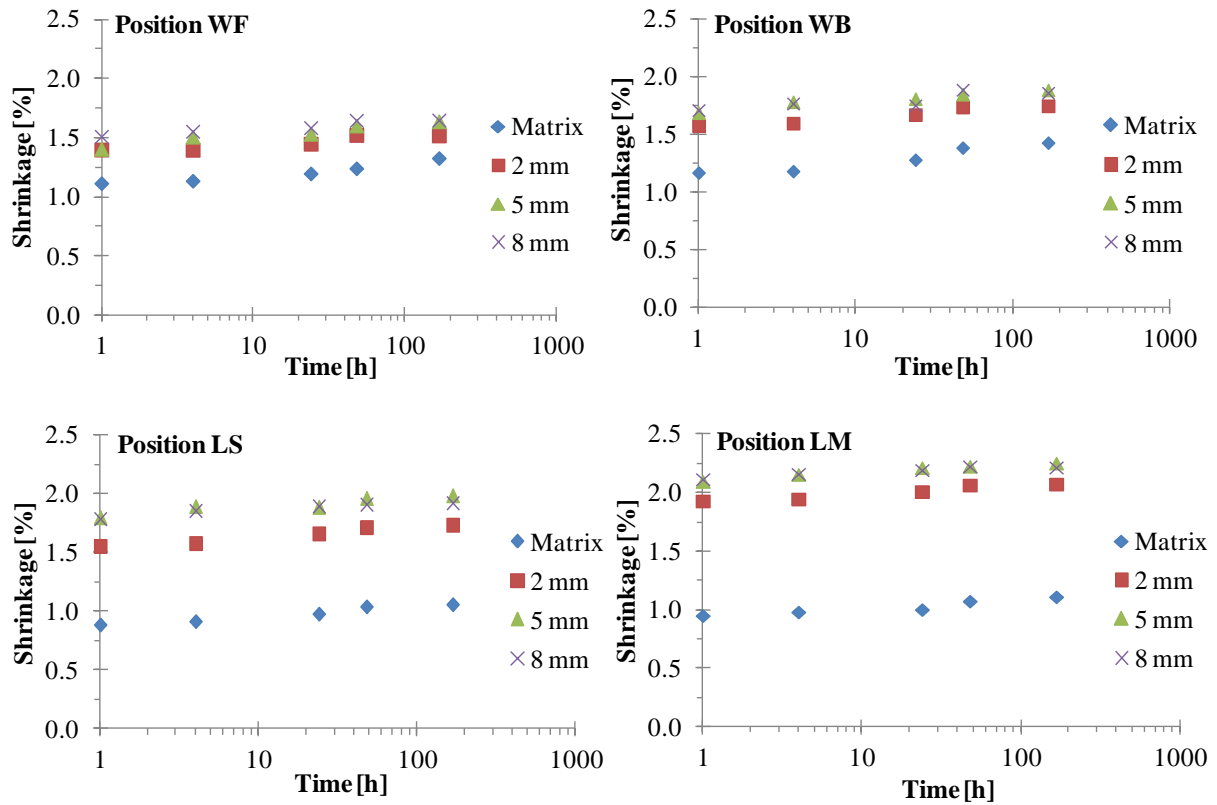
Figure 62. Shrinkage of rPP and all-PP(R) composite specimens with different fibre length (2, 5, 8 mm; 70 wt%) in different directions (WF: Width Front; WB: Width Back; LS: Length Side; LM: Length Middle)

The results show that the shrinkage of the thermoplastic fibre reinforced all-PP(R) composites with different fibre length increased in all directions. The highest increment can be detected in parallel to the flow direction in the middle zone. 2 mm fibres increased significantly the shrinkage compared to the matrix. Using 5 mm and 8 mm fibre length similar shrinkage behaviour can be detected. In flow direction the values were two times higher than the matrices.

Shrinkage of the injection moulded specimens with different fibre volume content is shown in Figure 63.
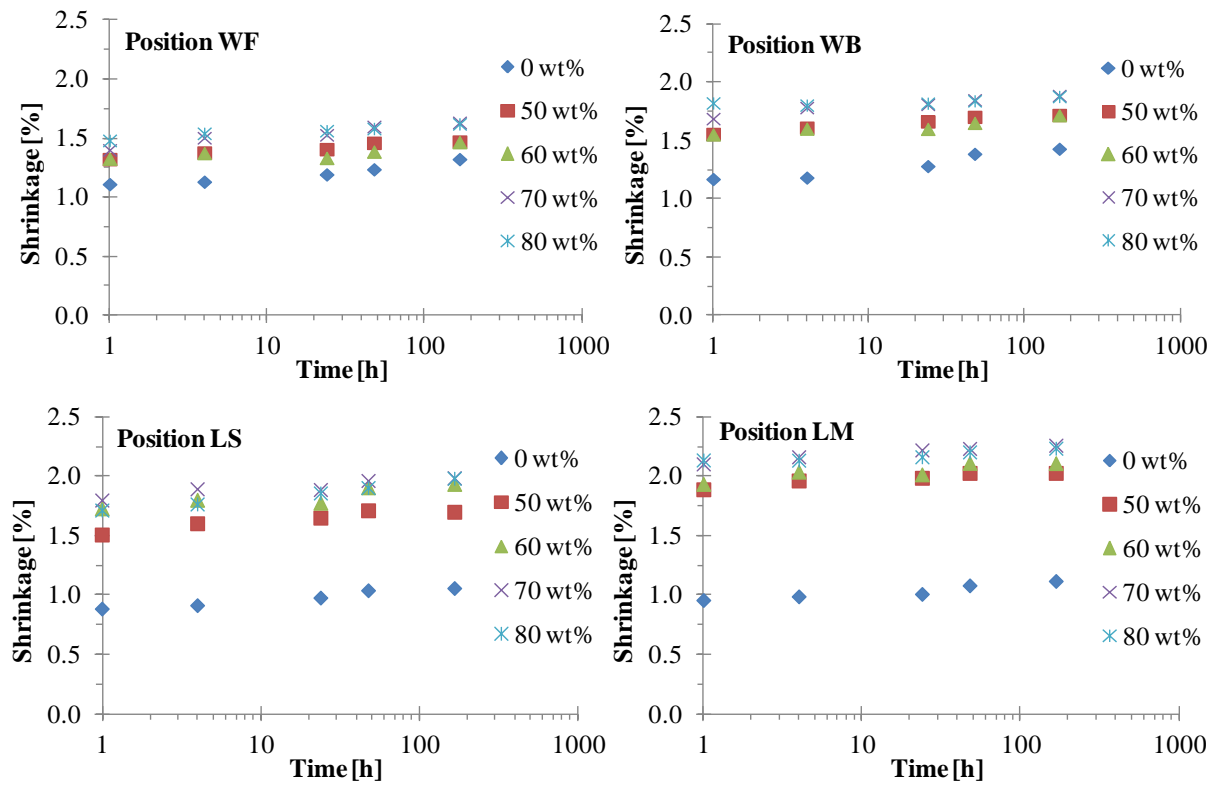
Figure 63. Shrinkage of rPP and all-PP(R) composite specimens having different fibre contents (50, 60, 70, 80 wt%) in different directions (WF: Width Front; WB: Width Back; LS: Length Side; LM: Length Middle)

Shrinkage of thermoplastic fibre-reinforced composites with different fibre volume content increased in all directions compared to that of the matrix material, which is in contrast to the shrinkage behaviour of conventional fibre-reinforced composites (*e.g.* glass fibre). This effect is attributed to the relaxation of the thermoplastic fibres. Shrinkage of the matrix material is approximately 1%, which is in agreement with the literature [147]. Increasing the thermoplastic fibre content resulted in higher shrinkage. The highest shrinkage occurred parallel to the flow direction at the middle of the specimen. As expected, the least shrinkage was observed near the gate due to the local pressure. Despite the increased technological shrinkage (measured 1 h after injection moulding) in fibre-reinforced composites, subsequent post shrinkage does not differ from that in unreinforced composites. Thus, calculating (with Equation 2) [134, 148] the proper shrinkage for the mould construction could make the part dimensions stable over long time.

$$S(t) = S_t + m \cdot \log(t), \qquad (2)$$

where S (t) is the shrinkage of the composite in time [1;168 h], S_t is the technological shrinkage and *m* is the slope of the post shrinkage (time factor).

Plotting the results an exponential relation between technological shrinkage (measured 1 h after the process) and fibre content can be deduced. Based on the observations Figure 64 and the time dependent behaviour description of the fibre reinforced materials.
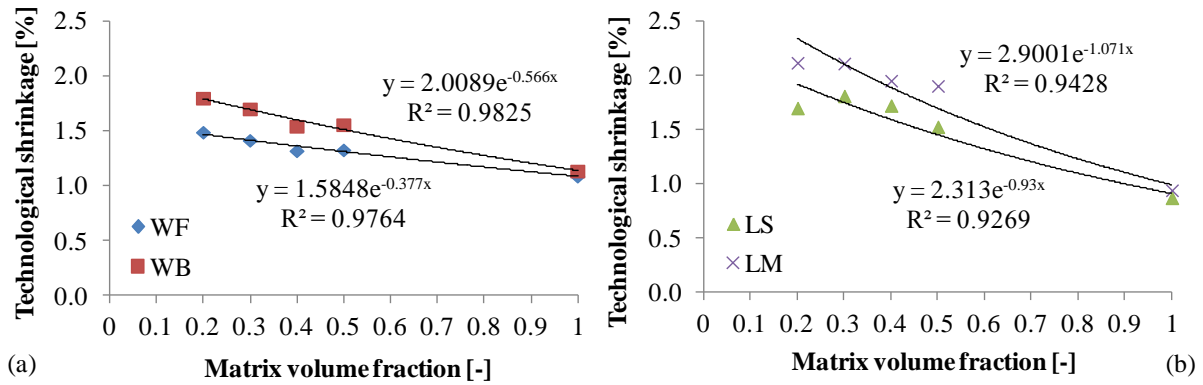
Figure 64. Technological shrinkage of the all-PP(R) composites as a functional of matrix volume fraction in perpendicular (a) and parallel (b) to the flow direction

The shrinkage of the all-PP(R) composites used in this study can be calculated with the following equation (3):

$$S(t) = C_1 \cdot e^{-C_2\left(1-\frac{\Phi}{100}\right)} + m \cdot \log(t),$$

(3)

where $S(t)$ is the shrinkage of the composite in time [1;168 h] and direction, C_1 is a constant which is proportional to the relaxation of the fibres, C_2 is a constant which is proportional to the fibre orientation in the specimen, Φ is the fibre content of the composite, and m is the slope of the post shrinkage (time factor).

Table 3 lists the value of the constants (C_1 and C_2) for different directions, which are data fitted coefficients.

	C1	C2
WF	1.6	0.4
WB	2.0	0.6
LS	2.3	0.9
LM	2.9	1.1

Table 4. Value of the C1 and C2 constant in different directions

3.3.3. Elastomeric polypropylene based all-PP composite (all-PP(E))

The results of the rPP based all-PP composites show that the processing temperature is a key parameter which affects the relaxation of the reinforcing fibres and thereby the resulting mechanical properties of the PP based all-PP composites. To produce all-PP composites with wider processing window (than for rPP) polypropylene-based thermoplastic elastomer was selected which ensures 50-70°C wider processing temperature range than for rPP.

Dynamic mechanical analysis (DMA)

DMA tests were done that show the effect of the different processing temperature to the all-PP(E) composites. The storage modulus and tanδ as a function of temperature are shown in Figure 65.
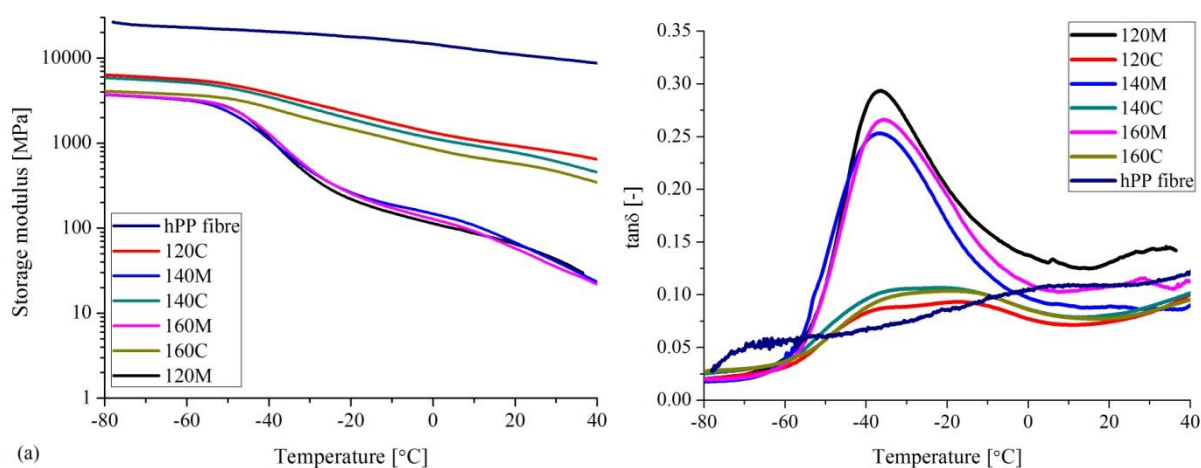
Figure 65. DMA traces of the all-PP(E) composites (70 wt%) (C) and ePP matrix (M) material injection moulded at different temperatures (120, 140, 160°C) compared to the DMA traces of the hPP fibre

The DMA traces evidenced that the matrix material can efficiently be reinforced by hPP fibres. Increasing processing temperature was accompanied with a decrease in the storage modulus that was attributed to the relaxation of the hPP fibres. The glass transition temperature of the matrix (T$_g$=-38°C based on the tanδ peak temperature) broadened by the hPP reinforcement and any peak value could hardly be determined.

Static tensile tests

Figure 66 shows the yield stress and tensile modulus of the all-PP(E) composites.
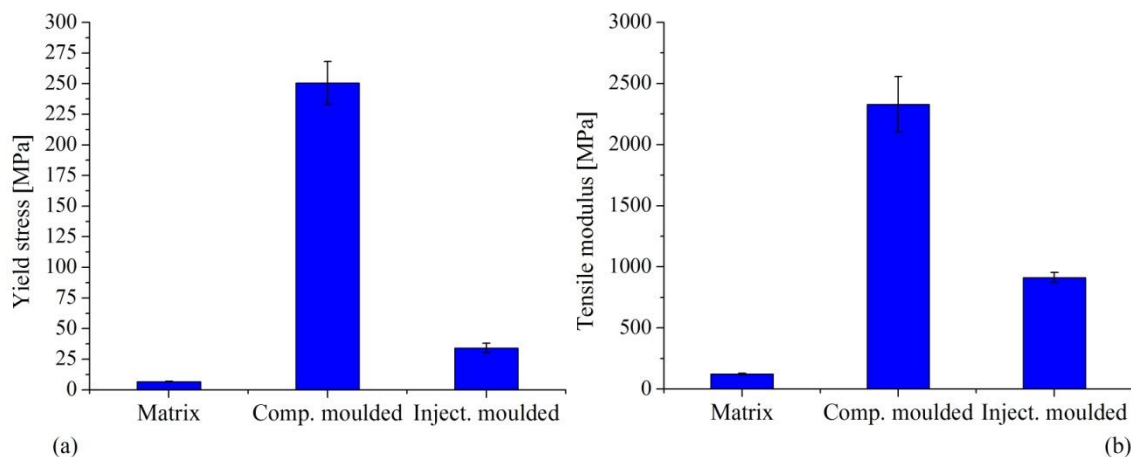
Figure 66. Yield stress (a) and tensile modulus (b) of the ePP matrix and all-PP(E) composites (70 wt%) produced by injection and compression moulding at 140°C

Using both compression and injection moulding the yield stress and the tensile modulus of the composites were increased significantly compared to the matrix material. Note that the mechanical parameters of the injection moulded all-PP(E) specimens agree with those conventional hPP grades (σ_Y=25-30 MPa, E=950-1000 MPa). The yield stress of the all-PP(E) composites in flow direction is shown in Figure 67.
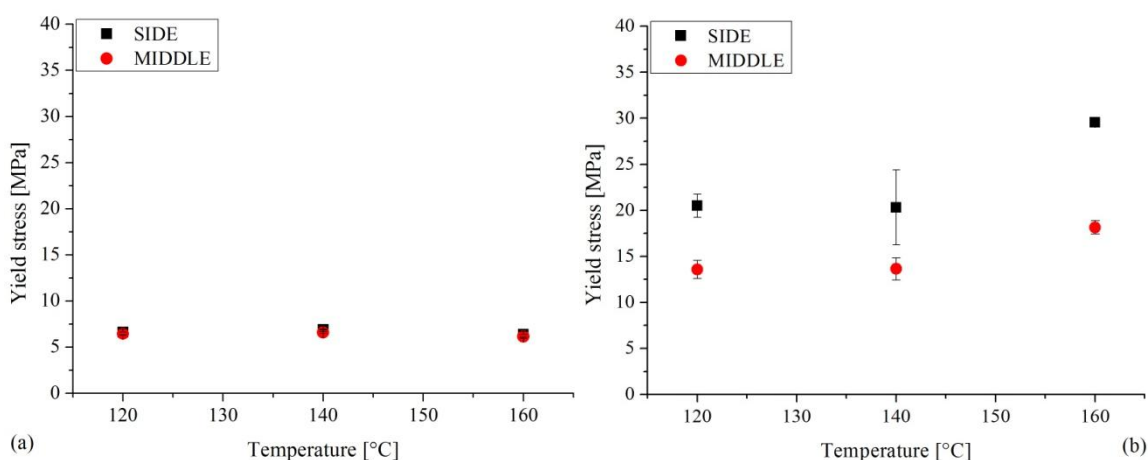
Figure 67. Yield stress, measured in flow direction at the side and middle sections, for the ePP matrix (a) and the all-PP(E) composites (70 wt%) (b) as a function of processing temperatures

It can be seen that the yield stress of the all-PP(E) composites depended on the processing temperature and on the analysed place of the plaque. With increasing processing temperature the yield stress values of the composites increased. Specimens injection moulded at 160°C showed a yield stress of about 30 MPa which is very close to that of conventional PP homopolymers [149]. The yield stress in the side region was higher than in the middle region when measured in flow direction. The yield stress of the matrix did not show orientation

77

dependence. The tensile modulus of the ePP matrix and all-PP(E) composites as a function of processing temperature and specimen cut-off are displayed in Figure 68.
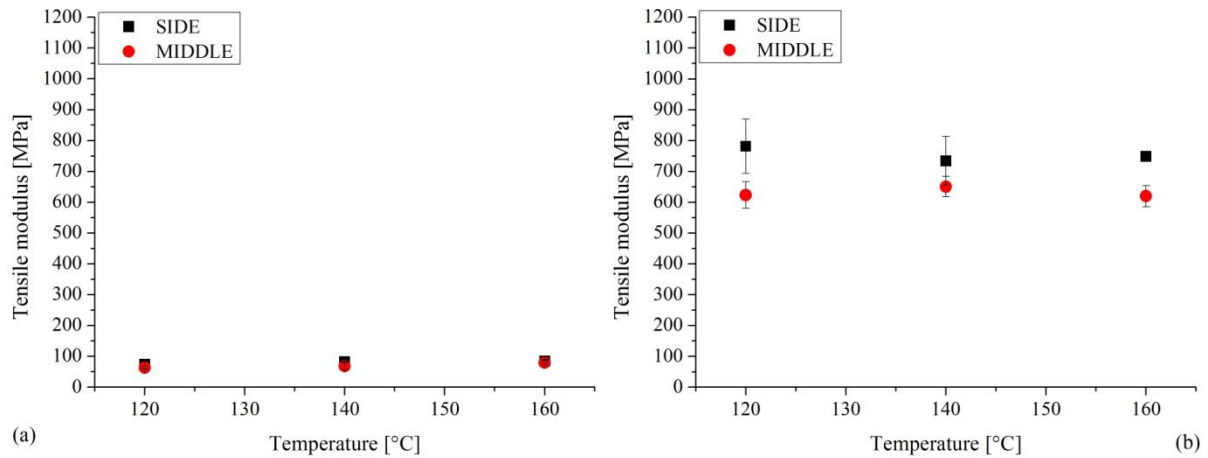
Figure 68. Tensile modulus, measured in flow direction at the side and middle sections, for the ePP matrix (a) and the all-PP(E) composites (70 wt%) as a function of processing temperatures

The tensile modulus of the composite in flow direction was significantly increased compared to the ePP matrix. Further difference between the moduli, measured in the side and the middle regions of the moulded plaques can also be determined for the composites. This can be attributed to the fibre alignment during the mould filling.

The yield stress data of the specimens measured perpendicular to the flow direction are given in Figure 69.
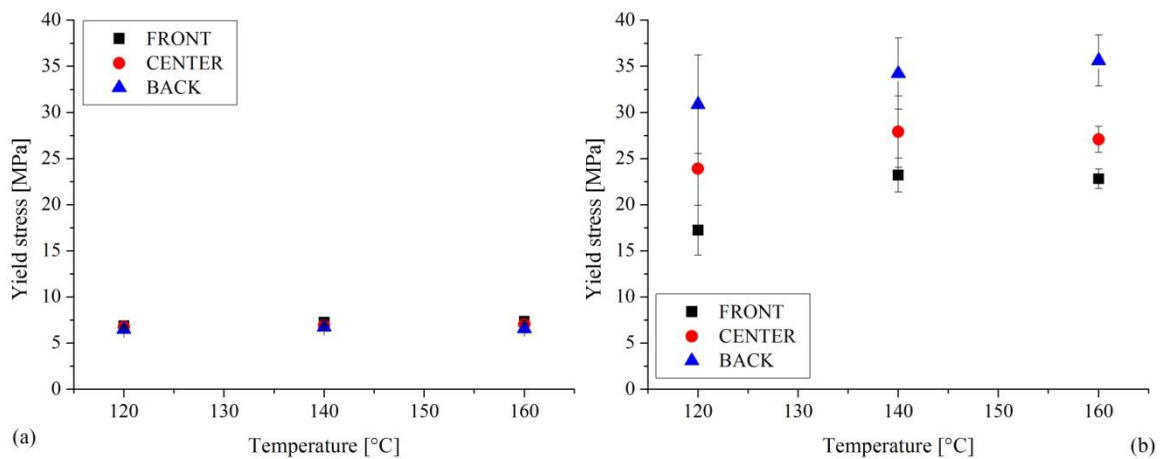
Figure 69. Yield stress, measured perpendicular to the flow direction at the front, centre and back sections, for the ePP matrix (a) and the all-PP(E) composites (70 wt%) (b) as a function of processing temperatures

Results in Figure 69 suggest that the mould filling process affected the mechanical properties via the related fibre alignment. The yield stress perpendicular to the flow direction depended on the analysed place. With increasing length from the gate the yield stress increased and

reached 35 MPa. The difference on the yield stress values in the front and the back regions were 12-15 MPa. With increasing processing temperature this difference slightly increased. The tensile moduli of the specimens determined perpendicular to the flow direction are displayed in Figure 70.
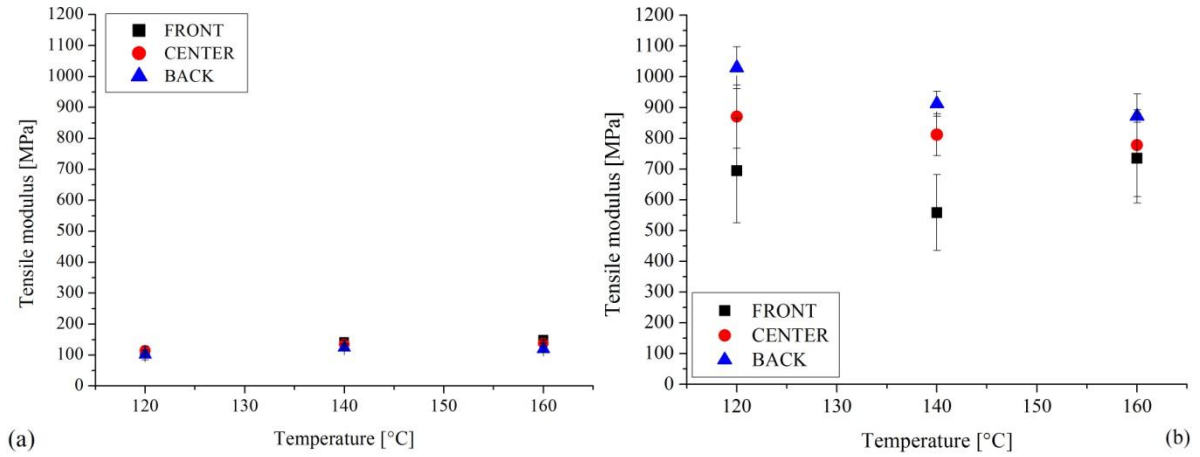
Figure 70. Tensile modulus measured perpendicular to the flow direction at the front, centre and back sections, for the ePP matrix (a) and the all-PP(E) composites (70 wt%) (b) as a function of processing temperatures

In case of the tensile moduli of the all-PP(E) composites significant difference was also observed perpendicular to the flow direction. This is again due to the effect of the fibre orientation which is different along the plaque. In the back region of composite plaque tensile moduli of 900-1000 MPa were achieved. By contrast, the tensile modulus of ePP did not change either with the processing temperature or with the position of specimen cut-off.

Instrumented falling weight impact tests (IFWI)

        Perforation energy of the ePP matrix and all-PP(E) composites are shown in Figure 71.
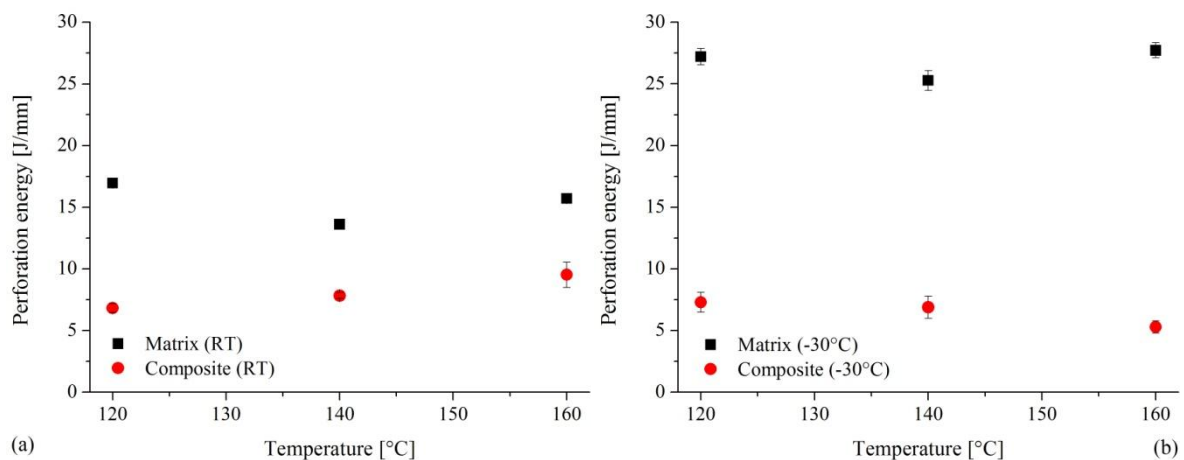
Figure 71. Perforation energy of the matrix (ePP) and all-PP(E) composite (70 wt%) at room temperature (a) and -30°C (b) as a function of processing temperature

Note that the perforation energy decreased at both room temperature and at -30°C for the composites compared to the neat matrix. Nonetheless, all values exceed that of the conventional random PP copolymer (0.5-1 J/mm). The processing temperature had small effect on the perforation energy of the matrix and related composites at both testing temperatures. Most striking feature is that the matrix material at -30°C showed markedly higher perforation energy than at room temperature. This is due to the fact that the testing temperature, -30°C, is very close to that of the T_g of the ePP which is associated with some "embrittlement".

Recall that according to the DMA results the storage modulus (see Figure 65) increased already in the vicinity of T_g (-38°C). This caused higher force values than at room temperature in the related IFWI fractograms (*cf.* Figure 72). For ductile polymers the toughness goes through a maximum at the T_g which is frequency dependent itself [150]. Note that the frequency range of the IFWI test is in kHz range (*cf.* Figure 72) which means already a shift in the T_g toward higher temperatures compared to the DMA (frequency: 1 Hz). Nonetheless, the typical failure occurred by plastic deformation of the ePP at both testing temperatures.
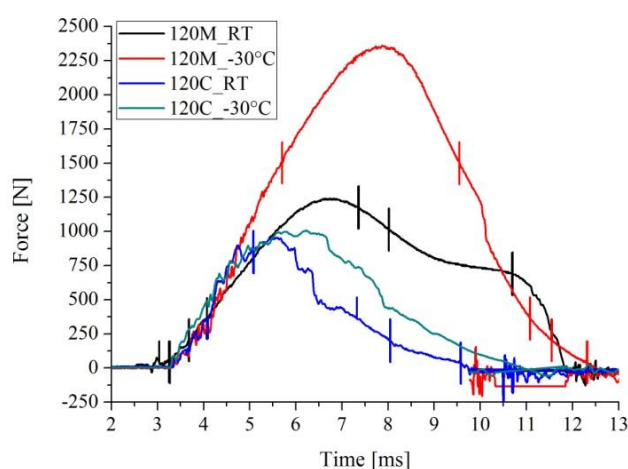
Figure 72. Force-time curves registered in IFWI testing at room temperature (RT) and -30°C for the ePP matrix (M) and all-PP(E) composite (C) injection moulded at 120°C

Light microscopy (LM)

LM frames taken from the polished cross sections of the all-PP(E) composites processed at different temperatures are shown in Figure 73.
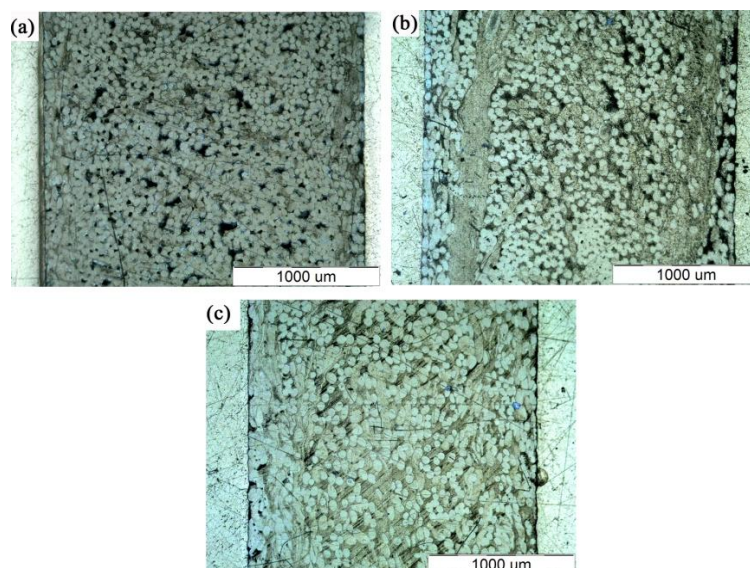
Figure 73. Cross sections of the all-PP(E) composites in flow direction (Side)
Designations: processing (melt) temperatures a) 120°C; b) 140°C; c) 160°C

The LM images in Figure 73 suggest that with increasing processing temperature the composites became better consolidated. It can be stated that skin-core effect on the cross section cannot be found contrast to injection moulded parts with rigid discontinuous fibres (such as glass) [151]. This effect can be attributed to the high fibre content (70 wt%) and the flexible reinforcement. The single fibres from the multifilament structure are disjoined gradually and form a quasi homogenous structure. Pictures from the central zone in flow direction (Figure 74) show that the single fibres are not laying perpendicular to the analysing plane.
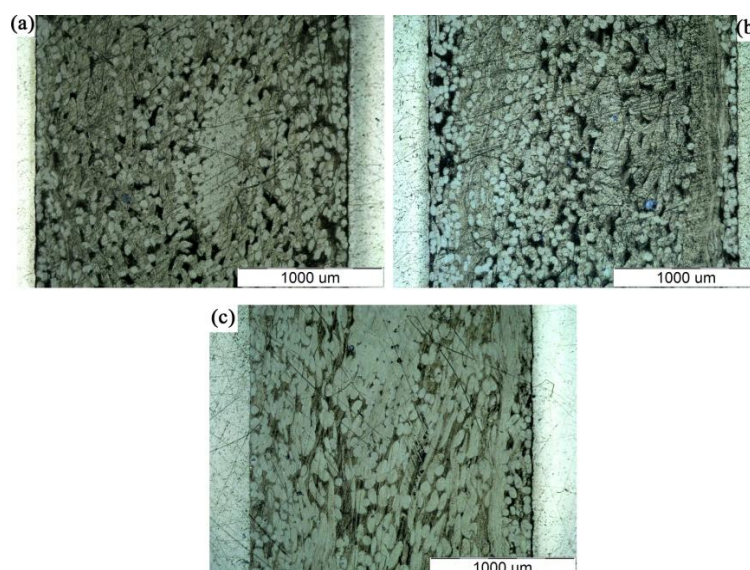
Figure 74. Cross sections of the all-PP(E) composites in flow direction in the middle region as a function of the processing temperature. Designations: processing temperatures: a) 120°C; b) 140°C; c) 160°C

81

In perpendicular direction to the flow in the front region LM pictures (Figure 75) showed the presence of skin layers. Their formation was likely caused by the difference in the thicknesses between the specimen (2.1 mm) and the fan gate (2 mm).
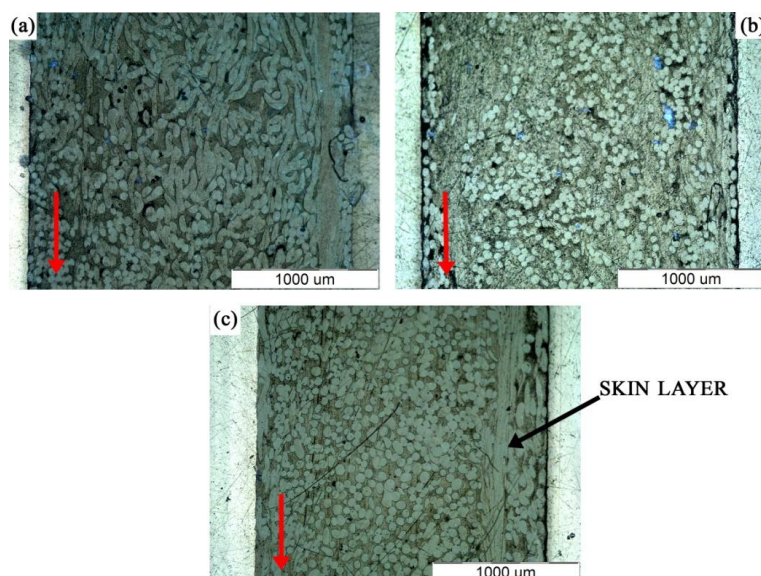
Figure 75. Cross sections of the all-PP(E) composite perpendicular to the flow direction in the front region produced at different processing temperatures: a) 120°C; b) 140°C; c) 160°C (Red arrows designate the flow direction)

It is the right place to underline that using a fan type and 2 mm thick gate markedly contributed to reduce the heat generation in the gate section (spare injection moulding can be achieved) and thus to maintain the hPP fibres.

Scanning electron microscopy (SEM)

Figure 76 shows the fracture surfaces (after tensile tests) of the all-PP(E) composites injection moulded at different temperatures.
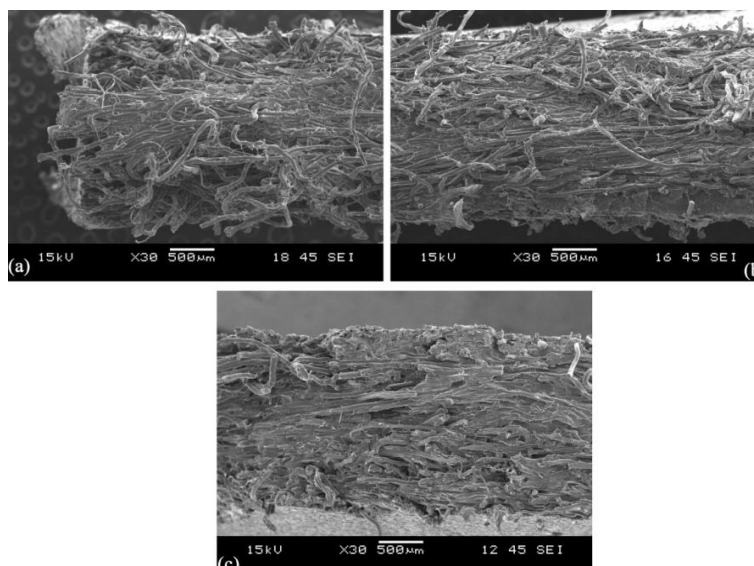
Figure 76. Fracture surfaces of the all-PP(E) composites injection moulded in the flow direction (Side) at a) 120°C; b) 140°C; c) 160°C

Similarly to the LM pictures a quasi-homogenous distribution of individual fibres can be found in the cross section and skin-core structure cannot be found. The reinforcing hPP fibres are well impregnated by the matrix and good adhesion exists between them (Figure 77).
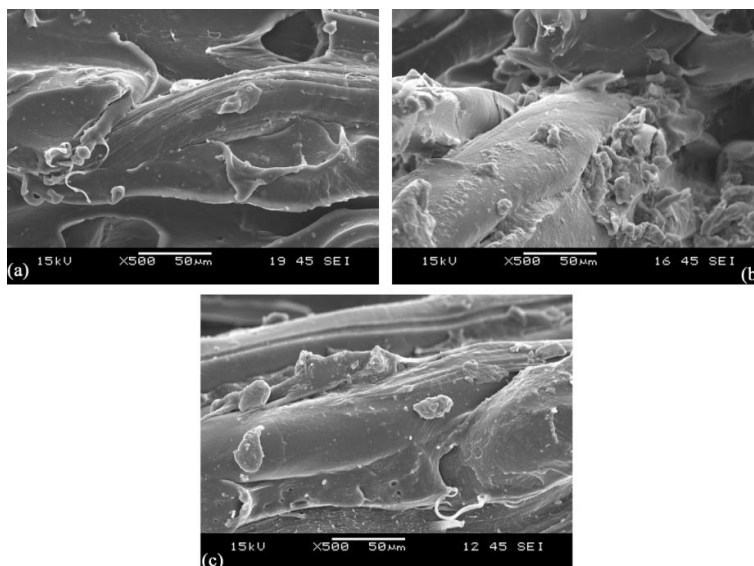
Figure 77. SEM pictures demonstrating the fibre/matrix adhesion on fracture surfaces of all-PP(E) composites injection moulded at a) 120°C; b) 140°C; c) 160°C in the flow direction (Side)

SEM pictures in Figure 77 confirm that the good mechanical performance of the all-PP(E) composites is guaranteed by the good fibre/matrix adhesion.

Shrinkage tests

The shrinkage of the injection moulded all-PP(E) specimens produced at different processing temperatures is demonstrated in Figure 78.
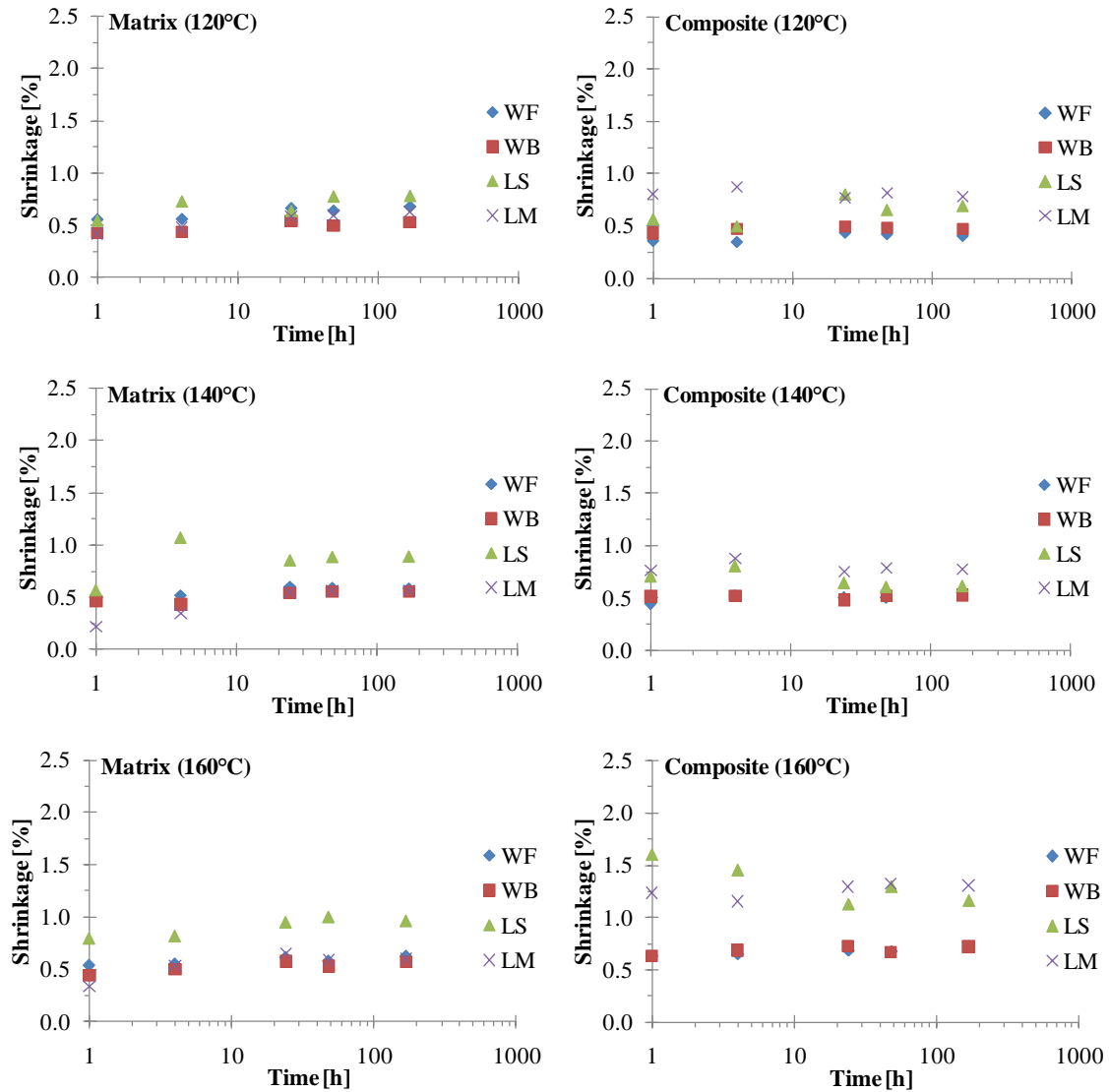
Figure 78. Shrinkage of the all-PP(E) composites at different processing temperature

The results show that the shrinkage data of the all-PP(E) composites at 120°C and 140°C are the same. The average shrinkage of the all-PP(E) composite at 120°C and 140°C was of ca. 0.8% which is in good agreemant with the shrinkage value of the conventional PP. The highest shrinkage was detected in longitudinal direction which is opposite to the glass fibre reinforced and glass bead filled products where the shrinkage (and warpage) in flow direction decreased. Injection moulding the composite at 160°C the shrinkage of the specimens

increased in longitudinal direction (also in side and middle locations) which can be assigned to the relaxation of thermoplastic fibres.

Like in the conventional fiber reinforced polymer composites the cross flow directional shrinkage does not changed significantly as the melt temperature increased. The flow directional shrinkage increased considerably as a function of the melt temperature because of the PP fiber relaxation (Figure 79).
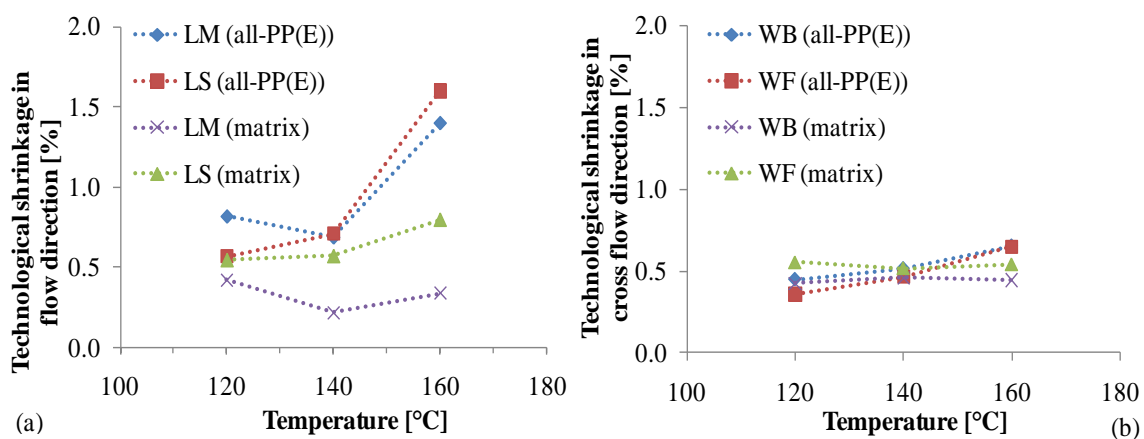
Figure 79. Technological shrinkage of the ePP matrix and all-PP(E) composite at different processing temperature and directions

4. Summary

The aim of my dissertation was to develop and characterize injection mouldable all-polypropylene composite. Further aim was to analyse the selected materials, the pre-product for injection moulding and to define the morphological and mechanical properties of injection moulded all-polypropylene composite.

Review of the literature of the self-reinforced materials and composites emphasized that reinforcing effect can be achieved by in- or *ex-situ* methods. *In-situ* reinforcing techniques (SCORIM, VIM) have not been spread widely because the designing the reinforcing part of the material is very difficult. Using ex-situ reinforcing (co-extrusion, film-stacking) limited geometries (e.g. sheet-like form pre- or final products) are available. Manufacturing of these are strongly limited (only thermoformed products with uniform wall thickness, *e.g.* shells, panels etc.). 3D products with complex geometry cannot be produced with conventional technologies (*e.g.* injection moulding).

To achieve my aims broad range of preliminary tests were done where in the first step material couples were chosen. My intention was to achieve the largest difference in melting temperature (processing window) between the matrix and thermoplastic reinforcement. Two kinds of material combination (rPP/PP (two types)) were applied. Both matrices and reinforcements were characterized by DSC tests. The results showed that the widest processing window was 20°C. The reinforcements were also analysed by single fibre and SEM/EDS tests. Based on the EDS results sizing agent exists on the surface of the Innegra S PP fibres.

To produce pre-product for injection moulding in the first series mixing technology was applied. The results showed that the hPP multifilament became roughened, formed agglomerates and a cold slug formed that blocked the standard flat nozzle during injection moulding. The reinforcement fibre content could not be guaranteed, and even distribution of reinforcement fibres could not be achieved.

In the next step new pre-product material was developed. To avoid agglomeration of reinforcing fibres, extrusion coating was applied prior to injection moulding in the second series with using rPP matrices. In case of PP systems coated multifilament was successfully produced and 0-40 wt% reinforcement content could be achieved. PP coated multifilament was granulated into 1-10 mm long cylindrical pellets and used for injection moulding. The PP based pre-product could be injection moulded (with using heated flat nozzle), and the results

showed that the thermoplastic reinforcement did not melt in the core section of the specimens during manufacturing.During the injection moulding tests with PP-based pre-product different parameters (applied processing temperature and fibre length, holding pressure) were analysed. The optimal processing temperature was determined as 160°C, where the processing method was stable and the reinforcing fibres kept their form. Varying the fibre length and holding pressure did not affect the mechanical properties. The mechanical tests of the all-PP systems revealed that a slight reinforcing effect (yield stress ~10% higher compared to that of the matrix) could be detected. The microscopy images showed that neither the distribution of the single fibres nor the impregnation of matrix material was perfect. These problems can be assigned to the improper impregnation of the coated pre-product; therefore it was concluded that the impregnation process had to be improved.

Based on the preliminary tests pre-impregnated PP-based pre-product was developed. From the selected random polypropylene matrix 50 µm thick film was produced using an extrusion film blowing technique. The matrix film and the reinforcing hPP multifilament were laminated prestressed onto an aluminium core with filament winding according to the film-stacking method, which resulted in unidirectionally aligned (UD) fibres. Different nominal fibre content (50-80 wt%) was set (by the number of the applied matrix foils) and thereafter this sandwich structure was consolidated at 180°C. The consolidated sheets were chopped for small pellets having a dimension of 5x5 mm. In order to investigate the effect of the reinforcing fibre length 70 wt% reinforcement containing all-PP(R) composites were also chopped for 5x2 and 5x 8 mm. Note that the length of the pre-products determined the length of the reinforcing fibres. From the pre-products 2.0 mm (all-PP(R) composites) thick 80 x 80 mm plaque specimens were injection moulded with an Arburg Allrounder 370S 700-290. To avoid cold slug formation heated, flat nozzle with holes 4 mm in diameter was used during injection moulding process. To compare the effect of the gate height on the characteristics of the produced injection moulded specimens two different gate types were used: conventional film gate (gate thickness: 1 mm) and fan gate (gate thickness: 2 mm).

With these new pre-impregnated pellets injection moulded products could be produced successfully. The mechanical tests showed that by increasing the fibre content (50-70 wt%) of the pre-product the yield stress and perforation energy significantly increased compared to the matrix material and the conventional hPP (TVK H388F) materials. By increasing the fibre length of the pre-product highest values (σ_Y=38 MPa) with lower deviation can be achieved when the reinforcing fibre length is 5 mm (stable injection moulding processing could be

achieved without injection plasticising problems). With 8 mm fibre length injection volume problem appeared. The applied fan gate resulted in more homogeneous tensile properties and greater perforation energy than the applied conventional film gate. Use of a 2 mm thick fan gate decreased the evolved heat in the gate region and thus contributed to the reinforcing efficiency of hPP fibres. The optical micrographs demonstrated that the fibre-matrix adhesion (impregnation) and single fibre distribution could be increased compared to the coated pre-product. Based on the results, all-PP composite showed greater shrinkage than the rPP matrix and the reinforcement did not decrease the shrinkage contrast to the conventional fibre reinforcement. This effect can be attributed to the relaxation of the thermoplastic reinforcement.

To achieve the wider (more than 20°C) processing window polypropylene based thermoplastic elastomer was applied as matrix material. From the ePP pellets a 50 µm thick foil was prepared by extrusion film-blowing and 70 wt% reinforcement content all-PP(E) composite was produced by filament winding and compression moulding (consolidation temperature was 140°C). From the consolidated plates chopped pellets were made in dimension of 5x5 mm and applied for injection moulding. During injection moulding tests the previously successfully applied fan gate was used. From the results it can be stated that PP-based thermoplastic elastomer is a suitable matrix material for all-polypropylene composites, since it ensures a wide processing window (~90°C). This processing window is by 50-70°C higher than that of the conventionally applied technologies (hot compaction, co-extrusion and film-stacking method). The shrinkage of the all-PP(E) composites was comparable with that of conventional polypropylene. The thermoplastic hPP worked as efficient reinforcement and significantly increased the yield stress and tensile modulus of the corresponding composites. The perforation energy of the all-PP(E) composite exceeds the values of the convention polypropylene at room temperature and at -30°C, as well. Light microscopy and SEM pictures demonstrated perfect single fibre distribution and good adhesion between the ePP matrix and the hPP fibres.

4.1. Theses

Based on the results, achieved in the framework of this PhD Thesis, the following theses have been deduced:

1st thesis

I have demonstrated that using cut, adequately pre-impregnated prefabricates with high fibre content (50-80 wt.%) polypropylene-based self-reinforced composites can be processed by traditional injection moulding [152-157].

2nd thesis

I have shown that converging melt flow sections during injection moulding (sprue, gate), affecting the fibres' orientation and distribution, govern the relaxation of the reinforcing polypropylene fibres, and thus the mechanical performance, namely the perforation impact energy, static yield strength and elastic modulus of the resulting self-reinforced composite mouldings. I have confirmed experimentally by selecting a 2 mm thick fan gate that the 80 wt% fibre containing self-reinforced polypropylene composites outperformed the corresponding matrix (random polypropylene copolymer). The perforation impact energy at room temperature and at -30°C was by more than 1100 and 900% higher, the static yield strength and elastic modulus at room temperature by more than 40% and 70% higher, respectively, of the composite than those of the matrix [156].

3rd thesis

I have demonstrated that the perforation impact energy of the self-reinforced polypropylene-based composites could be prominently enhanced, and especially at -30°C, when thermoplastic polypropylene-based elastomer served as matrix instead of random polypropylene copolymer of similar melt flow characteristics. Accordingly, the perforation impact energy values at room temperature and at -30°C proved to be by 100 and 150% higher, respectively, for the elastomer matrix-based than for the copolymer-based composites. This was attributed to the fact that the injection moulding processing window, defined as the difference between the melt temperatures of the reinforcing fibre and matrix, was markedly broader for the thermoplastic elastomer (ca. 70°C) than for the polypropylene copolymer (ca. 20°C) as well as the applied fan gate. As a consequence, self-reinforced composites with thermoplastic elastomer matrix could be injection moulded at lower temperatures than those with random polypropylene copolymer. This was associated with a low extent of relaxation of the reinforcing fibres via which the latter could maintain their efficient reinforcing in the moulded parts [157].

4th thesis

I have shown that the injection moulding-induced shrinkage of the all-polypropylene composites is higher than those with glass fibre reinforcements. This was argued to be an effect of heat shrinkage of the reinforcing fibres, the thermal expansion of which is markedly higher than those of glass fibres [156-157].

4.2. Applicability

In the recent decade, request for the environmental friendly and easily recyclable materials has been increased. The self-reinforced or all-polymer composites give a good alternative to replace materials in the automotive (*e.g.* underbody) and suitcase industry. Hitherto self-reinforced products only without undercut in sheet-like form have been produced. This new injection mouldable all-PP composite is assured to produce arbitrary 3D shapes in large-scale. The great impact behaviour of the polypropylene based composites provides better mechanical properties of the products (*e.g.* suitcase) than the conventional PP material especially below 0°C.

4.3. Further tasks to be solved

After summarizing and evaluating the results the following questions have risen:

- Further development of the all-PP pre-product. Pultrusion technology may be adopted to produce impregnated pre-products for injection moulding.
- In this work only polypropylene based materials were used (successfully) for injection moulding. The development should be extended for other materials as well (polyesters, polyamides, biodegradable materials etc.)
- Based on the literature analysis of the fracture and failure behaviourof the all-PP composites are also recommended.
- To analyze the reusing and recycling of the injection moulded all-PP composites

5. References

1. Directive 2000/53/EC of European Parliament and of the Council of 18 September 2000

2. Cvikovszky T., Nagy P., Gaál J.: A polimertechnika alapjai. Műegyetemi Kiadó, Budapest (2000).

3. Kmetty Á., Bárány T., Karger-Kocsis J.: Self-reinforced polymeric materials: A review. Progress in Polymer Science, 35, 1288-1310 (2010).

4. Pornnimit B., Ehrenstein G. W.: Extrusion of self-reinforced polyethylene. Advances in Polymer Technology, 11, 91-98 (1991).

5. Kornfield J., Kimata S., Sakurai T., Nozue Y., Kasahara T., Yamaguchi N., Karino T., Shibayama M.: Molecular Aspects of Flow-Induced Crystallization of Polymers. Progress of Theoretical Physics Supplement, 10-16 (2008).

6. Prox M., Pornnimit B., Varga J., Ehrenstein G. W.: Thermoanalytical investigations of self-reinforced polyethylene. Journal of Thermal Analysis, 36, 1675-1684 (1990).

7. Farah M., Bretas R. E. S.: Characterization of i-PP shear-induced crystallization layers developed in a slit die. Journal of Applied Polymer Science, 91, 3528-3541 (2004).

8. Huang H. X.: Continuous extrusion of self-reinforced high density polyethylene. Polymer Engineering and Science, 38, 1805-1811 (1998).

9. Huang H. X.: High property high density polyethylene extrudates prepared by self-reinforcement. Journal of Materials Science Letters, 17, 591-593 (1998).

10. McHugh A. J., Tree D. A., Pornnimit B., Ehrenstein G. W.: Flow-induced crystallization and self-reinforcement during extrusion. International Polymer Processing, 6, 208-211 (1991).

11. Huang H. X.: Self-reinforcement of polypropylene by flow-induced crystallization during continuous extrusion. Journal of Applied Polymer Science, 67, 2111-2118 (1998).

12. Čermák R., Obadal M., Habrová V., Stoklasa K., Verney V., Commereuc S., Fraïsse F.: Self-reinforcement of polymers as a consequence of elongational flow. Rheologica Acta, 45, 366-373 (2006).

13. Song J., Prox M., Weber A., Ehrenstein G.W.: Self-reinforcement of polypropylene. in 'Polypropylene: Structure, Blends and Composites' (eds.: Karger-Kocsis J.) Chapman and Hall, London, Vol 1, 271-291 (1994).

14. Prox M., Ehrenstein G. W.: Polypropylene beim Spritzgießen eigenverstärken. Kunststoffe, 81, 1057-1060 (1991).

15. Allan S. P., Bevis I. M., Zadhoush A.: The development and application of shear controlled orientation technology. Iranian Journal of Polymer Science and Technology, 4, 50-55 (1995).

16. Ogbonna C. I., Kalay G., Allan P. S., Bevis M. J.: The self-reinforcement of polyolefins produced by shear controlled orientation in injection-molding. Journal of Applied Polymer Science, 58, 2131-2135 (1995).

17. Lei J., Jiang C. D., Shen K. Z.: Biaxially self-reinforced high-density polyethylene prepared by dynamic packing injection molding. I. Processing parameters and mechanical properties. Journal of Applied Polymer Science, 93, 1584-1590 (2004).

18. Kalay G., Bevis M. J.: Processing and physical property relationships in injection molded isotactic polypropylene. 1. Mechanical properties. Journal of Polymer Science Part B-Polymer Physics, 35, 241-263 (1997).

19. Guan Q., Shen K. Z., Ji L. L., Zhu J. M.: Structure and properties of self-reinforced polyethylene prepared by oscillating packing injection-molding under low-pressure. Journal of Applied Polymer Science, 55, 1797-1804 (1995).

20. Guan Q., Zhu X. G., Chiu D., Shen K. Z., Lai F. S., McCarthy S. P.: Self-reinforcement of polypropylene by oscillating packing injection molding under low pressure. Journal of Applied Polymer Science, 62, 755-762 (1996).

21. Chen L. M., Shen K. Z.: Biaxial self-reinforcement of isotactic polypropylene prepared in uniaxial oscillating stress field by injection molding. I. Processing conditions and mechanical properties. Journal of Applied Polymer Science, 78, 1906-1910 (2000).

22. Kalay G., Bevis M. J.: Processing and physical property relationships in injection-molded isotactic polypropylene 2. Morphology and crystallinity. Journal of Polymer Science Part B-Polymer Physics, 35, 265-291 (1997).

23. Li Y. B., Chen J., Shen K. Z.: Self-reinforced isotactic polypropylene prepared by melt vibration injection molding. Polymer-Plastics Technology and Engineering, 47, 673-677 (2008).

24. Li Y. B., Shen K. Z.: Effect of low-frequency melt vibration on HDPE morphology. Polymer International, 58, 484-488 (2009).

25. Naundorf I., Eyerer P.: 'Living' or plastic hinges. in 'Polypropylene an A-Z Reference' (eds.: J. Karger Kocsis) Kluwer Publishers, Dordrecht, Vol 383-391 (1999).

26. Ward I. M., Coates P. D., Dumoulin M. M.: Solid Phase Processing of Polymers. Hanser, Munich (2000).

27. Farrell C. J., Keller A.: Direct ram extrusion of polyethylene; a correlation between chain-folding and tensile modulus. Journal of Materials Science, 12, 966-974 (1977).

28. Legros N., Ajji A., Dumoulin M. M.: Ram extrusion of high-density polyethylene and polypropylene in solid state: Process conditions and properties. Polymer Engineering and Science, 37, 1845-1852 (1997).

29. Li J. X., Lee Y. W.: Evolution of morpholgy in high-molecular-weight polyethylene during die drawing. Journal of Materials Science, 28, 6496-6502 (1993).

30. Taraiya A. K., Ward I. M.: The production and properties of die-drawn biaxially oriented polypropylene tubes. Plastics Rubber and Composites Processing and Applications, 15, 5-11 (1991).

31. Mohanraj J., Chapleau N., Ajji A., Duckett R. A., Ward I. M.: Production, properties and impact toughness of die-drawn toughened polypropylenes. Polymer Engineering and Science, 43, 1317-1336 (2003).

32. Taraiya A. K., Mirza M. S., Mohanraj J., Barton D. C., Ward I. M.: Production and properties of highly oriented polyoxymethylene by die-drawing. Journal of Applied Polymer Science, 88, 1268-1278 (2003).

33. Endo R., Kanamoto T.: Superdrawing of polytetrafluoroethylene virgin powder above the static melting temperature. Journal of Polymer Science Part B-Polymer Physics, 39, 1995-2004 (2001).

34. Bigg D. M., Smith E. G., Epstein M. M., Fiorentino R. J.: High modulus semi-crystalline polymers by solid-state rolling. Polymer Engineering and Science, 22, 27-33 (1982).

35. Ajji A., Legros N.: Solid-state forming of polypropylene. in 'Polypropylene an A-Z reference' (eds.: K. K. J.) Kluwer Publishers, Dordrecht, Vol 744-751 (1999).

36. Morawiec J., Bartczak Z., Kazmierczak T., Galeski A.: Rolling of polymeric materials with side constraints. Materials Science and Engineering a-Structural Materials Properties Microstructure and Processing, 317, 21-27 (2001).

37. Bartczak Z.: Deformation of high-density polyethylene produced by rolling with side constraints. I. Orientation behavior. Journal of Applied Polymer Science, 86, 1396-1404 (2002).

38. Bartczak Z., Morawiec J., Galeski A.: Deformation of high-density polyethylene produced by rolling with side constraints. II. Mechanical properties of oriented bars. Journal of Applied Polymer Science, 86, 1405-1412 (2002).

39. Bartczak Z., Morawiec J., Galeski A.: Structure and properties of isotactic polypropylene oriented by rolling with side constraints. Journal of Applied Polymer Science, 86, 1413-1425 (2002).

40. Galeski A.: Strength and toughness of crystalline polymer systems. Progress in Polymer Science, 28, 1643-1699 (2003).

41. Mohanraj J., Morawiec J., Pawlak A., Barton D. C., Galeski A., Ward I. M.: Orientation of polyoxymethylene by rolling with side constraints. Polymer, 49, 303-316 (2008).

42. Smith P., Lemstra P. J.: Ultrahigh-strength polyetylene filaments by solution spinning/drawing. 2. Influence of solvent on the drawability. Makromolekulare Chemie-Macromolecular Chemistry and Physics, 180, 2983-2986 (1979).

43. Barham P. J., Keller A.: High-Strength Polyethylene Fibers From Solution and Gel Spinning. Journal of Materials Science, 20, 2281-2302 (1985).

44. Pennings A. J., Vanderhooft R. J., Postema A. R., Hoogsteen W., Tenbrinke G.: High-speed gel-spinning of ultra-high molecular weight polyethylene. Polymer Bulletin, 16, 167-174 (1986).

45. Elyashevich G. K., Karpov E. A., Kudasheva O. V., Rosova E. Y.: Structure and time-dependent mechanical behavior of highly oriented polyethylene. Mechanics of Time-Dependent Materials, 3, 319-334 (1999).

46. Elyashevich K. G., Karpov A. E., Rosova Y. E., Streltses V. B.: Orientational crystallization and orientational drawing as strengthening methods for polyethylene. Polymer Engineering and Science, 33, 1341-1351 (1993).

47. Baranov A. O., Prut E. V.: Ultra-high modulus isotactic polypropylene. 1. The influence of orientation drawing and initial morphology on the structure and properties of oriented samples. Journal of Applied Polymer Science, 44, 1557-1572 (1992).

48. Morawiec J., Bartczak Z., Pluta M., Galeski A.: High-strength uniaxially drawn tapes from scrap recycled poly(ethylene terephthalate). Journal of Applied Polymer Science, 86, 1426-1435 (2002).

49. Marikhin V. A., Myasnikova L. P.: Structural basis of high-strength high-modulus polymers. in 'Oriented Polymer Materials' (eds.: S. Fakirov) Hüthing & Wepf Verlag Zug, Heidelberg, Vol 38-98 (1996).

50. Alcock B., Cabrera N. O., Barkoula N. M., Peijs T.: The effect of processing conditions on the mechanical properties and thermal stability of highly oriented PP tapes. European Polymer Journal, 45, 2878-2894 (2009).

51. Karger-Kocsis J., Wanjale S. D., Abraham T., Bárány T., Apostolov A. A.: Preparation and characterization of polypropylene homocomposites: Exploiting polymorphism of PP homopolymer. Journal of Applied Polymer Science, 115, 684-691 (2010).

52. Ward I. M.: Developments in oriented polymers, 1970-2004. Plastics Rubber and Composites, 33, 189-194 (2004).

53. Ward I. M., Hine P. J.: The science and technology of hot compaction. Polymer, 45, 1413-1427 (2004).

54. Hine P. J., Ward I. M.: High stiffness and high impact strength polymer composites by hot compaction of oriented fibers and tapes, in Mechanical Properties of Polymers based on Nanostructure and Morphology. in 'Mechanical properties of polymers based on nanostructure and morphology' (eds.: F. J. Baltá-Calleja and G. H. Michler) CRC Press, Boca Raton, Vol 1, 677-698 (2005).

55. Rasburn J., Hine P. J., Ward I. M., Olley R. H., Bassett D. C., Kabeel M. A.: The hot compaction of polyethylene terephthalate. Journal of Materials Science, 30, 615-622 (1995).

56. Rojanapitayakorn P., Mather P. T., Goldberg A. J., Weiss R. A.: Optically transparent self-reinforced poly(ethylene terephthalate) composites: molecular orientation and mechanical properties. Polymer, 46, 761-773 (2005).

57. Hine P. J., Ward I. M., El Matty M. I. A., Olley R. H., Bassett D. C.: The hot compaction of 2-dimensional woven melt spun high modulus polyethylene fibres. Journal of Materials Science, 35, 5091-5099 (2000).

58.   Hine P. J., Ward I. M., Jordan N. D., Olley R. H., Bassett D. C.: A comparison of the hot-compaction behavior of oriented, high-modulus, polyethylene fibers and tapes. Journal of Macromolecular Science-Physics, B40, 959-989 (2001).

59.   Hine P. J., Ward I. M.: Hot compaction of woven nylon 6,6 multifilaments. Journal of Applied Polymer Science, 101, 991-997 (2006).

60.   Al Jebawi K., Sixou B., Seguela R., Vigier G., Chervin C.: Hot compaction of polyoxymethylene, part 1: Processing and mechanical evaluation. Journal of Applied Polymer Science, 102, 1274-1284 (2006).

61.   El-Maaty M. I. A., Bassett D. C., Olley R. H., Hine P. J., Ward I. M.: The hot compaction of polypropylene fibres. Journal of Materials Science, 31, 1157-1163 (1996).

62.   Wright-Charlesworth D. D., Lautenschlager E. P., Gilbert J. L.: Hot compaction of poly(methyl methacrylate) composites based on fiber shrinkage results. Journal of Materials Science-Materials in Medicine, 16, 967-975 (2005).

63.   Ward I. M., Hine P. J.: Novel composites by hot compaction of fibers. Polymer Engineering and Science, 37, 1809-1814 (1997).

64.   Ratner S., Weinberg A., Marom G.: Neat UHMWPE filament wound composites by crosslinking compaction. Advanced Composites Letters, 12, 205-210 (2003).

65.   Karger-Kocsis J.: Interphase with lamellar interlocking and amorphous adherent - A model to explain effects of transcrystallinity. Advanced Composites Letters, 9, 225-227 (2000).

66.   Ratner S., Pegoretti A., Migliaresi C., Weinberg A., Marom G.: Relaxation processes and fatigue behavior of crosslinked UHMWPE fiber compacts. Composites Science and Technology, 65, 87-94 (2005).

67.   Orench I. P., Balta-Calleja F., Hine P. J., Ward I. M.: A microindentation study of polyethylene composites produced by hot compaction. Journal of Applied Polymer Science, 100, 1659-1663 (2006).

68.   Hine P. J., Ward I. M., Teckoe J.: The hot compaction of woven polypropylene tapes. Journal of Materials Science, 33, 2725-2733 (1998).

69.   Teckoe J., Olley R. H., Bassett D. C., Hine P. J., Ward I. M.: The morphology of woven polypropylene tapes compacted at temperatures above and below optimum. Journal of Materials Science, 34, 2065-2073 (1999).

70.   Jordan N. D., Olley R. H., Bassett D. C., Hine P. J., Ward I. M.: The development of morphology during hot compaction of Tensylon high-modulus polyethylene tapes and woven cloths. Polymer, 43, 3397-3404 (2002).

71.   Hine P. J., Ward I. M., Jordan N. D., Olley R., Bassett D. C.: The hot compaction behaviour of woven oriented polypropylene fibres and tapes. I. Mechanical properties. Polymer, 44, 1117-1131 (2003).

72.   Jordan N. D., Bassett D. C., Olley R. H., Hine P. J., Ward I. M.: The hot compaction behaviour of woven oriented polypropylene fibres and tapes. II. Morphology of cloths before and after compaction. Polymer, 44, 1133-1143 (2003).

73. Bozec L. Y., Kaang S., Hine P. J., Ward I. M.: The thermal-expansion behaviour of hot compacted polypropylene and polyethylene composites. Composites Science and Technology, 60, 333-344 (2000).

74. Hine P. J., Olley R. H., Ward I. M.: The use of interleaved films for optimising the production and properties of hot compacted, self reinforced polymer composites. Composites Science and Technology, 68, 1413-1421 (2008).

75. McKown S., Cantwell W. J.: Investigation of strain-rate effects in self-reinforced polypropylene composites. Journal of Composite Materials, 41, 2457-2470 (2007).

76. Prosser W., Hine P. J., Ward I. M.: Investigation into thermoformability of hot compacted polypropylene sheet. Plastics Rubber and Composites, 29, 401-410 (2000).

77. Romhány G., Bárány T., Czigány T., Karger-Kocsis J.: Fracture and failure behavior of fabric-reinforced all-poly(propylene) composite (Curv(R)). Polymers for Advanced Technologies, 18, 90-96 (2007).

78. Jenkins M. J., Hine P. J., Hay J. N., Ward I. M.: Mechanical and acoustic frequency responses in flat hot-compacted polyethylene and polypropylene panels. Journal of Applied Polymer Science, 99, 2789-2796 (2006).

79. Hine P. J., Astruc A., Ward I. M.: Hot compaction of polyethylene naphthalate. Journal of Applied Polymer Science, 93, 796-802 (2004).

80. Bárány T., Karger-Kocsis J., Czigány T.: Development and characterization of self-reinforced poly(propylene) composites: carded mat reinforcement. Polymers for Advanced Technologies, 17, 818-824 (2006).

81. Bárány T., Izer A., Karger-Kocsis J.: Impact resistance of all-polypropylene composites composed of alpha and beta modifications. Polymer Testing, 28, 176-182 (2009).

82. Izer A., Bárány T., Varga J.: Development of woven fabric reinforced all-polypropylene composites with beta nucleated homo- and copolymer matrices. Composites Science and Technology, 69, 2185-2192 (2009).

83. Izer A., Bárány T.: Hot consolidated all-PP composites from textile fabrics composed of isotactic PP filaments with different degrees of orientation. Express Polymer Letters, 1, 790-796 (2007).

84. Varga J.: Beta-modification of isotactic polypropylene: Preparation, structure, processing, properties, and application. Journal of Macromolecular Science Part B—Physics, 41, 1121-1171 (2002).

85. Varga J., Mudra I., Ehrenstein G. W.: Highly active thermally stable beta-nucleating agents for isotactic polypropylene. Journal of Applied Polymer Science, 74, 2357-2368 (1999).

86. Karger-Kocsis J. Composite composed of polypropylene reinforcement and polypropylene matrix and various production methods thereof. German Patent DE 102 37 803, 2007.

87. Bárány T., Izer A., Czigány T.: On consolidation of self-reinforced polypropylene composites. Plastics Rubber and Composites, 35, 375-379 (2006).

88. Varga J., Ehrenstein G. W., Schlarb A. K.: Vibration welding of alpha and beta isotactic polypropylenes: Mechanical properties and structure. Express Polymer Letters, 2, 148-156 (2008).

89. Abraham T. N., Siengchin S., Karger-Kocsis J.: Dynamic mechanical thermal analysis of all-PP composites based on beta and alpha polymorphic forms. Journal of Materials Science 43, 3697-3703 (2008).

90. Bhattacharyya D., Maitrot P., Fakirov S.: Polyamide 6 single polymer composites. Express Polymer Letters, 3, 525-532 (2009).

91. Chen J., Yang W., Yu G. P., Wang M., Ni H. Y., Shen K. Z.: Continuous extrusion and tensile strength of self-reinforced HDPE/UHMWPE sheet. Journal of Materials Processing Technology, 202, 165-169 (2008).

92. Zhang G., Jiang L., Shen K. Z., Guan Q.: Self-reinforcement of high-density polyethylene/low density polyethylene prepared by oscillating packing injection molding under low pressure. Journal of Applied Polymer Science, 71, 799-804 (1999).

93. Zhang G., Fu Q., Shen K. Z., Jian L., Wang Y.: Studies on blends of high-density polyethylene and polypropylene produced by oscillating shear stress field. Journal of Applied Polymer Science, 86, 58-63 (2002).

94. Zhang A. Y., Jisheng E., Allan P. S., Bevis M. J.: Enhancement in micro-fatigue resistance of UHMWPE and HDPE processed by SCORIM. Journal of Materials Science, 37, 3189-3198 (2002).

95. Capiati N. J., Porter R. S.: The concept of one polymer composites modelled with high density polyethylene. Journal of Materials Science, 10, 1671-1677 (1975).

96. Peijs T.: Composites for recyclability. Materials Today, 6, 30-35 (2003).

97. Alcock B., Cabrera N. O., Barkoula N. M., Loos J., Peijs T.: Interfacial properties of highly oriented coextruded polypropylene tapes for the creation of recyclable all-polypropylene composites. Journal of Applied Polymer Science, 104, 118-129 (2007).

98. Cabrera N., Alcock B., Loos J., Peijs T.: Processing of all-polypropylene composites for ultimate recyclability. Proceedings of the Institution of Mechanical Engineers Part L-Journal of Materials-Design and Applications, 218, 145-155 (2004).

99. Alcock B., Cabrera N. O., Barkoula N. M., Loos J., Peijs T.: The mechanical properties of unidirectional all-polypropylene composites. Composites Part A-Applied Science and Manufacturing, 37, 716-726 (2006).

100. Alcock B., Cabrera N. O., Barkoula N. M., Peijs T.: Low velocity impact performance of recyclable all-polypropylene composites. Composites Science and Technology, 66, 1724-1737 (2006).

101. Alcock B., Cabrera N. O., Barkoula N. M., Reynolds C. T., Govaert L. E., Peijs T.: The effect of temperature and strain rate on the mechanical properties of highly oriented polypropylene tapes and all-polypropylene composites. Composites Science and Technology, 67, 2061-2070 (2007).

102. Alcock B., Cabrera N. O., Barkoula N. M., Spoelstra A. B., Loos J., Peijs T.: The mechanical properties of woven tape all-polypropylene composites. Composites Part A-Applied Science and Manufacturing, 38, 147-161 (2007).

103. Alcock B., Cabrera N. O., Barkoula N. M., Wang Z., Peijs T.: The effect of temperature and strain rate on the impact performance of recyclable all-polypropylene composites. Composites Part B-Engineering, 39, 537-547 (2008).

104. Barkoula N. M., Alcock B., Cabrera N. O., Peijs T.: Fatigue properties of highly oriented polypropylene tapes and all-polypropylene composites. Polymers & Polymer Composites, 16, 101-113 (2008).

105. Karger Kocsis J.: Fatigue performance of polypropylene and related composites. in 'Polypropylene: An A-Z Reference' (eds.: J. Karger-Kocsis) Kluwer Publishers, Dordrecht, Vol 227-232 (1999).

106. Banik K., Abraham T. N., Karger-Kocsis J.: Flexural creep behavior of unidirectional and cross-ply all-poly(propylene) (PURE(R)) composites. Macromolecular Materials and Engineering, 292, 1280-1288 (2007).

107. Banik K., Karger-Kocsis J., Abraham T.: Flexural creep of all-polypropylene composites: Model analysis. Polymer Engineering and Science, 48, 941-948 (2008).

108. Kim K. J., Yu W. R., Harrison P.: Optimum consolidation of self-reinforced polypropylene composite and its time-dependent deformation behavior. Composites Part A-Applied Science and Manufacturing, 39, 1597-1605 (2008).

109. Cabrera N. O., Alcock B., Klompen E. T. J., Peijs T.: Filament winding of co-extruded polypropylene tapes for fully recyclable all-polypropylene composite products. Applied Composite Materials, 15, 27-45 (2008).

110. Cabrera N., Reynold C. T., Alcock B., Peijs T.: Non-isothermal stamp forming of continuous tape reinforced all-polypropylene composite sheet. Composites Part A, 39, 1455-1466 (2008).

111. Alcock B., Cabrera N., Barkoula N., Peijs T.: Direct forming of all-polypropylene composites products from fabrics made of co-extruded tapes. Applied Composite Materials, 16, 117-134 (2009).

112. Cabrera N. O., Alcock B., Peijs T.: Design and manufacture of all-PP sandwich panels based on co-extruded polypropylene tapes. Composites Part B-Engineering, 39, 1183-1195 (2008).

113. Shalom S., Harel H., Marom G.: Fatigue behaviour of flat filament-wound polyethylene composites. Composites Science and Technology, 57, 1423-1427 (1997).

114. Houshyar S., Shanks R. A.: Morphology, thermal and mechanical properties of poly(propylene) fibre-matrix composites. Macromolecular Materials and Engineering, 288, 599-606 (2003).

115. Houshyar S., Shanks R. A.: Tensile properties and creep response of polypropylene fibre composites with variation of fibre diameter. Polymer International, 53, 1752-1759 (2004).

116. Houshyar S., Shanks R. A., Hodzic A.: Tensile creep behaviour of polypropylene fibre reinforced polypropylene composites. Polymer Testing, 24, 257-264 (2005).

117. Houshyar S., Shanks R. A., Hodzic A.: Influence of different woven geometry in poly(propylene) woven composites. Macromolecular Materials and Engineering, 290, 45-52 (2005).

118. Houshyar S., Shanks R. A.: Mechanical and thermal properties of flexible poly(propylene) composites. Macromolecular Materials and Engineering, 291, 59-67 (2006).

119. Houshyar S., Shanks R. A.: Mechanical and thermal properties of toughened polypropylene composites. Journal of Applied Polymer Science, 105, 390-397 (2007).

120. Bárány T., Izer A., Czigány T.: High performance self-reinforced polypropylene composites. Materials Science Forum, 567-538, 121-128 (2007).

121. Izer A., Bárány T.: Effect of consolidation on the flexural creep behaviour of all-polypropylene composite. Express Polymer Letters, 4, 210-216 (2010).

122. Kitayama T., Utsumi S., Hamada H., Nishino T., Kikutani T., Ito H.: Interfacial properties of PP/PP composites. Journal of Applied Polymer Science, 88, 2875-2883 (2003).

123. Wu C. M., Chen M., Karger-Kocsis J.: Interfacial shear strength and failure modes in sPP/CF and iPP/CF microcomposites by fragmentation. Polymer, 42, 129-135 (2001).

124. Bárány T., Izer A., Menyhárd A.: Reprocessability and melting behaviour of self-reinforced composites based on PP homo and copolymers. Journal of Thermal Analysis and Calorimetry, 101, 255-263 (2010).

125. Ruan W. H., Zhang M. Q., Wang M. H., Rong M. Z., Bárány T., Czigány T.: Preparation and properties of nano-silica filled self-reinforced polypropylene. Advanced Materials Research, 47, 318-321 (2008).

126. Pegoretti A. Z. A., Migliaresi C.: Preparation and tensile mechanical properties of unidirectional liquid crystalline single-polymer composites. Composites Science and Technology, 66, 1970-1979 (2006).

127. Pegoretti A., Zanolli A., Migliaresi C.: Flexural and interlaminar mechanical properties of unidirectional liquid crystalline single-polymer composites. Composites Science and Technology, 66, 1953-1962 (2006).

128. Pegoretti A.: Trends in composite materials: the challenge of single-polymer composites. Express Polymer Letters, 1, 710-710 (2007).

129. Matabola K. P., de Vries A. R., Luyt A. S., Kumar R.: Studies on single polymer composites of poly(methyl methacrylate) reinforced with electrospun nanofibers with a focus on their dynamic mechanical properties. Express Polymer Letters, 5, 635-642 (2011).

130. Chen J. C., Wu C. M., Pu F. C., Chiu C. H.: Fabrication and mechanical properties of self-reinforced poly(ethylene terephthalate) composites. Express Polymer Letters, 5, 288-237 (2011).

131. Wu C. M., Chang C. Y., Wang C. C., Lin C. Y.: Optimum consolidation of all-polyester woven fabric-reinforced composite laminates by film stacking. Polymer Composites, 33, 245-252 (2012).

132. Kovács J. G., Solymossy B.: Effect of Glass Bead Content and Diameter on Shrinkage and Warpage of Injection-Molded PA6. Polymer Engineering and Science, 49, 2218-2224 (2009).

133. Kovács J. G.: Shrinkage Alteration Induced by Segregation of Glass Beads in Injection Molded PA6: Experimental Analysis and Modeling. Polymer Engineering and Science, 51, 2517-2525 (2011).

134. Kovács J. G.: Fröccsöntött termékek tervezése és szimulációja. PhD Thesis. BME (2007).

135. Sikló B., Cameron K., Kovács J. G.: Deformation analysis of short glass fiber-reinforced polypropylene injection-molded plastic parts. Journal of Reinforced Plastics and Composites, 30, 1367-1372 (2011).

136. Jansen K. M. B., Van Dijk D. J., Freriksen M. J. A.: Shrinkage anisotropy in fiber reinforced injection molded products. Polymer Composites, 19, 325-334 (1998).

137. Kovács J. G., Sikló B.: Test method development for deformation analysis of injection moulded plastic parts. Polymer Testing, 30, 543-547 (2011).

138. Sikló B.: Fröccsöntött termékek vetemedésének mérési módszerei és csökkentési lehetőségei. PhD Thesis. BME (2012).

139. Kovács J. G., Sikló B.: Investigation of cooling effect at corners in injection molding. International Communications in Heat and Mass Transfer, 38, 1330-1334 (2011).

140. Bánhegyi G.: Szállal erősített műanyagok. Műanyagipari Szemle, 4, 16-18 (2005).

141. Thomason J. L.: The influence of fibre length and concentration on the properties of glass fibre reinforced polypropylene: 5. Injection moulded long and short fibre PP. Composites Part a-Applied Science and Manufacturing, 33, 1641-1652 (2002).

142. Thomason J. L.: The influence of fibre length and concentration on the properties of glass fibre reinforced polypropylene. 6. The properties of injection moulded long fibre PP at high fibre content. Composites Part a-Applied Science and Manufacturing, 36, 995-1003 (2005).

143. Thomason J. L.: The influence of fibre length and concentration on the properties of glass fibre reinforced polypropylene: 7. Interface strength and fibre strain in injection moulded long fibre PP at high fibre content. Composites Part a-Applied Science and Manufacturing, 38, 210-216 (2007).

144. Kumar K. S., Bhatnagar N., Ghosh A. K.: Development of long glass fiber reinforced polypropylene composites: Mechanical and morphological

characteristics. Journal of Reinforced Plastics and Composites, 26, 239-249 (2007).

145. Bürkle E., Sieverding M., Mitzler J.: Hosszú üvegszállal erősített PP fröccsöntése. Műanyag és Gumi, 40, 308-310 (2003).

146. Bernd H., Wunder H.: Tulajdonságok javítása hosszú üvegszál erõsítéssel a hőre lágyuló műanyagok példáján. Műanyag és Gumi, 41, 11-15 (2004).

147. Karian H. G.: Part shrinkage behavior of polypropylene resins and polypropylene composites. in 'Handbook of polypropylene and polypropylene composites' (eds.: H. G. Karian) Marcel Dekker, New York, Vol 19, 675-706 (2003).

148. Relling M., Belina K., MC. Crindle R.: Fröccsöntési paraméterek hatása izotaktikus polipropilén (iPP) hosszú idejű zsugorodására. Műanyag és Gumi, 40, 71-73 (2003).

149. Ehrenstein G. W.: Polymeric Materials. Hanser, Munich (2001).

150. Karger-Kocsis J., Friedrich K.: Temperature and strain rate effects on the fracture toughness of PEEK and its short glass fibre reinforced composite. Polymer, 27, 1753-1760 (1986).

151. Gibson A. G.: Processing and properties of reinforced polypropylenes. in 'Polypropylene' (eds.: J. Karger Kocsis) Chapman&Hall, Cambridge, Vol 3, 82-90 (1995).

152. Izer A., Kmetty Á., Bárány T.: Környezetbarát önerősítéses polimer kompozitok. Műanyag és Gumi, 45, 463-467 (2008).

153. Kiss Z., Kmetty Á., Bárány T.: Investigation of the weldability of the self-reinforced polypropylene composites. Materials Science Forum, 659, 25-30 (2010).

154. Kmetty Á., Bárány T.: Fröccsöntéssel feldolgozható önerősítéses polipropilén kompozit fejlesztése. Műanyag és Gumi, 48, 331-334 (2011).

155. Bocz K., Toldy A., Kmetty Á., Bárány T., Igricz T., Marosi G.: Development of flame retarded self-reinforced composites from automotive shredder plastic waste. Polymer Degradation and Stability, 97, 221-227 (2012).

156. Kmetty Á., Tábi T., Kovács J. G., Bárány T.: Development and characterisation of injection moulded all-polypropylene composites. Express Polymer Letters,7, 134-145, (2013).

157. Kmetty Á., Bárány T., Karger-Kocsis J.: Injection moulded all-polypropylene composites composed of polypropylene fibre and polypropylene based thermoplastic elastomer. Composites Science and Technology, 73, 72-80 (2012).

158. Huang H. X.: Mechanical anisotropy of self-reinforced polyethylene crystallized during continuous-melt extrusion. Journal of Materials Science Letters, 18, 225-228 (1999).

159. Hine P., Broome V., Ward I.: The incorporation of carbon nanofibres to enhance the properties of self reinforced, single polymer composites. Polymer, 46, 10936-10944 (2005).

6. Appendices

Num.	Processing	Materials	Processing conditions	Results	Comment	Ref.
1	Self-reinforced extrusion	HDPE	Entrance semi-angel of 45°, p= 60-100 MPa, T_{mould}= 180°C	σ_B= 160 MPa, E_t= 2-17 GPa	Fibrillar structure (next to the die wall), Shish-kebab structure	[4]
			Entrance semi-angel of 60°, p= 30-60 MPa, T_{mould}= 128°C	σ_B= 130-192 MPa,	Fibrillar structure, Micro hardness and light permeability are increasing	[8-9, 158]
		PP	p= 30-70 MPa, T= 160°C v= 160-200 mm/min	σ_B=60 MPa, E_t= 3.3 GPa	-	[13]
2	Self-reinforced injection moulding	hPP	T_{melt}= 160-190°C, T_{mould}= 25-80°C,	σ_B= 62-95 MPa, E_t= 2-3 GPa	-	[13-14]
3	SCORIM /OPIM	HDPE	T_{melt}= 140-180°C, p_{proc}= 25-28 MPa T_{mould}= 40-60°C	$\sigma_{B,L}$= 24-29 MPa, $a_{cN,L}$= 5-6 kJ/m^2, $\sigma_{B,T}$= 25-30 MPa, $a_{cN,T}$= 5-6 kJ/m^2	Static packing	[17]
				$\sigma_{B,L}$= 36-56 MPa, $a_{cN,L}$=8-14 kJ/m^2 $\sigma_{B,T}$= 23-36 MPa, $a_{cN,T}$= 2-3 kJ/m^2	Dynamic packing (f=0.2-0.5 Hz)	
			p_{proc}= 32-48 MPa, T_{melt}= 220°C, T_{mould}=42°C,	σ_B= 70-90 MPa, E_t= 3-6 GPa		[19]
		PP	T_{mould}= 42°C, T_{melt}= 210-240°C,	σ_B= 34-35 MPa	Static packing	[20]
				σ_B= 47-53 MPa	Dynamic packing (f= 0.3-1 Hz)	
		iPP	T_{mould}= 20-80°C, p_{proc}= 40 MPa,	$\sigma_{B,L}$= 44 -55 MPa, $a_{cN,L}$= 7-13 kJ/m^2 $\sigma_{B,T}$= 35-45 MPa, $a_{cN,T}$= 2-3 kJ/m^2	Dynamic packing f=0.125-0.5 Hz	[21]
		PP copolymer	p_{proc}= 100 MPa, T_{mould}= 60-110°C, T_{melt}= 220-250°C,	σ_y= 50-59 MPa, E_t= 2-3 GPa	Different packing mode	[18, 22]
		iPP	p_{proc}= 100-160 MPa, T_{mould}= 60°C, T_{melt}= 205-250°C,	σ_y= 38-77 MPa, E_t= 2-3 GPa	Different packing mode	
4	VIM	iPP	p_{proc}= 100 MPa, T_{mould}= 40°C, T_{melt}= 210-230°C, f= 0-2.5 Hz, p_A=0-73.5 MPa	σ_y= 32-38 MPa, a_{cN}=11-32 kJ/m^2	-	[23]
		HDPE	p_{proc}= 39.5 MPa, T_{mould}= 40°C, T_{melt}= 180-200°C, f= 0-2.33 Hz, p_A=0-59.4 MPa	Crystallinity= 60-70%	Laminar and shish-kebab structure	[24]

Table 5. Production method, conditions and product characteristics of single-component SRPMs produced in one-step (in-situ)

Num.	Process	Materials	Processing conditions	Results	Comment	Ref.
1	Ram extrusion	HDPE	Entrance semi-angel of 30°, p=40-110 MPa, T=90-120°C	E_t=0.2-0.9 GPa	high friction, low extrusion rates	[26]
		HDPE	p=0-100 MPa, λ=3.75-6, T=105°C	E_t=1.1 GPa, Thermal conductivity = 0.4-0.5 W/mK	thermal relaxation after leaving the die	[28]
		PP	p=0-100 MPa, λ=3.75-6 , T=130°C	E_t=1.7 GPa, Thermal conductivity = 0.1 W/mK	lubrication applied	[28]
2	Hydrostatic extrusion	UHMPE	v=1-50 cm/min, p=0-250 MPa	E_t=10-60 GPa	batch process	[26]
3	Die-drawing	HMWPE	λ=1-13, T= 115°C	λ=1-7 elongated spherules λ=7-12 lamella structure	decreased creep	[29]
		PP	λ=6-11, T= 200°C	E_t=1-12 GPa	increased tenacity	[30-31]
		POM	Entrance semi-angel of 5-20°, λ= 1-16	E_b=3-26 GPa	increased crystallinity	[32]
4	Super drawing	PTFE	λ=6-160	E_t=38-102 GPa, σ_B=0.7-1.4 GPa	increased crystallinity	[33]
5	Rolling	HDPE	λ=2-9	E_t=3-15 GPa, σ_B=30-290 MPa	increased crystallinity	[26, 36-38]
		PP	λ=2-9	E_t=4-10 GPa, σ_B=30-350 MPa	increased crystallinity	[26, 39]
6	Gel drawing	UHMWPE	λ=3-22	E_t=10-90 GPa, σ_B=0.3-3.5 GPa	increased crystallinity	[42-44]
7	Orientation drawing	HDPE	T_D=110-120°C, λ=5.8-30	E_t=6-35 GPa, σ_B=250-1200 MPa	micro-cracking	[45-46]
		iPP	T_D=163-164°C, λ=21.5-35.5	E_t=18.5-24.7 GPa, σ_B=0.6-1.1 GPa	physical aging	[47]
8	Hot compaction	UHMPE*	T_{proc}=134-154°C, p=0.7-21 MPa	E_t=9.9-85 GPa, σ_B=200 MPa	unidirectional, woven structure	[54, 57-58, 63, 67, 70]
		UHMWPE	T_{proc}=145°C, p=31-49 MPa	E_t=0.4 GPa, σ_B=3.7 MPa	crosslinked	[64, 66]
		PP*	T_{proc}=164-195°C, p=1.1-14 MPa	E_t=1.6-3.9 GPa, σ_B=25-168 MPa	high acoustic output	[61, 68, 71-78]
		PET	T_{proc}=249-256°C, p=1.9-32.4 MPa	E_t=11.5-13 GPa, $\sigma_{B,T}$=15-35 MPa	good adhesion	[55]
		PEN	T_{proc}=268-276°C,	E_t=2-9.6 GPa, σ_B=22-207 MPa	0/90 multifilament	[54, 79]
		PA-6.6	p=2.8 MPa	E_t=4.1 GPa, σ_B=50 MPa	woven structure	[59]
		PPS	$T_{proc,opt}$=288°C,	E_t=5.2 GPa, σ_B=80 MPa	chemical resistance	[54]
		PP/CNF	T_{proc}=230°C, T_{mold}=190°C	E_t=1.5-2.7 GPa	2, 4, 6, 10, 20 wt% of CNF	[159]
		POM	$T_{proc,opt}$=182°C	E_t=1.9-5.3 GPa,	POM powder	[60]
		PMMA	T_{proc}=100-125°C	σ_B =65-165 MPa	unidirectional structure	[62]
		PEEK	$T_{proc,opt}$=347°C	E_t=3.65 GPa ,σ_B=100 MPa	woven structure	[54]
9	Film-stacking	β-PP/α-iPP	T_{proc}=150-170°C, p=7 MPa	$E_{t,L}$=2.4-2.7 GPa, $\sigma_{B,L}$=20-100 MPa $E_{t,T}$=1.6-2.4 GPa, $\sigma_{B,T}$=20-43 MPa	carded needle-punched mat	[80]
		β-PP/PP	T_{proc}= 156-186°C, p=7 MPa	E_t=2.5-3 GPa, σ_Y=90-100 MPa	PP woven textile	[81-82]
		iPP/iPP	T_{proc}=160-170°C, p=6 MPa	E_t=2.1-2.5 GPa, σ_B=29-140MPa	knitted, carded and needle punched mats	[83]
		β-PP/α-PP	T_{proc}=160°C, p=7 MPa	E_t=2.3 GPa, σ_B=60 MPa	winding	[89]

Table 6. Production methods, conditions and product characteristics of single-component SRPMs produced in multi-step (ex situ); *Summerized results

Num.	Processing	Materials	Processing conditions	Results	Comment	Ref.
1	Self-reinforced extrusion	HDPE/UHMWPE	T_{proc}=125-180°C, p=2…30 MPa	σ_B=20-170 MPa	specially designed fish-tail shaped extrusion die	[91]
2	SCORIM/ OPIM	HDPE/LDPE	T_{melt}=200°C p_{proc}=90 MPa T_{mould}=25°C	σ_B=21-109 MPa	shish-kebab structure (WAXD)	[92]
		HDPE/PP	T_{melt}=220°C p_{proc}=32-48 MPa T_{mould}=42°C	σ_B=25-90 MPa	(< 10 wt% PP)	[93]
		HDPE/UHMWPE	-	μ=0.3-0.5 (0.3) Load-carrying capacity= 70 N (35 N)	micro-cracks parallel to the surface (conventional packing)	[94]

Table 7. Production methods, conditions and product characteristics of multi-component SRPMs produced in single-step (in situ)

Num.	Processing	Materials	Processing conditions	Results	Comment	Ref.
1	Coextrusion	rPP/PP	T_{proc}=140, 160°C, p=2.4 MPa, λ=17	$\sigma_{B,L}$=385 MPa, $E_{t,L}$=13 GPa $\sigma_{B,T}$=5 MPa, $E_{t,T}$=1.5GPa	unidirectional structure	[99]
		rPP/PP	T_{proc}=140…170°C, p=17 MPa, λ=16	σ_F=205 MPa, E_B= 6 GPa	woven structure	[98]
		rPP/PP	T_{proc}=140°C, p=1-15 MPa, λ= 17	σ_B=20-230 MPa, E_t=2-7 GPa	woven structure, increasing impact-energy absorption	[100-103]
		rPP/PP	T_{proc}=145°C, p=2.4 MPa	σ_F=90-160 MPa, E_B=3-12 GPa	consolidation in vacuum bag (UD, 0/90 structure)	[106-107]
2	Film-stacking	HDPE/PE	T_{proc}=137°C, p=16.5 MPa	σ_Y=34-190 MPa, E_t=2-7 GPa	winding angels (30-45°)	[113]
		rPP copolymer/PP	T_{proc}=155-160°C, p=16.5 MPa	σ_Y=15-30 MPa, E_t=1.6-1.8 GPa	transcrystalline structure (light microscopy)	[114]
		rPP copolymer/PP	T_{proc}=158°C, p=11-14 kPa,	σ_B=17-26 MPa, E_t=2-3 GPa	different woven structure	[117]
		rPP copolymer-EP/PP	T_{proc}=152°C	σ_B=17-26 MPa, E_t=0.3-0.7 GPa	0-30 wt% EP	[119]
		rPP/PP	T_{proc}=147-177°C, p=7 MPa	σ_Y=110-120 MPa, E_t=2-2.5 GPa	highly stretched split PP tapes	[81-82]
		β-rPP/ PP	T_{proc}=136-166°C, p=7 MPa	σ_Y=100-110 MPa, E_t=1.5-2 GPa	highly stretched split PP tapes	[81-82]
		rPP/hPP	T_{proc}=150-163°C, p=1.9 MPa	σ_B=14-42 MPa, E_t=0.4-0.5 GPa	transcrystalline structure (TEM)	[122]
		LCP/LCP	T_{proc}=260-285°C, p=4.4 MPa	σ_F=24-36 MPa, E_B=36-42 GPa	unidirectional structure	[126-127]
		PMMA/PMMA	T_{proc}= 140-160°C, p= 0.2 MPa		electrospun nanofibres	[129]
		Polyester/PET	T_{proc}= 215-235°C, p= 5-10 MPa	σ_Y=30 MPa, E_t=3.0-3.2 GPa	biodegradable and convention polyester resin	[130-131]

Table 8 Production methods, conditions and product characteristics of multi-component SRPMs produced in multi-step (ex-situ)
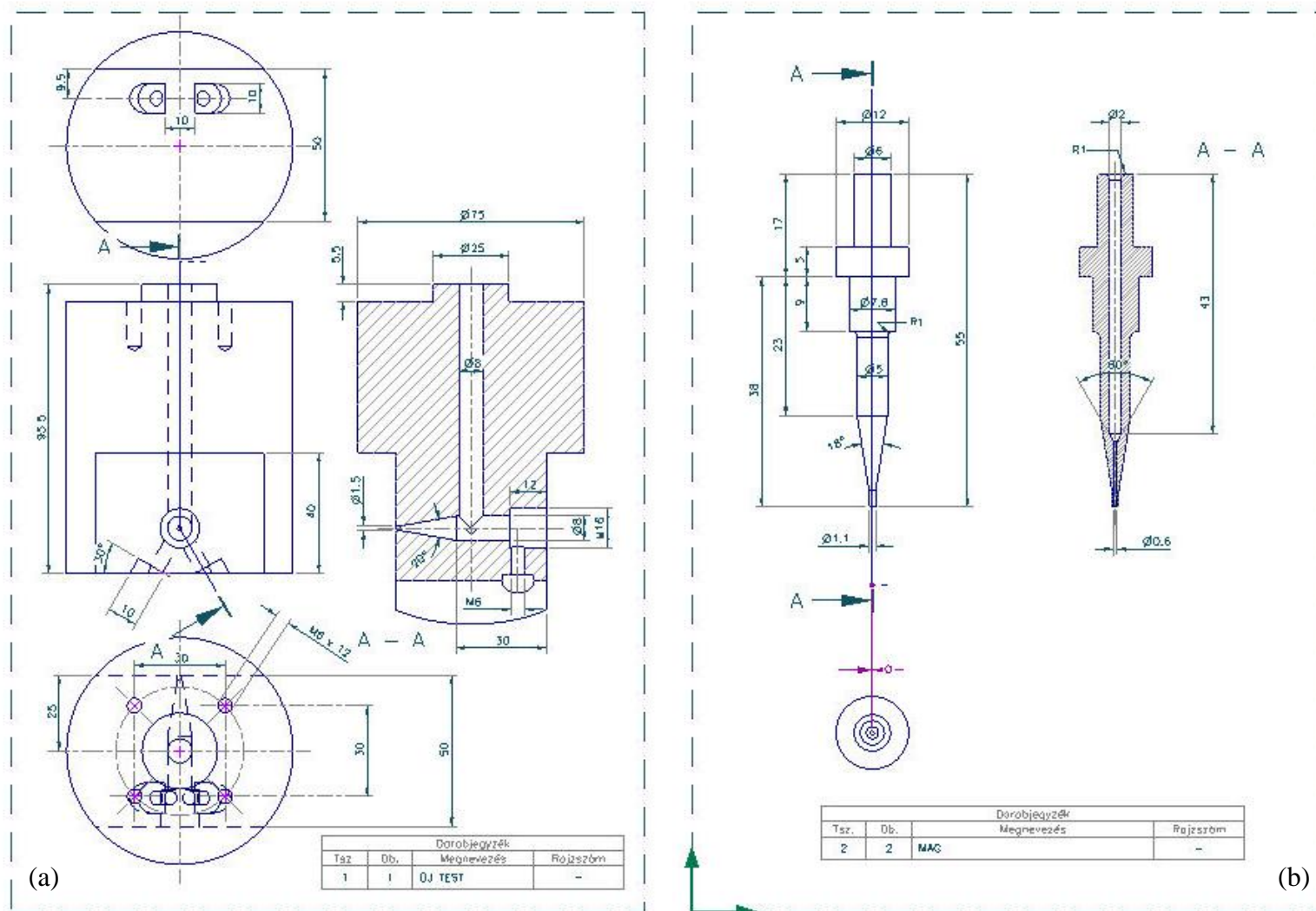
Figure 80. Developed special extruder die (a) with self-aligning core (b)